universität wien

DISSERTATION

Titel der Dissertation

„Characterization of potential vaccine antigens from *Moraxella catarrhalis* and nontypeable *Haemophilus influenzae* with focus on iron metabolism“

Verfasserin

Mag.rer.nat. Margarita Smidt

angestrebter akademischer Grad

Doktorin der Naturwissenschaften (Dr.rer.nat.)

Wien, 2011

Studienkennzahl lt. Studienblatt:	A 091 441
Dissertationsgebiet lt. Studienblatt:	Genetik - Mikrobiologie
Betreuer:	Univ. Prof. Dr. Alexander von Gabain

Acknowledgements

As this section of my thesis might be the most frequently read I feel obliged to put an extra effort into this part by considering and remembering everyone who supported me during my PhD.

There are many people who either directly or indirectly supported me throughout the past three years. Very special thanks go to Alexander von Gabain and Eszter Nagy for giving me the opportunity to do my PhD at Intercell AG and for the most interesting discussions in our student seminars.

I have (fortunately) encountered more supervisors than work-related problems during my time at Intercell. All of my supervisors have provided me with extremely valuable scientific advice and support. I always appreciated Axel Niebisch´s scientific and technical support during the first months of my PhD. Martin B. Oleksiewicz´s organizational talent has impressed me from the very beginning and I keep my fingers crossed that I have adopted this capability at least to a certain extent. I would like to thank him for the supervision. Thanks a lot to Andreas Meinke for the support during the final few months of my thesis. It would have been very hard to finalize my thesis without his input.

In a project meeting a colleague once called me "Moraxella" – some people might call that a Freudian slip, however, I was getting a little worried about identifying too much with my topic. Like couples, or people and their dogs starting to resemble each other over the years, maybe scientists and their "scientific objects" also become alike. Well, even more concerning that I actually felt addressed…

However, many of my colleagues as well as family and friends helped me overcome this problem ;).

I am grateful that my colleagues (Molecular Microbiology department) made sure that the chocolate concentration in the office was always maintained at a constant level, leading to a very enjoyable and relaxed atmosphere at work.

I would especially like to thank Zehra Visram, Andrea Fritzer, Tina Satke and Verena Salletmayer for the numerous scientific discussions which were typically accompanied by caffeine intake, due to efficacy reasons. Tina, thank you also for being a very reliable and motivated friend with regard to the early morning runs. It would have been a lot less fun running along the Prater Hauptallee all by myself. It did not only keep us fit and

healthy, but it was also a necessity after all the chocolate consumption mentioned before as well as an opportunity to bridge incubation times.

I never want to forget to mention Birgit Noiges in my acknowledgements, as she provided us with constant help. She has the ability to listen to any kind of problem/concern/wish with a patience and tranquility that is remarkable.

Thanks to all staff scientists and group leaders (Urban Lundberg and Sanja Selak) for their scientific input. Ulrike Schirmer helped me with the planning of some experiments - thanks a lot for that and also for reviewing parts of my thesis! Thanks to Wolfgang Schüler for the bioinformatic support, to Markus Hanner for the help with protein-related problems and to Petra Schlick for scientific discussions.

Many thanks go to Peter Hermans for providing the opportunity to perform the Microarray analyses in the "Pediatric Infectious Diseases" group of the Radboud University Medical Center in Nijmegen (The Netherlands). Special thanks to Stefan de Vries and Hester Bootsma for their technical and scientific support during my stay.

Additionally, I would like to thank Patrick Bättig from the Karolinska Institutet (Sweden) for testing the *M. catarrhalis* antigens in the mouse model and John Hays from the ERASMUS Medical Centre (The Netherlands) for providing the *M. catarrhalis* plasmid pEMCJH04-KAN.

I would like to thank all members of the OMVac consortium as well as my PhD committee (Thomas Decker, Alexander von Gabain and Martin B. Oleksiewicz) for numerous interesting scientific discussions.

My friends Julia Zach and Michaela Wladasch deserve many, many thanks! Our get-togethers have always been so much fun and also extremely motivating when times during my PhD were not so easy.

Last but not least I would like to thank my parents Ena and Stefan for their love and their mental and also financial support. Thanks also to my sisters Isabel and Laura and their families for being there for me whenever I need you.

Andreas, I want to thank you for your love, support and for your motivation. Thank you for always being there for me and for all your understanding!

1 Abstract

Otitis media, a very common disease of early childhood is caused by three major bacterial pathogens – *Streptococcus pneumoniae*, nontypeable *Haemophilus influenzae* (NTHI) and *Moraxella catarrhalis*. An increasing resistance to antibiotics and the economic burden associated with otitis media raise the demand for a vaccine to prevent this disease.

These studies focussed on the identification, selection and characterization of potential novel vaccine antigens from NTHI and *M. catarrhalis*, the second and third most frequent antigens associated with otitis media. The list of antigens generated by the antigenome approach (AIP®) in previous studies provided the basis for these studies. Out of 214 *M. catarrhalis* and 156 NTHI antigens, approximately 20 proteins per pathogen were chosen for further research based on gene distribution, antigenome-screen hits and peptide ELISA. In parallel, proteomic analyses were performed in order to verify and complement the results obtained by the antigenome approach. Whole membrane preparations (NTHI and *M. catarrhalis*), outer membrane preparations (NTHI) as well as outer membrane vesicles (OMVs) (*M. catarrhalis*) were subjected to mass spectrometric analysis. Thus, an enrichment of membrane proteins was achieved, leading to the identification of the membrane proteomes of *M. catarrhalis* and NTHI. Furthermore, OMVs isolated from *M. catarrhalis* cultures grown in iron-depleted medium were isolated and subjected to SDS-PAGE. This revealed that especially proteins between 70 and 130 kDa were upregulated during iron-limiting conditions. Due to these observations, the frequent selection of iron transport proteins by AIP®, and their crucial role in pathogenesis, one main focus of these studies was the examination of iron-regulated proteins. In the present studies, iron transporters were shown to be overexpressed during iron limitation *in vitro* by Western blot analysis and flow cytometry (NTHI) as well as Microarray analysis (*M. catarrhalis*). Moreover, eight selected gene deletion mutants were generated in *M. catarrhalis* to examine the essentiality of the genes for survival and bacterial growth. The *msp22* (MCR_1416) gene deletion mutant appeared to be more sensitive to iron limitation compared to the wild type and all other gene deletion mutants. Thus, Msp22 was chosen for further characterization. Msp22 is a cytochrome *c* homologue, and immunization with the recombinant protein conferred protection in a mouse pulmonary clearance model. Moreover, vaccination with two additional

candidate antigens, the "plug" domain of a TonB-dependent receptor (MCR_0076) as well as OppA (MCR_1303), enhanced pulmonary clearance upon bacterial challenge. Finally, Msp22 was heterologously expressed in *M. catarrhalis* using *M. catarrhalis* shuttle plasmid pEMCJH04-KAN, and subsequently purified on Ni-sepharose columns. Purified Msp22 was demonstrated to be covalently bound to heme and to exhibit heme-dependent peroxidase activity.

In summary, these studies strongly supported the characterization and evaluation of potential novel *M. catarrhalis* and NTHI antigens for the development of an otitis media vaccine.

2 Kurzfassung

Otitis media, die Mittelohrentzündung, ist eine weitverbreitete Krankheit bei Kindern unter drei Jahren und wird hauptsächlich durch drei bakterielle Erreger verursacht - *Streptococcus pneumoniae*, nontypeable *Haemophilus influenzae* (NTHI) und *Moraxella catarrhalis*. Ein Ansteigen der Antibiotikaresistenz sowie die mit der Krankheit assoziierte finanzielle und ökonomische Last für die Gesundheitssysteme von Staaten begründen den Bedarf eines Impfstoffes gegen die Mittelohrentzündung.

Meine Studien beschäftigten sich mit der Identifikation, Selektion und Charakterisierung potentieller neuer Impfstoffantigene von NTHI und *M. catarrhalis*, den zweit- und dritthäufigsten Erregern der Mittelohrentzündung. Die Antigenliste, welche durch die Anwendung der Antigenomtechnologie (AIP®) in vorangegangenen Studien generiert wurde, stellte die Basis für diese Studien dar. Von 214 *M. catarrhalis* und 156 NTHI Antigenen wurden etwa 20 Proteine zur weiteren Evaluierung basierend auf Gendistribution, Antigenom-Screen hits und Peptide ELISA selektiert. Parallel und ergänzend zur Antigenomtechnologie wurden Proteomanalysen durchgeführt, indem Proteine in Membranpreparationen (gesamte Membran, äußere Membran, Membranvesikel) mittels Massenspektrometrie identifiziert wurden. Dies erlaubte eine Anreicherung an Membranproteinen sowie die Bestimmung der Membranproteome der beiden Bakterien. Weiters wurden Membranvesikel von *M. catarrhalis* Kulturen, die unter eisenlimitierenden Bedingungen gewachsen sind, isoliert. Vergleichende SDS-PAGE zeigte, dass speziell Proteine zwischen 70 und 130 kDa unter eisenlimitierenden Bedingungen überexprimiert wurden. Aufgrund dieser Daten und der häufigen Selektion von Eisentransportern mittels AIP® stellte der Eisenmetabolismus einen Schwerpunkt dieser Studien dar. Da die Konzentration an freiem Eisen im menschlichen Körper sehr gering ist, scheinen diese Proteine eine wichtige Rolle in der Pathogenese und Virulenz zu spielen. Im Zuge dieser Studien wurde mittels Western blot und Durchflusszytometrie (NTHI) sowie Microarrayanalysen (*M. catarrhalis*) gezeigt, dass die Expression jener Antigene, die am Eisentransport beteiligt sind, durch Eisen reguliert wird. Außerdem wurden acht selektierte Gendeletionsmutanten in *M. catarrhalis* generiert, um die Wesentlichkeit der jeweiligen Gene für das Überleben und das bakterielle Wachstum zu bestimmen. Die *msp22* (MCR_1416) Gendeletionsmutante weiste erhöhte Sensitivität gegenüber eisenlimitierenden Bedingungen auf und wurde

daher zur weiteren Charakterisierung herangezogen. Msp22 ist ein Cytochrom *c* Homolog und Immunisierung mit rekombinantem Protein führte zu Protektion in einem Mausinfektionsmodell. Außerdem führte die Vakzination mit zwei weiteren Proteinen, der „plug"-Domäne eines TonB-abhängigen Rezeptors (MCR_0076) sowie OppA (MCR_1303) zu einer stark verminderten Bakterienzahl in der Mauslunge nach Infektion mit *M. catarrhalis*. Zusätzlich wurde Msp22 mittels des Shuttlevektors pEMCJH04-KAN heterolog in *M. catarrhalis* exprimiert und anschließend über Ni-Sepharosesäulchen gereinigt. Es konnte gezeigt werden, dass das gereinigte Protein kovalent an Häm gebunden ist und häm-abhängige Peroxidaseaktivität aufweist.

Zusammenfassend unterstützten diese Studien die Charakterisierung und Evaluierung potentieller neuer *M. catarrhalis* und NTHI Antigene für die Entwicklung eines Impfstoffs gegen Otitis media.

3 Introduction

3.1 Otitis media – a polymicrobial and multifactorial disease

3.1.1 Otitis media disease and pathogens causing otitis media

Otitis media, the middle ear infection, is one of the most common childhood infections and represents an inflammatory disease accompanied by the production of cytokines (44, 115, 149, 166, 200). It develops through various disease stages including acute otitis media (AOM), recurrent acute otitis media, and otitis media with effusion (OME) (31, 138). AOM leads to inflammation of the middle ear resulting in earache, night restlessness and fever (95). Complications such as mastoiditis contribute to the aggravation of the disease (1, 175). OME can precede an acute infection or it can be the consequence of AOM, and may lead to hearing problems due to the collection of fluid within the middle ear space (70). Recurrent acute otitis media is characterized by the repetitive development of AOM within a short period of time (≥ three episodes within six months) (36, 149). In the United States, the prevalence of recurrent otitis media increased dramatically in the 1980s which was mainly due to a change in social parameters such as the more frequent use of child care (100).

Otitis media is a polymicrobial disease that can be caused by multiple pathogens, the most frequent being *Streptococcus pneumoniae*, nontypeable *Haemophilus influenzae* (NTHI) and *Moraxella catarrhalis* (37). Table 3-1 represents relative frequencies of the most abundant pathogens causing otitis media.

Table 3-1: Pathogens causing otitis media. *S. pneumoniae*, NTHI and *M. catarrhalis* are the most frequent pathogens associated with otitis media. The incidence of otitis media caused by *S. pyogenes* has been increasing.

Pathogen	Relative frequency in OM	Reference
S. pneumoniae	19 – 50%	(122)
NTHI	16 – 45%	(122)
M. catarrhalis	7 – 23%	(122)
S. pyogenes	~ 4 - 7%	(154, 160)
Respiratory viruses	≤ 30%	(36, 73, 74)

S. pneumoniae is a gram-positive, alpha-hemolytic, lancet-shaped coccus that is a major cause of morbidity and mortality in elderly people in the developed world and children in developing countries. It is the number one cause of AOM, and a major cause

of meningitis, pneumonia, and bacteraemia. A rapidly rising resistance to antibiotics has been observed, making treatment a challenge. The most important virulence factor of *S. pneumoniae* is its polysaccharide capsule, which is also the basis for differentiation between serotypes and for vaccine development. In total, over 90 polysaccharide serotypes have been recognized to date. The capsule enables the bacterium to evade the host immune system by protection against complement-mediated opsonophagocytosis as well as Fc binding to its receptor (91).

Haemophilus influenzae is a fastidious, gram-negative coccobacillus. Six encapsulated strains (a-f) as well as unencapsulated strains which are referred to as nontypeable *H. influenzae* (NTHI) due to the lack of a polysaccharide capsule, are known. NTHI accounts for approximately 16 – 45% of all AOM cases and causes a number of respiratory tract infections including sinusitis and bronchitis (122). In the nasopharynx, NTHI is a commensal and colonization starts with the interaction with the mucosa via adhesion molecules. Bacterial multiplication and subsequent adherence to respiratory epithelial cells in combination with overcoming the local immune response eventually lead to disease (170).

M. catarrhalis is a gram-negative bacterium that has not been considered a pathogen for a long time (26). It has a relatively small genome of less than 2 Mbp, with genes expressing a number of adhesion molecules and other virulence factors. Adhesion to the epithelium precedes the invasion of host cells for the purpose of hiding from the host immune system. Furthermore, a fast increase in resistance of this pathogen to beta-lactam antibiotics has been observed in the recent years (21, 39).

In addition to otitis media, all three pathogens play a significant role in exacerbations of chronic obstructive pulmonary disease (COPD) (121, 195). Beside the major causative agents *S. pneumoniae*, NTHI and *M. catarrhalis*, otitis media may also result from other bacterial or viral infections. Interestingly, *Streptococcus pyogenes* has become an important cause of otitis media as could be shown by a five-year study in Israel that was initiated in the late 1990s (160). Moreover, respiratory viruses such as respiratory syncytial virus, rhinovirus or (para)influenza viruses are frequently isolated from middle ear fluids of children suffering from AOM (35, 36, 73, 74). *Neisseria meningitidis* and *Staphylococcus aureus* have also been detected in middle ear effusions of patients that went through tympanostomy tube placement for middle ear disease, however, these bacteria are only rarely associated with otitis media disease (141).

3.1.2 Interactions of *M. catarrhalis* and NTHI with the immune system and mechanisms of immune evasion

The initial contact of bacteria with the human host immune system occurs during the colonization of mucosal surfaces. The mucosa represents a physical barrier equipped with local defense mechanisms. Pattern recognition receptors such as toll-like receptors allow the unspecific recognition of structures that are common to many pathogens. The ability of the immune system to differentiate between commensals and pathogenic bacteria allows the selective clearance of pathogens from human tissues. However, bacteria have developed several mechanisms in order to escape host immune responses.

Phase variation represents a major feature of *M. catarrhalis* and NTHI with regard to immune evasion. It is characterized by a change in protein expression as a response to changing environments. Thus, random phenotype variations arise, allowing the selection for the best adapted variant to a certain condition (170). Phase variation often affects phenotypes which are linked to virulence. The variability of surface antigen expression thus complicates the evaluation and interpretation of strain comparison data (49). Hemoglobin-haptoglobin binding proteins A and B of NTHI (32) or MID (116) and UspA1 (99) of *M. catarrhalis* are only a few examples of proteins which have been identified to be subject to phase variation.

Complement resistance (serum resistance) plays an important role in *M. catarrhalis* and NTHI pathogenesis (80, 127). The complement system can be activated in different ways. If IgM or IgG is bound to antigen, the C1 complex is activated, resulting in a series of events, which finally lead to the formation of the membrane attack complex (classical pathway). The alternative pathway is triggered by spontaneous hydrolysis of C3. *M. catarrhalis* is capable of triggering both pathways of complement activation (184). However, mechanisms allowing survival of bacteria leading to serum resistance have evolved. Antigens involved in serum resistance include UspA1 (68), UspA2 (7), CopB (77), OmpCD (83) and OmpE (124). It has been shown that patients harbor a higher number of serum resistant *M. catarrhalis* isolates than healthy children, thus leading to the conclusion that complement resistance is an important virulence factor that is closely linked to disease (80).

In general, encapsulated *H. influenzae* strains are more resistant to human serum than nontypeable strains. However, the degree of sensitivity to human serum varies among

NTHI strains and correlates with the severity of disease (69, 194). Nakamura *et al*. (127) have recently shown that the expression of genes encoding proteins which contribute to the surface structure of NTHI correlates with an increased serum resistance as well as a reduction in IgM binding. Therefore, serum resistant strains are less sensitive to the bactericidal activity of antibodies. Additionally, NTHI isolates from the lower respiratory tract are associated with an increased serum resistance compared to isolates from the upper respiratory tract.

Innate and adaptive immune responses are essential for the human host to protect from bacterial colonization and infection. Immune mechanisms involve the action of a number of phagocytic cells (e.g. macrophages) and the complement system on the one hand, and the activation and effector functions of T- and B-cells on the other hand. These mechanisms allow the specific recognition of bacterial and other pathogens and the subsequent clearance from human tissues. King *et al*. (93) analyzed adaptive immune responses to NTHI, a pathogen that causes not only a number of respiratory tract infections, but may even cause systemic infection (132). Predominantly, the cytokines IFN-γ and IL-2 were produced in healthy control subjects (Th1 response). Additionally, CD40L production (a protein which is mainly expressed on activated T-cells) was significantly higher in the healthy control group. IFN-γ as well as CD40L act as activation signals for macrophages. However, a different immune response was elicited in subjects with bronchiectasis who mainly produced IL-4 and IL-10 (Th2 response) (93). Strain-specific IgG antibodies against NTHI are predominant compared to other immunoglobulins in the middle ear (51, 53). The presence of antibodies negatively correlates with the number of viable bacteria in the middle ear fluid, indicating that the antibodies exhibit bactericidal activity (52). When analyzing acute and convalescent antibody titers to outer membrane proteins D, OMP26 and P6 of NTHI, IgG levels are increased in non-otitis prone children compared to otitis prone children after AOM (92, 197).

For *M. catarrhalis* it was shown that not only whole bacteria, but also outer membrane vesicles (OMVs) which are secreted and carry outer membrane proteins including virulence factors, have the capacity to modulate immune responses (156). They bind B-cells and activate them via toll-like receptor 9. This mechanism is dependent on the protein Hag (MID) (186). Moreover, *M. catarrhalis* is capable of modifying innate immune responses by the inhibition of pro-inflammatory responses induced by toll-like receptor

2. This involves binding of UspA1 to the CEACAM1 receptor on host cells which eventually results in the inhibition of the NF-κB pathway and thus prevents a pro-inflammatory response (167, 168). Additionally, UspA2 of *M. catarrhalis* is capable of binding C3 and thus inactivates especially the alternative pathway of complement activation (131). OMVs contain UspA1/A2, and UspA1/A2-dependent C3 binding and inactivation leads to increased survival of NTHI when grown in human serum in the presence of *M. catarrhalis* OMVs (172).

3.1.3 Risk factors for otitis media

In general, both environmental and genetic factors play a role in the development of otitis media disease. Age is one of the most dominant risk factors for the development of otitis media. Children aged between six months and three years are especially prone to AOM as a result of the anatomic proportion of the nasopharynx. The Eustachian tube which connects the nasopharynx with the middle ear and ensures pressure equalization is still short and wide and therefore easily accessible for bacteria and other pathogens. The ascension of bacteria from the nasopharynx to the middle ear is thus facilitated. Moreover, respiratory viruses can pave the way for bacterial AOM due to a damaged and more sensitive mucosa, and worsen the outcome of the disease (73, 74). Figure 3-1 summarizes the most important risk factors contributing to the development of otitis media. The immune system of children is still immature and therefore not capable of developing a protective immune response. Early onset of the disease (in the first few months of life) represents an important risk factor for recurrent middle ear infections (101). Children in daycare programs (100) and children living in households with smokers (19, 176) are also at higher risk. However, breast-feeding reduces the risk of becoming infected compared to bottle-feeding (155, 163). Genetic predispositions such as polymorphisms of inflammatory genes or immunodeficiency also contribute to the development and susceptibility to otitis media (64, 88, 134).

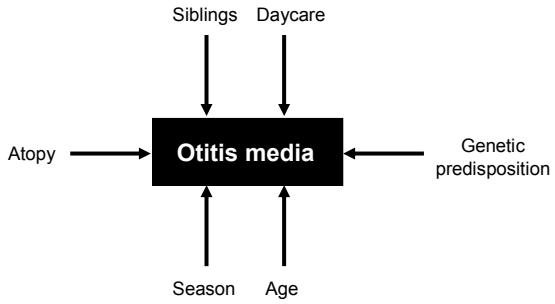

Figure 3-1: Factors contributing to the development of otitis media. Adapted from Rovers *et al*. (149). Age represents the major risk factor in association with otitis media. Children in daycare and children with older siblings are more prone to the development of otitis media. Genetic predispositions including immunodeficiency as well as allergies increase the probability of suffering from otitis media.

The large variety of risk factors together with the multitude of pathogens makes otitis media one of the most frequent childhood diseases with extremely high rates both in developed as well as developing countries (136, 149).

3.1.4 The burden of otitis media and current treatment

About 60% of children have suffered at least once from AOM by one year of age and up to 85% have developed at least one episode by three years of age. Numerous doctor´s visits, the use of antibiotics, the necessity of surgeries and the high prevalence of otitis media in general globally lead to very high costs and subsequently to an extreme economic burden for the health systems. Moreover, long-term effects of otitis media lead to delayed speech and language development and hearing impairment, thus causing major social problems. Additionally, complications including mastoiditis and in some cases even meningitis may develop as a result of a middle ear infection (36, 122).

Nowadays, diagnosis of AOM is done by otoscopic examination and the analysis of symptoms associated with otitis media including inflammation, fever and pain (94, 146). The current treatment of AOM involves the use of nose drops in order to reduce the swelling of the nasopharyngeal mucosa and to unblock the Eustachian tube. The use of a grommet upon repeated infections allows the passage of air to the middle ear and alleviation of hearing loss (110). Frequently, antibiotics are being prescribed for the treatment of AOM (146). Amoxicillin-clavulanate appears to be one of the most effective antibiotics currently in use (79). However, an increasing resistance of bacteria to certain antibiotics has emerged, and the overuse of antibiotics may cause a requirement for even

more expensive drugs. Notably, most clinical isolates of *M. catarrhalis* (21, 36, 38, 109) and NTHI isolates (17, 179) have been shown to produce β-lactamase.

As the current treatments combat the symptoms rather than the causative agents of otitis media disease, there is a need for a vaccine in order to prevent colonization and infection. In their review, Cripps *et al*. (36) suggest that a vaccine should target the three predominant bacteria causing AOM as well as viral strains which are responsible for the destruction of the respiratory tract epithelium. By applying this approach, the vast majority of otitis media cases would be prevented.

3.2 Vaccines against otitis media: achievements and challenges

There is currently no vaccine against otitis media available due to the fact that it is an extremely challenging endeavour to develop a vaccine against a polymicrobial disease. Three pneumococcal conjugate vaccines (based on the pneumococcal polysaccharide capsule) that partially protect against otitis media have been launched so far (Table 3-2).

Table 3-2: Vaccines on the market which partially protect against otitis media disease. All three vaccines are pneumococcal conjugate vaccines.

Vaccine	Protein carrier	Pneumococcal polysaccharide serotypes	Manufacturing Company
Prevnar®	Diphtheria CRM_{197} protein	4, 6B, 9V, 14, 18C, 19F, 23F	Wyeth
Prevnar 13®	Diphtheria CRM_{197} protein	1, 3, 4, 5, 6A, 6B, 7F, 9V, 14, 18C, 19A, 19F, 23F	Pfizer
Synflorix®	NTHI protein D	1, 4, 5, 6B, 7F, 9V, 14, 18C, 19F, 23F	GlaxoSmithKline

As these vaccines cover only a limited number of capsule serotypes (seven for Prevnar®, ten for Synflorix®, and 13 for Prevnar 13® out of over 90 pneumococcal polysaccharide serotypes), the incidence of serotypes included in the vaccine decreases, whereas the incidence of serotypes not included in the vaccines relatively increases. Therefore, it is very difficult to estimate the efficacy of pneumococcal vaccination against AOM (36, 182). Prevnar® and Prevnar 13® are pneumococcal conjugate vaccines, the latter providing expanded protection against six additional pneumococcal polysaccharide serotypes. In general, both vaccines show a similar safety profile (20, 199). Prevnar® has been shown to reduce invasive disease caused by *S. pneumoniae*, however, otitis media disease is only prevented to a limited extent (25). The introduction of Prevnar® as well as the increased use of antibiotics has led to a more frequent infection by pneumococcal serotype 19A. Pneumococcal conjugate vaccines containing 19F polysaccharide were analyzed for cross-

protection against serotype 19A. However, protection is dependent on the vaccine formulation as well as the number of doses (71, 183). Therefore, the subsequent vaccine Prevnar 13® does contain serotype 19A as well.

Synflorix® developed by GlaxoSmithKline is a pneumococcal *H. influenzae* protein D conjugate vaccine and thus the first vaccine containing an NTHI antigen. The vaccine is licensed for the active immunization against *S. pneumoniae* infections and AOM. The vaccine is conjugated to NTHI protein D, and protein D is non-lipidated in this vaccine. The exact function of protein D remains to be elucidated, however, it is most probably involved in pathogenesis, surface-exposed and conserved among the majority if not all NTHI strains (46, 142). Immune responses to the vaccine have been analyzed showing that antibodies induced upon vaccination with Synflorix® inhibit glycerophosphodiester phosphodiesterase activity of protein D which may play a role in virulence (178). Immunization with recombinant protein D, however, results in less that 40% efficacy against AOM caused by NTHI (89, 144).

Given the fact that not even all otitis media cases resulting from pneumococcal infection may be prevented by the currently available pneumococcal vaccines, two major considerations arise (123). On the one hand, an otitis media vaccine should preferably contain pneumococcal protein antigens which are conserved among all pneumococcal strains regardless of the serotype. On the other hand, a vaccine should include NTHI as well as *M. catarrhalis* antigens, and potentially also *S. pyogenes* antigens in addition in order to broadly protect against bacterial otitis media disease and to reduce the morbidity associated with it.

3.3 Animal models for otitis media and correlates of protection

Finding an appropriate animal model for exclusively human pathogens is a major challenge with regard to vaccine development against otitis media. The mouse model has become one of the most common animal models for the study of otitis media (107, 152, 180). However, this is not the most adequate model, as mice do not develop otitis media disease and clear infection by NTHI and *M. catarrhalis* rather quickly. Still, it is the model that is widely used due to the extensive experience, easy accessibility of murine reagents and reasonable prices. Several vaccine antigens of NTHI and *M. catarrhalis* have been studied in mouse models including NTHI proteins P4 (85), P6 (8), *M. catarrhalis* LOS

(lipooligosaccharide) conjugated to protein (86), OmpCD (105) and Hag (MID) (57). Moreover, the utilization of the mouse model allows the efficient and easy study of specific immune responses and virulence factors as well as the analysis of mechanisms of host-pathogen interactions (180).

The chinchilla model is utilized for the study of otitis media as the anatomic proportion of the chinchilla´s nasopharynx is similar to that of children. It is a suitable tool to study polymicrobial diseases such as otitis media (10). Pneumococcal otitis media has been studied using this model and small inocula applied intranasally or by injection into the middle ear are sufficient to cause disease (62). Moreover, Johnson *et al*. (89) analyzed NTHI-induced otitis media and the function of protein D during disease in this model. Furthermore, mucosal immunization with detoxified lipooligosaccharide of NTHI conferred protection in the chinchilla model (84). Despite the fact that chinchillas represent a valuable animal model for the study of otitis media, the availability of the animals as well as their distinct breeding cycle cause obstacles for research in this field.

Another method to study infection is the utilization of a pressure cabin which allows transfer of bacteria into the middle ear by the application of pressure. This "natural" way of colonization allows a non-invasive infection of the middle ear via the Eustachian tube. This model may be used in a rat model as well as in a mouse model of infection (177).

The route of vaccination is crucial for the development of a protective immune response. Mucosal vaccination has been shown to be effective against otitis media disease as it induces mucosal immunity as well as systemic immunity. Nevertheless, problems including low immunogenicity of antigens that are administered mucosally and antigenic heterogeneity will need to be solved. The use of good adjuvants may help to overcome these obstacles. It is desirable that a vaccine elicits protective antibodies locally in the nasopharynx as well as in the middle ear as mucosal immunity represents the first line of defense against several pathogens. Thus, a combination of protective innate and adaptive immune responses is required for the purpose of combating otitis media (152).

The identification of suitable correlates of protection facilitates and accelerates the development of vaccines. The most suitable correlate of protection from NTHI infection is the presence of serum bactericidal antibody. The situation for *M. catarrhalis* is slightly more complicated as to date no correlate of protection has been identified. Thus, (novel) *in vitro* as well as *in vivo* assays will need to be developed and optimized in order to be able to determine correlates of protection. An additional challenge is the fact that NTHI

and *M. catarrhalis* are exclusively human pathogens colonizing the respiratory tract. Thus, adequate animal models which mimic human infection remain a difficult problem that requires additional research (121, 122).

3.4 Evaluation of vaccine antigens for the prevention of otitis media

Disease caused by *M. catarrhalis* and NTHI is mediated by a variety of outer membrane proteins including virulence factors, adhesins and other surface-exposed structures rather than by one single antigen or toxin. In fact, several antigens contribute to virulence and pathogenesis and are therefore investigated for their potential as vaccine candidates. The prerequisites for promising vaccine antigens are the initiation of a protective immune response and the conservation among the majority of bacterial strains.

3.4.1 Potential vaccine antigens and virulence factors of *M. catarrhalis*

To date, a number of potential vaccine antigens of *M. catarrhalis* have been identified by various research groups and are currently being tested in animal models for future vaccine use. Table 3-3 lists the most important candidate antigens including their (predicted) functions in bacterial metabolism.

Table 3-3: Potential vaccine antigens of *M. catarrhalis*. *All *Moraxella* strains express either UspA2 or UspA2H (a hybrid form of UspA1 and UspA2). *M. catarrhalis* strain RH4 expresses UspA2H. AIP®, Antigen Identification Program. CopB, TbpB and LbpB are involved in iron metabolism.

Antigen	(Predicted) function	Involvement in iron metabolism	Identified by AIP® (number of hits)	Reference
UspA1	Adherence, phase variation	-	46	(27, 28)
UspA2*	Serum resistance, phase variation	-	0	(27, 28)
UspA2H*	Adherence	-	85	(98)
OmpCD	Adherence	-	3	(5, 83, 111)
OmpE	Fatty acid transport	-	0	(111)
CopB	Iron uptake	+	35	(4, 76, 111)
Hag (MID)	Adherence, hemagglutination	-	493	(57)
TbpB	Iron uptake from Transferrin	+	9	(111, 126)
LbpB	Iron uptake from Lactoferrin	+	39	(14, 111)

Hag (MID), one of the most promising vaccine candidates is involved in the binding to human IgD as well as in agglutination of human erythrocytes and adherence to type II alveolar epithelial cells (56). Bullard *et al*. (22) demonstrated its direct involvement in adherence to human middle ear epithelial cells. The property of adherence by Hag (22) as

well as parts of its gene sequence (116) are conserved among *M. catarrhalis* strains. Moreover, immunization with truncated Hag protein enhances bacterial clearance in a mouse pulmonary clearance model (57).

The UspA proteins are highly immunogenic, and immunization with UspA elicits antibodies with bactericidal activity (28). Additionally, bacterial clearance is enhanced following vaccination of mice in a pulmonary challenge model. Two genes named *uspA1* and *uspA2* encode the protective epitope (3). Antibodies to both, UspA1 and UspA2 are present in humans of all age groups, are cross-reactive and exhibit bactericidal activity. Antibody titers are significantly higher in adults than in children indicating that they play an essential role in protection from *M. catarrhalis* infection (3, 27). UspA2H, a protein mediating adherence replaces UspA2 in some *M. catarrhalis* strains and represents a hybrid form of UspA1 and UspA2 (98).

CopB is a conserved, iron-inducible protein (4). In a mouse lung model of infection, clearance from *M. catarrhalis* can be achieved by active immunization as well as by passive transfer of polyclonal antibodies (76, 161). Aebi *et al*. (2) identified the protective epitope of this protein (residues 293 – 302 of *M. catarrhalis* strain O35E). In addition, it was shown that CopB is a major target for human immune responses (75).

OmpCD is a highly conserved protein with surface-exposed epitopes. It mediates adherence of the bacterium to A549 human lung cells and middle ear mucin. However, the immunodominant regions do not seem to correspond to the region responsible for adhesion (5). Furthermore, it could be demonstrated that vaccination with this protein results in increased clearance of bacteria from the lung in a mouse model of infection (105).

The majority of promising vaccine antigens are outer membrane proteins which are exposed to the bacterial surface. Outer membrane vesicles (OMVs) are secreted by many gram-negative bacteria including *M. catarrhalis*, they are approximately 50 – 250 nm in size, and contain a number of outer membrane proteins as well as periplasmic proteins (Figure 3-2) including Hag (MID) (186) and the UspA (172) proteins.

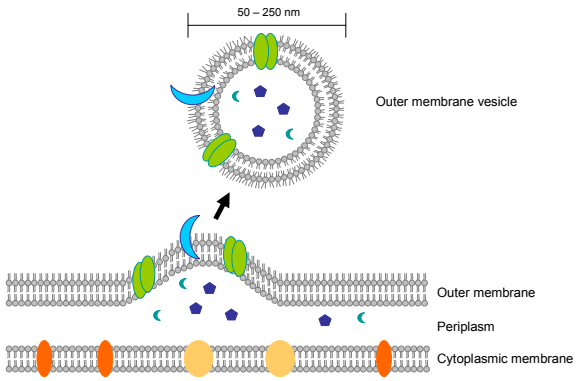

Figure 3-2: Formation of *M. catarrhalis* outer membrane vesicles. The release of OMVs is stimulated by heat-EDTA treatment *in vitro*. OMVs are 50 – 250 nm in size and contain several outer membrane proteins as well as periplasmic proteins and LPS. Adapted from Kuehn *et al*. (96).

There is evidence that OMVs are secreted *in vivo* during infection. Therefore, these vesicles are virulence factors and could play an important role in pathogenesis (172). Immunization of mice with OMVs leads to the production of antibodies specific for a number of outer membrane proteins and LPS. Moreover, enhanced clearance of *M. catarrhalis* is achieved upon vaccination of mice with OMVs (108).

Potential vaccine antigens involved in iron metabolism will be described in section 3.5.2. The antigens described in this chapter (*M. catarrhalis* and NTHI antigens) do not represent the complete list of currently examined vaccine antigens, but an overview of the most important virulence factors / protein antigens which have been studied in most detail.

3.4.2 Potential vaccine antigens and virulence factors of NTHI

Strong efforts have been made in the recent years to identify NTHI vaccine candidates. Table 3-4 represents the major candidate antigens and virulence factors of NTHI showing their (predicted) functions in bacterial metabolism.

Table 3-4: Potential vaccine antigens of NTHI. *Hia is not found in all NTHI strains, but expressed in most strains that lack HMW-like proteins. AIP®, Antigen Identification Program.

Antigen	(Predicted) function	Involvement in iron metabolism	Identified by AIP® (number of hits)	Reference
Protein D	Adherence	-	3	(145)
TbpB	Iron uptake from Transferrin	+	19	(190)
HMW1	Adherence	-	44 (HMW1A)	(12, 170)
HMW2	Adherence	-	111 (HMW2A)	(12, 170)
Hia*	Virulence, adhesion	-	-	(142, 170, 196)
Hap	Adherence	-	27	(103, 170)
IgA protease	IgA cleavage	-	52	(170)

The first and only NTHI antigen to be included in a vaccine was protein D, which acts as carrier protein in a pneumococcal conjugate vaccine (Synflorix®, GlaxoSmithKline). Protein D is expressed *in vivo* in a chinchilla model of otitis media. However, it is not certain whether expression of this protein is diminished during chronic infection. Furthermore, adherence of NTHI to mucosal epithelial cells can be reduced by the deletion of protein D (GlpQ) as well as by antibodies directed against protein D (GlpQ) (89).

The two High-molecular-weight (HMW) proteins HMW1 and HMW2 are involved in adhesion and increased bactericidal activity is associated with an augmentation of serum antibodies against the HMW proteins (12, 13, 171). HMW proteins are localized on distinct regions of the cell surface and have been shown to be secreted (11). These features as well as the presence of these genes in most strains make these proteins promising vaccine candidates.

Secretory IgAs represent a major immune defense mechanism of mucosal tissues. NTHI produces an IgA1 protease that is capable of cleaving IgA1 within the hinge region. This leads to the segregation of the antigen recognition function and the effector function of the antibody. Thus, bacterial clearance can no longer be performed by the host. However, antigen can still be recognized by the antigen recognition fragment and thus binding by intact antibodies is inhibited. In NTHI, IgA1 proteases are genetically and antigenically more diverse than in *H. influenzae* type b strains. The activity of this enzyme is significantly higher in NTHI strains that were isolated from clinical infections as compared to colonizing strains. These observations indicate that IgA1 protease may play a critical role in infection and might thus be an interesting vaccine candidate (187).

Hap triggers interactions between bacteria for the purpose of aggregation, and mediates evasion of the host immune response by the invasion of epithelial cells (147). Moreover, immunization of mice with recombinant Hap leads to the reduction of CFU counts in the murine lung, indicating that Hap represents a potential vaccine antigen (103).

3.5 The importance of iron for pathogenesis

Iron is essential for the survival of almost every single living organism. It plays an important role in metabolic pathways, microbial growth, protection against oxidative stress and the regulation of gene expression. Iron forms insoluble ferric hydroxides in the

presence of oxygen, thus aerobic environments lead to a low level of freely available iron. A number of enzymes contain iron and carry out crucial functions necessary for the survival of the cell. Several iron-containing enzymes contain heme as a cofactor. Heme (iron-protoporphyrin IX) serves as nutrient for many microorganisms and is involved in a large number of redox-reactions (202).

Free iron *in vivo* in mammalian hosts is scarce and therefore severely affecting microbial growth and metabolism. On the one hand, most iron is intracellular such as in the form of ferritin or heme. On the other hand, high-affinity iron-binding proteins such as transferrin and lactoferrin bind extracellular iron, thus inhibiting bacterial growth and having a major effect on host – pathogen interactions (42, 66). Iron also plays an important role in virulence as low levels of iron induce the expression of virulence factors (169).

3.5.1 Iron metabolism in bacteria – NTHI and *M. catarrhalis*

Special mechanisms have evolved in bacteria to overcome iron-limiting conditions. Siderophores are low-molecular-weight compounds that may be sequestered in order to chelate iron from host sources. They specifically bind, solubilize, and deliver iron to microbial cells via receptors (129). However, NTHI and *M. catarrhalis* rely on siderophore-independent pathways, expressing a number of iron transporters which allow them to obtain iron from the human host (23, 139). In this case, a direct interaction between the bacterial surface and the human iron-bound proteins such as hemoglobin, transferrin and lactoferrin is required. Iron transporters are generally upregulated during iron-limiting conditions thus enabling more efficient iron uptake from iron-bound proteins (23, 189, 192).

Iron transport is a highly complex process in bacteria due to the fact that numerous iron uptake systems exist in parallel. It appears that there is a certain redundancy in pathways. However, there seems to be a necessity that bacteria have developed several mechanisms to obtain iron from their host and to keep up with the evolution of high-affinity iron-binding proteins.

Iron uptake is strictly controlled in bacteria. The protein associated with the function of iron homeostasis is the Ferric-uptake regulator (Fur) (9). Its function has been studied in detail in *E. coli*, however, as most of the Fur homologs of other bacteria are capable of

complementing an *E. coli fur* mutant, it is assumed that the mechanisms of transcriptional regulation are commonly shared by many bacteria (59). High iron concentrations lead to the binding of Fur to Fe^{2+}. Under these circumstances, Fur can bind target DNA sequences of genes encoding iron-repressible proteins (9).

Figure 3-3 represents the proteins involved in iron uptake for both, *M. catarrhalis* and NTHI as well as the iron sources from the human host.

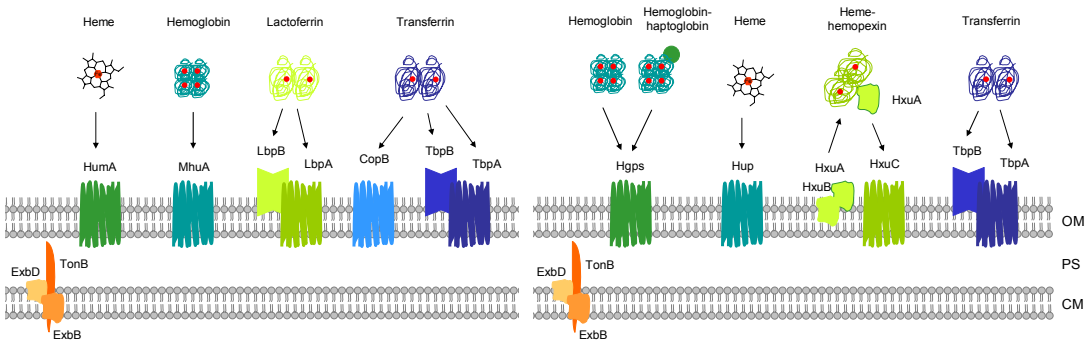

Figure 3-3: Iron metabolism in *M. catarrhalis* (left) and NTHI (right). Transferrin-binding proteins (TbpA, TbpB), heme transporters (HumA, Hup) and hemoglobin transporters (MhuA, Hgps) are present in both organisms. *M. catarrhalis* additionally expresses lactoferrin-binding proteins (LbpA, LbpB). NTHI can obtain iron from heme-hemopexin via the heme-hemopexin-binding proteins (HxuA, HxuB, HxuC). HxuA is secreted and complexes heme-hemopexin. HxuC is required for internalization of the heme-hemopexin-HxuA complex. OM, outer membrane; PS, periplasmic space; CM, cytoplasmic membrane.

TonB plays a key role in iron metabolism even though it is not directly involved in iron uptake. TonB-dependent proteins are outer membrane transporters requiring energy from the proton motive force which is transduced to the outer membrane by the TonB-ExbB-ExbD complex (130). TonB is only found in gram-negative bacteria. The variability of TonB between different species is rather vast with huge differences in length. Furthermore, the number of TonB copies varies between species (30).

The transferrin-binding proteins (Tbp) are comprised of two proteins, TbpA and TbpB. TbpA deficient *M. catarrhalis* strains are incapable of utilizing transferrin as a sole source of iron *in vitro*, indicating that TbpA is essential for iron uptake from this source (106). *H. influenzae* gene deletion mutants lacking TbpA or TbpB ($TbpA^{-}TbpB^{+}$ or $TbpA^{+}TbpB^{-}$) showed reduced binding to transferrin, a double mutant completely lost this ability. Moreover, the lack of the Tbps resulted in an inability to grow with transferrin as the only iron source (65). TbpA is a transmembrane protein with extracellular loops, and TbpB is a surface-exposed lipoprotein. TbpB has a bilobal structure, however, the exact

mechanisms of interaction with human transferrin remain to be elucidated. Furthermore, TbpB preferably binds to the iron-loaded form of transferrin (117).

M. catarrhalis is capable of obtaining iron from lactoferrin by expressing lactoferrin-binding proteins (Lbp). Lbps are surface-exposed and could thus be interesting vaccine candidates (18). The interaction of lactoferrin-binding proteins with the human glycoprotein is specific, and allows the bacterium to overcome the bacteriostatic effect of lactoferrin (157).

NTHI requires a heme source under aerobic growth conditions. In addition to the previously mentioned iron transporters, NTHI expresses the heme-hemopexin-binding proteins (Hxu) HxuA, HxuB and HxuC which constitute a gene cluster (*hxuCBA*). Secreted HxuA complexes heme-hemopexin, and this complex is most probably internalized by HxuC (33). Each component of the *hxuCBA* cluster is necessary for the bacterium to utilize heme-hemopexin as a sole iron source. Additionally, HxuC is essential for the utilization of heme-albumin complexes (118).

The Hxu proteins are required for iron uptake from heme-hemopexin complexes. However, hemoglobin-haptoglobin complexes require the expression of another transporter, namely hemoglobin-haptoglobin-binding proteins (Hgp) (159). Yet, only NTHI, but not *M. catarrhalis* is able to obtain iron from these high-affinity iron-binding proteins.

Overall, it is essential for bacteria to maintain iron homeostasis by the strict regulation of the expression of iron transporters. Moreover, bacteria have developed mechanism to overcome the bactericidal effect of human iron-binding proteins and to obtain this essential micronutrient from various sources.

3.5.2 Iron-regulated proteins as potential vaccine candidates

The human host represents a hostile environment for bacteria with extremely low concentrations of freely available iron. Bacterial iron transporters are therefore upregulated during iron-limiting conditions and repressible by high iron concentrations. These transporters will thus be strongly upregulated by pathogens *in vivo* during colonization and infection of the human host. There are several examples in the literature which indicate that proteins involved in iron metabolism play an important role in pathogenesis and could thus be suitable vaccine candidates if they elicit protective

immune responses. Mainly, the receptors which bind transferrin and lactoferrin have been studied in this context.

TbpB of several species was shown to be a promising vaccine candidate. Efforts have been made for pathogens including *H. influenzae* type b, *Neisseria gonorrhoeae* (174), *Neisseria meningitidis* (148) and *Actinobacillus pleuropneumoniae* to study this protein with respect to vaccine development (82). There is evidence that this protein is expressed *in vivo* during infection (81, 193). Additionally, TbpB has been shown to elicit bactericidal antibodies (143). Recombinant TbpB from both NTHI and *M. catarrhalis* is highly immunogenic after immunization and was shown to enhance clearance of NTHI in a rat lung model (126, 190). Anti-TbpA antibodies can block uptake of iron from transferrin in *N. meningitidis*. However, the role of anti-TbpA antibodies is not completely understood and therefore the potential of TbpA as a vaccine candidate is still controversial (140).

Studies by Yu *et al*. (201) demonstrated that LbpB of *M. catarrhalis* is immunogenic in humans. Sera raised against LbpA are not bactericidal, anti-LbpB serum, however, is slightly bactericidal (43). However, *N. meningitidis* Lbps were shown to be immunogenic and antibodies raised against these proteins exhibit bactericidal activity (137). As these receptors are necessary for survival, surface-exposed, and essential for iron uptake from lactoferrin, they should be considered potential vaccine candidates (14).

Furthermore, the hemoglobin-haptoglobin-binding proteins as well as HxuC of NTHI play an important role in virulence. The deletion of either *hxuC* or the *hgp* genes did not decrease virulence in a rat model of invasive disease. However, a quadruple mutant was considerably affected by the gene deletion, resulting in significantly impaired virulence of this strain (159).

These findings suggest that iron transporters play a complex role in pathogenesis, and that single candidates or combinations of these proteins might be effective as vaccines to induce protective immunity.

3.6 Defining the antigenome of *M. catarrhalis* and NTHI

The development of subunit vaccines is primarily dependent on the identification of potential vaccine antigens. In previous studies, the antigenomes of NTHI and *M. catarrhalis* were identified. Figure 3-4 describes the antigenome technology that was applied to NTHI and *M. catarrhalis*, the second and third most frequent pathogens

associated with otitis media. This technology aims at the identification of genetically conserved and immunogenic proteins for vaccine development.

Human IgG pools from otitis media patients as well as healthy individuals were utilized for the screening of *E. coli* surface display libraries expressing fragments of potentially every antigen of NTHI and *M. catarrhalis*, respectively. This led to the identification of over 150 antigen candidates for NTHI and more than 200 antigen candidates for *M. catarrhalis*.

An antigen needs to fulfill certain criteria in order to be a suitable vaccine candidate. This includes the accessibility for antibodies and other effector immune cells, *in vivo* expression during disease, conservation among most or all strains and protection in animal models (112, 113). Therefore, these 150 – 200 selected candidates were further validated by peptide ELISA as well as gene conservation and gene distribution analyses. The vaccine candidates that were present in most of the 47 selected strains (> 80%) were analyzed for their patent status which also served as selection criterion. Finally, approximately 20 antigens remained for further analysis.

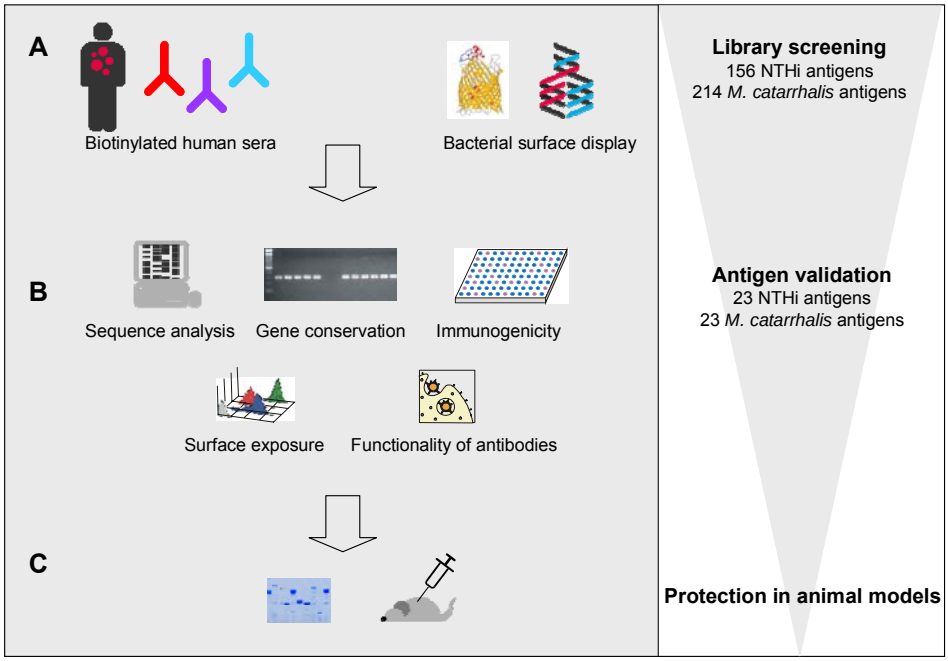

Figure 3-4: Defining the antigenomes of NTHI and *M. catarrhalis*. **A**: Collection and characterization of human sera for subsequent screening of bacterial surface display libraries. **B**: Antigen validation: sequence analysis, determination of gene conservation by PCR, peptide ELISA to define immunogenic epitopes, surface exposure by flow cytometry, testing of functionality of antibodies by *in vitro* assays. **C**: Recombinant proteins are produced and tested for protection in animal models.

Interestingly, eight out of the 23 NTHI candidate antigens and at least two out of 23 *M. catarrhalis* are predicted to be involved in iron metabolism. Selected NTHI candidates include the *hxuCBA* cluster which encodes heme-hemopexin-binding proteins, transferrin-binding protein B and TonB. *M. catarrhalis* MhuA protein, a hemoglobin utilization protein as well as a putative TonB-dependent receptor were among the most frequently selected candidates. Furthermore, several hypothetical proteins and proteins for which only limited literature is available have been selected for further analysis as vaccine candidates against otitis media disease.

3.7 Aim of the studies

The overall aim of these studies was the identification and characterization of potential vaccine antigens from NTHI and *M. catarrhalis* for the purpose of developing a vaccine against otitis media disease. The antigenomes identified for both pathogens in previous studies provided the basis for these studies.

- In order to complement the antigenome approach (AIP®), analysis of the membrane proteomes of *M. catarrhalis* as well as NTHI was performed. This independent approach allowed the verification of the surface localization of proteins, the identification of additional candidate antigens, mainly membrane proteins, and thus contributed to the selection of antigens for further examination.
- For the purpose of identifying protective candidate antigens, recombinant proteins of the antigens or antigen fragments were produced in *E. coli* for immunization experiments. Moreover, recombinant proteins were used to generate hyperimmune sera in mice to obtain antibodies for *in vitro* assays.
- Due to the frequent selection of iron-regulated proteins by the antigenome approach, a major part of these studies focussed on iron metabolism. The influence of iron-limiting conditions was analyzed *in vitro* by growth experiments, and protein expression levels were examined and compared by Microarray analysis and Western blot. Moreover, the surface exposure of selected candidate antigens was examined under different growth conditions.
- The generation of selected gene deletion mutants provided information about the essentiality of the vaccine candidates for bacterial growth, virulence and survival.
    - Msp22, a *M. catarrhalis* protein, appeared to be an interesting candidate antigen due to the *msp22*Δ phenotype and was selected for functional characterization.

In summary, these studies aimed at evaluating a set of novel and conserved antigens of *M. catarrhalis* and NTHI to eventually fulfill the unmet need of including proteins from these two pathogens in a future otitis media vaccine.

4 Materials and methods

4.1 Bacterial strains and plasmid constructs

Bacterial strains used in this study are summarized in Table 4-1. *M. catarrhalis* strain RH4 and NTHI strain 86-028NP were used for all experiments and modified as required (e.g. for the generation of gene deletion mutants).

Table 4-1: Bacterial strains. c*, complemented bacteria transformed with pEMCJH04-KAN-Msp22. *M. catarrhalis* gene deletion mutants were generated in strain RH4. The NTHI gene deletion mutant was generated in strain 86-028NP.

Strain	Description
***M. catarrhalis* RH4**	
wild type	wild type strain RH4, isolated from blood of an infected patient
wild type c*	wild type transformed with pEMCJH04-KAN-Msp22
*msp22*Δ	Gene deletion mutant lacking *msp22* (MCR_1416)
*msp22*Δ c*	Gene deletion mutant lacking *msp22*, transformed with pEMCJH04-KAN-Msp22
*msrAB*Δ	Gene deletion mutant lacking *msrAB* (MCR_0686)
*mhuA*Δ	Gene deletion mutant lacking *mhuA* (MCR_0739)
*oppA*Δ	Gene deletion mutant lacking *oppA* (MCR_1303)
MCR_0076Δ	Gene deletion mutant lacking TonB-dependent receptor
MCR_0136Δ	Gene deletion mutant lacking hypothetical protein MCR_0136
MCR_0560Δ	Gene deletion mutant lacking hypothetical protein MCR_0560
MCR_0996Δ	Gene deletion mutant lacking hypothetical protein MCR_0996
NTHI 86-028NP	
wild type	wild type strain 86-028NP, recovered from the nasopharynx of a child with chronic otitis media (Harrison *et al*., 2005)
*hxuA*Δ	Gene deletion mutant lacking *hxuA*
E. coli	
DH5α	ElectroMAX™ DH5α-E™ Cells (Invitrogen)
DH10B	ElectroMAX™ DH10B™ Cells (Invitrogen)
BL21-CodonPlus®	Competent cells (Stratagene)

Plasmids used for cloning and expression as well as complementation studies are listed in Table 4-2.

Table 4-2: Plasmid constructs. pET28b+ was used for recombinant expression of *M. catarrhalis* and NTHI antigens in *E. coli*. pEMCJH04-KAN and its variants were utilized for complementation studies and recombinant expression of Msp22 in *M. catarrhalis*.

Plasmid	Description	Reference
pET28b+	Kan^R, expression vector (5368 bp)	-
pET28bnHIS	Kan^R, expression vector (5311 bp)	-
pR412T7	$Spec^R$, (4640 bp)	-
pEMCJH04-KAN	Kan^R, complementation plasmid for *M. catarrhalis* (4740 bp)	(72)
pEMCJH04-KAN-Msp22	Kan^R, expression of Msp22 (5400 bp)	This study
pEMCJH04-KAN-Msp22-HIS	Kan^R, expression of HIS-tagged Msp22 (5418 bp)	This study

4.2 General methods

4.2.1 SDS-Polyacrylamide gel electrophoresis

For SDS-PAGE, 4-20% Lonza PAGEr® Gold Precast Gels were used. Proteins were separated at 200 V for 40 min in Laemmli Buffer. Lane marker non-reducing sample buffer (40 mM DTT final concentration) was added to the samples prior to electrophoresis. Prestained protein ladder plus (Fermentas) was used as molecular weight marker. Gels were stained with SimplyBlue™ SafeStain (Invitrogen).

4.2.2 Agarose gel electrophoresis

Agarose gels were prepared with UltraPure™ Agarose (Invitrogen) resuspended in 1xTAE buffer. 0.2 μg/ml Ethidium bromide were added to the liquid agarose for subsequent visualization of DNA bands. 6x Loading Dye Solution (Fermentas) was added to the samples prior to electrophoresis. TrackIt™ 1 kb DNA ladder (Invitrogen) was used as DNA marker. Agarose gel electrophoresis was performed at 120 V in 1xTAE buffer. Agarose gels were exposed to UV light for viewing DNA fragments.

4.2.3 Western blot analysis

For Western blot analysis, 5x lane marker non-reducing sample buffer was added to the samples (1x final concentration) which were subsequently heated at 95°C for approximately 3 min. SDS-PAGE of bacterial lysates for subsequent Western blot analysis was performed as described in 4.2.1. iBLOT® Gel Transfer Device and iBlot Gel Transfer Stacks Nitrocellulose (Invitrogen) were used for membrane blotting. The membrane was blocked with 5% milk in 1x PBS. Proteins were detected with mouse hyperimmune sera (1:2,500 – 1:5,000 dilution) or a Penta-His antibody (Qiagen, 1:3,000 dilution) as primary antibody. A HRP-linked anti-mouse antibody was used as secondary antibody (1:5,000 – 1:20,000 dilution), and detection of protein was achieved upon exposure to a film after incubation of the membrane with chemiluminescent substrate (ECL™ Western blotting detection reagent, GE Healthcare). Washes were done with 1x PBST (PBS + 0.1% Tween® 20) after incubation with antibody.

4.2.4 Southern blot analysis

About 5 µg of *Nco*I/*Afl*II digested genomic DNA fragments were separated for 4 hrs at 80 V on a 0.8% agarose gel. The agarose gel was submerged in Denaturation solution, Neutralization solution, and equilibrated in 20x SSC (see section 9.3 Buffers and media). Subsequently, the DNA was blotted onto a Nylon membrane overnight. The DNA was fixed on the membrane by exposure to UV light for 3 min. Prewarmed DIG Easy Hyb Hybridization solution (Roche) was added to the membrane and agitated gently at 42°C for approximately 50 min. Probes for the respective genes as well as the Spectinomycin resistance cassette were synthesized using the primers listed in Appendix II and the PCR DIG Probe Synthesis Kit (Roche). *M. catarrhalis* genomic DNA (gene-specific probes) and vector pR417T7 (Spectinomycin-specific probe) were used as template DNAs for probe synthesis (see Appendix II).

5 µl labeled PCR product (probe) was added to 50 µl ddH_2O and denatured in a waterbath at 100°C for 5 min. After cooling on ice, the labeled probe dilution was mixed with 5 ml DIG Easy Hyb Hybridization solution and added to the membrane at 42°C overnight. The following day, the membrane was washed with Low Stringency Buffer at RT and High Stringency Buffer at 65°C. For washing and blocking the DIG Wash and Block Buffer Set (Roche) were used. Subsequently, the antibody solution (DIG Luminescent Detection Kit, Roche) was added to the membrane 1:10,000 in blocking solution (30 min, RT). The membrane was washed and exposed to a film after incubation with Detection buffer containing substrate CSPD (provided by Roche).

4.2.5 Isolation of genomic DNA

Genomic DNA was isolated using the Wizard® Genomic DNA Purification Kit (Promega). Briefly, cell pellets were resuspended in Nuclei Lysis solution and incubated at 80°C for 5 min. After cooling to room temperature (RT), RN*ase* solution was added and the mixture was incubated at 37°C for 60 min. Protein precipitation was performed by adding Protein Precipitation solution and vortexing. After centrifugation (4,400 rpm, 20 min, 4°C) the supernatant was transferred to a clean tube containing isopropanol. DNA precipitation was followed by a wash with 70% ethanol. Genomic DNA was resuspended in ddH_2O at 65°C for 60 min.

4.2.6 Isolation of RNA

RNA was isolated using the RNeasy® kit (Qiagen) according to manufacturer´s instructions. TE buffer was autoclaved and 5 mg/ml lysozyme as well as 0.5 mg/ml proteinase K were added freshly prior to each RNA isolation. Cell pellets were resuspended in this solution and incubated at RT for 10 min, with vortexing every 2 min. Buffer RLT containing β-mercaptoethanol was added and the mixture was vortexed. After the addition of EtOH absolute, the lysate was transferred to an RNeasy spin column. The RNA bound to the column was washed with Buffer RW1 and Buffer RPE. The RNA was eluted with RN*ase*-free water.

In order to remove genomic DNA from the RNA preparation, the Turbo DNA-free kit (Ambion) was used. Turbo DN*ase* buffer and Turbo DN*ase* were added to the sample and incubated at 37°C for 30 min. 0.1 vol of the DN*ase* inactivation reagent were added, and the mixture was incubated for 5 min (occasional shaking) prior to centrifugation. The supernatant containing DNA-free RNA was transferred to a clean tube and stored at -80°C.

The quality of the RNA was determined by calculating the ABS_{260}/ABS_{280} ratio, and qRT-PCR analysis was performed to verify the complete removal of genomic DNA. If necessary, additional DN*ase* treatment of the RNA preparations was performed.

4.2.7 PCR

PCRs were done using the T3 Thermocycler (Biometra). Denaturation, annealing and elongation temperatures varied depending on template DNA and primer sequences. GoTaq® Polymerase (Promega) was used for colony PCRs, PWO DNA polymerase (Roche) was used to generate DNA fragments A and B for *M. catarrhalis* gene deletion mutants, and Expand HiFidelity DNA polymerase (Roche) was used for cloning purposes.

4.3 *M. catarrhalis* growth conditions

M. catarrhalis was grown in brain heart infusion (BHI) broth at 37°C with shaking (180 rpm) or on Columbia agar + 5% sheep blood at 37°C. In addition, a chemically defined

medium was used for *M. catarrhalis* growth. The protocol for the *M. catarrhalis* chemically defined medium was adapted from Juni *et al*. (90) (see section 9.3 Buffers and media).

For growth experiments, a single *M. catarrhalis* RH4 colony from a fresh overnight plate was inoculated in BHI broth and grown overnight (180 rpm, 37°C). When grown in BHI, the overnight culture was diluted in BHI medium. Otherwise, the cells were harvested (4,400 rpm, 4°C, 15 min) and resuspended in 1 ml chemically defined medium. Overnight cultures were prepared in chemically defined medium containing 0.1 mg/L $FeSO_4*7H_2O$. The next day, the overnight culture was diluted in chemically defined medium containing 0.5 mg/L $FeSO_4*7H_2O$ and Desferal® (Novartis) concentrations ranging from 0 – 2.5 μM. The Desferal® concentration in the BHI medium amounted to 30 μM. The optical density was measured at 600 nm (OD_{600}) at certain time points to follow the growth rate.

4.3.1 Autoagglutination of *M. catarrhalis*

M. catarrhalis cultures were grown as described in section 4.3. In order to determine the degree of autoagglutination, bacteria were either analyzed by microscopy (Axioskop 2 plus, Zeiss) or optical density (600 nm) measurement. For that purpose, the OD_{600} was initially measured during log-phase. The cuvette was let stand overnight and the OD_{600} was measured again.

4.4 NTHI growth conditions

NTHI was grown in BHI broth containing 10 μg/ml β-NAD and 1 - 10 μg/ml hemin (BHI^+) or on BBL™ Mueller Hinton Chocolate Agar (BD diagnostic systems) at 37°C in an atmosphere of 5% CO_2.

For growth experiments, a single NTHI86-028NP colony from a fresh overnight plate was inoculated in BHI^+ broth and grown overnight (37°C, 5% CO_2). The overnight culture was diluted in fresh BHI^+ broth, and Desferal® (Novartis) concentrations ranging from 0 – 500 μM. The optical density (OD_{600}) was measured at certain time points.

4.5 Preparation of bacterial lysates

M. catarrhalis and NTHI lysates were prepared from cultures grown in iron-rich medium containing 0 µM Desferal® and iron-depleted medium with different Desferal® concentrations. The cells were harvested, resuspended in 1x PBS and sonicated on ice using two 30 second bursts (5 x 10% cycle, 100% power). The protein concentration was measured by BCA protein assay reagent (Pierce).

4.6 Proteomic analysis

4.6.1 Preparation of whole membranes from *M. catarrhalis* and NTHI

Cells from a 1.5 L culture were harvested (4,500 rpm, 4°C, 60 min) and washed with 1x PBS. The pellet was resuspended in 100 mM Na_2CO_3 and sonicated on ice for 2 min (50%). After centrifugation (12,000 rpm, 4°C, 10 min) to remove cell debris, the supernatant was ultracentrifuged (40,000 rpm, 4°C, 90 min) and the pellet was washed with 1x PBS (40,000 rpm, 4°C, 90 min). Finally, the pellet was resuspended in 500 µl 1x PBS.

4.6.2 Preparation of outer membrane vesicles from *M. catarrhalis*

Cells from a 1.5 L culture were harvested (4,500 rpm, 4°C, 60 min) and washed with 1x PBS. The cells were resuspended in 50 ml EDTA buffer (0.05 M Na_2HPO_4, 0.15 M NaCl, 0.01 M EDTA, pH 7.4) and incubated at 56°C for 30 min at 75 rpm agitation with glassbeads (1.7 – 2 mm). The culture was centrifuged (3,500 rpm, RT, 15 min) twice, and the supernatant containing the membrane vesicles was ultracentrifuged (40,000 rpm, 4°C, 90 min). The pellet was washed with 1x PBS (40,000rpm, 4°C, 60 min) and resuspended in 500 µl 1x PBS.

4.6.3 Preparation of the outer membrane from NTHI

Cells from 1.5 L culture were harvested (7,000 g, 4°C, 15 min) and washed with 1x PBS. The pellet was resuspended in 20 ml 1x PBS and DN*ase* I (100 µg/ml final concentration) as well as protease inhibitor cocktails I and II (see section 9.3 Buffers and media) were

added. Sonication on ice was performed for 1 min and followed by centrifugation (7,000 g, 4°C, 15 min). The supernatant was ultracentrifuged (40,000 rpm, 4°C, 90 min) and the pellet was resuspended in 10 ml PBS/1% N-Lauroylsarcosine. After incubation on ice for 45 min, ultracentrifugation was performed again (40,000 rpm, 4°C, 90 min), the pellet was washed with 1x PBS/0.2% N-Lauroylsarcosine (40,000 rpm, 4°C, 90 min) and resuspended in 1 ml 1x PBS.

4.6.4 Mass spectrometry

Membrane preparations were analyzed by the University of Graz. The proteins were separated by 1D SDS-PAGE, and the bands were identified by nano-HPLC IT MS/MS after trypsin digestion. Additionally, a 2D nano-HPLC MS/MS approach was used (54, 61).

4.7 Cloning of antigens for recombinant expression

Genes or gene fragments were PCR amplified using genomic DNA as template. Appropriate restriction sites were added at the 5′ end of the primers. Digested DNA fragments were ligated with digested vector pET28b+ at 16°C overnight. After precipitation (1/10 vol 3 M Na-acetate pH5.3, 3 vol EtOH absolute, 20 µg glycogen), the ligation was transformed into electrocompetent *E. coli* DH5α cells by electroporation (2000 V, 25 µF, 1 mm cuvette), which were subsequently transferred to S.O.C. medium, incubated at 37°C (180 rpm) and plated on LB plates containing Kanamycin (50 µg/ml). Clones were analyzed by colony PCR using primers ICC102 and ICC103 (Appendix II).
Positive clones were subjected to enzymatic test digest using appropriate restriction enzymes. Sequence analysis of the recombinant constructs was performed to verify amplification of the correct sequence. Plasmids with the antigen inserts were transformed into BL21 Codon plus *E. coli* cells by chemical transformation. Briefly, 50 µl cells were added to 1 µl XL10-Gold β-Mercaptoethanol mix. After incubation on ice for 10 min, 1 µl plasmid DNA was added. Incubation on ice for 30 min was followed by 2 sec incubation at 42°C and 2 min on ice. After incubation at 37°C with shaking for 1 hour, 980 µl pre-warmed S.O.C. medium was added to the cells, and the transformation was plated on LB containing 50 µg/ml Kanamycin.

4.8 Recombinant expression of antigens in *E. coli*

50 ml enriched LB-medium (see section 9.3 Buffers and media) supplied with 50 μg/ml Kanamycin and 50 μg/ml Chloramphenicol was inoculated with single *E. coli* colonies (that heterologously express the HIS-tagged antigens) and grown overnight at 37°C with shaking. The overnight culture was transferred to 2 L enriched LB-medium and grown for at least 2 hours at 37°C (shaking). Induction with IPTG (100 μM final concentration) was followed by another 4 hours of growth with shaking at 37°C. Small scale analysis of the *E. coli* cultures expressing the candidate antigens (or fragments) was performed prior to large scale purification in order to determine the solubility of the proteins. The cultures were harvested (7000x g, 15°C, 10 min) and the cell pellets were washed with 1x PBS. Cells were resuspended in 250 ml lysis buffer (50 mM Tris pH8.0, 500 mM NaCl, 0.1% Tx-100, protease inhibitor cocktails I and II – see section 9.3 Buffers and media) and lysed with a high pressure homogenizer. Soluble and insoluble fractions were separated by centrifugation (7000x g, 15°C, 10 min). The insoluble fraction (inclusion bodies) was solubilized. The protein solution (from the soluble or insoluble fraction) was applied to a Ni-sepharose column, washed and the purfied protein was eluted (Table 4-3).

Table 4-3: Purification of soluble proteins. Wash and elution buffers are listed. W0, wash buffer with Tx-100; WØTx, wash buffer without Tx-100; W20, wash buffer with 20 mM imidazole; W40, wash buffer with 40 mM imidazole; EA and EE, elution buffers; CV, Column volume.

	Fraction	Buffer	Column volumes
1	Flow through		
2	W0	50 mM Tris/HCl pH8.0, 500 mM NaCl, 0.1% Tx-100	15 CV
3	WØTx	50 mM Tris/HCl pH8.0, 500 mM NaCl	10 CV
4	W20	50 mM Tris/HCl pH8.0, 500 mM NaCl, 20 mM imidazole	5 CV
5	W40	50 mM Tris/HCl pH8.0, 500 mM NaCl, 40 mM imidazole	5 CV
6	EA	50 mM Tris/HCl pH8.0, 150 mM NaCl, 250 mM imidazole	3 CV
7	EE	50 mM Tris/HCl pH8.0, 120 mM NaCl, 250 mM imidazole, 8 M Urea	3 CV

DTT was added to cysteine-containing proteins (lysis buffer and wash buffers) to a final concentration of 0.5 mM.

Protein concentrations were measured using BCA protein assay reagent (Pierce). Additionally, the LPS content of the purified proteins was determined using PyroGene® recombinant factor C endotoxin detection system (Lonza).

4.9 Generation of mouse hyperimmune sera against *M. catarrhalis* and NTHI recombinant proteins

HIS-tagged proteins expressed in *E. coli* were utilized for the generation of hyperimmune sera in mice. Female NMRI mice 6-8 weeks of age (Janvier, France) were bled by tail vein puncture to generate preimmune sera, and were immunized three times intraperitoneally (2 week intervals) with 50 μg recombinant antigen per immunization, using Complete Freund´s Adjuvant (CFA) for the first immunization and Incomplete Freund´s Adjuvant (IFA) for the second and third immunizations. Groups of 5 mice per antigen were vaccinated. Terminal bleeds were collected via the orbital sinus one week after the final immunization.

4.10 Determination of antibody titres by ELISA

Antibody titres in the inividual hyperimmune sera as well as preimmune serum pools (comprising serum of five mice) were determined by ELISA. Coating of 96-well MaxiSorp™ plates (Nunc) was performed overnight (4°C) using either 50 ng recombinant protein (hyperimmune sera) or 500 ng bacterial lysate (preimmune serum pools) per well. Wells were blocked with 1x PBS/1% BSA, followed by the addition of five-fold dilutions (1:1,000 – 1:3,125,000) of the hyperimmune sera in 1x PBS/0.1% BSA buffer. After 1.5 hours at 37°C, plates were washed with 1x PBS/1% Tween20, and incubated with HRP-linked anti-mouse antibody diluted 1:1,000 in 1x PBS/0.1% BSA. After 1 hour at 37°C, plates were washed with 1x PBS/0.1% Tween20, and developed with ABTS substrate.

4.11 Flow cytometry

Cultures were grown in iron-rich and iron-depleted medium as described in 4.4. About $5x10^5$ bacteria resuspended in 100 μl HBSS/2% BSA were added per well to round-bottomed 96-well plates, and mouse hyperimmune sera were added (diluted 1:100). After incubation at 4°C for 45 min, the bacteria were washed (HBSS/2% BSA), and the secondary antibody (Goat F(ab´)2 fragment anti-mouse IgG (H+L)-PE) was added at a 1:100 dilution (incubation at 4°C, 45 min). An additional wash (HBSS only) was followed by the addition of SYTO® 60 reagent (1:2,000). The cells were again washed and fixed in

2% paraformaldehyde (overnight, 4°C). The bacterial suspensions were analyzed on a Cell Lab Quanta™SC flow cytometer (Beckman Coulter).

4.12 *M. catarrhalis* gene deletion mutants

4.12.1 Generation of *M. catarrhalis* gene deletion mutants

M. catarrhalis gene deletion mutants were generated by amplifying a ~500 bp region up- and downstream of the gene to be deleted from genomic DNA using oligonucleotide primers L1, L2, R1 and R2 (see Appendix II).

These flanking regions of the gene were ligated by overlap-extension PCR with a Spectinomycin resistance cassette that was derived from the vector pR412T7. *M. catarrhalis* cells were rendered competent by washing with 1x PBS containing 0.15% bovine gelatin. Transformation was done by adding the DNA fragments to the competent cells, and subsequent plating on Spectinomycin-containing blood agar plates (100 μg/ml).

After incubation overnight at 37°C, test PCRs of selected colonies were performed to confirm the gene deletion by using primer pairs L1/R1, L1/A, L1/C, P1/P2 (see Appendix II). Additionally, gene deletions mutants were confirmed by sequencing. For that purpose, primers P1 and P2 were used for amplification, and the PCR product was sent for sequencing (MWG).

4.12.2 Antibiotic sensitivity test

In order to test the antibiotic sensitivity of gene deletion mutants, the Taxo™ Anaerobe Disc Set (BD diagnostic systems) was used. A volume of bacteria corresponding to 100 μl of an OD_{600} = 2 overnight culture was plated on blood agar, and 5 different antibiotic discs were put on the plate. After incubation overnight at 37°C, the inhibition zones were measured.

4.12.3 *M. catarrhalis* complementation using plasmid pEMCJH04-KAN

The plasmid pEMCJH04-KAN was obtained from John Hays (ERASMUS Medical Centre, Rotterdam). PCR of the gene including a region of ~220 bp upstream (region containing

potential prokaryotic promoters) was performed using 20 ng genomic DNA as template as well as primers 8825 and 8826 (see Appendix II).

The PCR amplified product was purified, *Bam*HI/*Pst*I digested and ligated with *Bam*HI/*Pst*I digested pEMCJH04-KAN. After precipitation of the plasmid construct, transformation into *M. catarrhalis* competent cells was performed. Briefly, several colonies from a blood agar plate were transferred to 1 ml PBS/0.15% bovine gelatin. A 1:25 dilution of the cell suspension was prepared in BHI and the cells were grown to exponential phase. Subsequently, a 1:5 dilution of the culture (400 µl BHI and 100 µl culture) was prepared and the plasmid DNA (~0.5 ng – 2.5 ng) was added. After 3 - 4 hrs growth (37°C, 180 rpm), 100 µl of transformed bacteria were plated on blood agar plates with a constant Kanamycin concentration of 50 µg/ml and different Spectinomycin concentrations (0, 20, 50, 100 µg/ml) for the transformed gene deletion mutant. Positive clones were confirmed by colony PCR (Primers 8835 and 8836, see Appendix II).

4.13 Characterization of Msp22

4.13.1 Cloning of *msp22* for expression in *M. catarrhalis*

Mini prep DNA of pEMCJH04-KAN-Msp22 was used as template DNA for PCR. Primers 8825 and 8860 (primer containing 6xHIS-tag) were used for amplification (see Appendix II). The fragment was *Bam*HI/*Pst*I digested and ligated with *Bam*HI/PstI digested pEMCJH04-KAN. Transformation of the ligation into competent *M. catarrhalis* wild type cells was performed as described in section 4.12.3. Transformed cells were plated on blood agar containing 50 µg/ml Kanamycin. Clones were analyzed by colony PCR using primers 8835 and 8836.

4.13.2 Purification of Msp22 from *M. catarrhalis*

M. catarrhalis wild type cells (negative control) and *M. catarrhalis* containing pEMCJH04-KAN-Msp22-HIS were plated on blood agar containing 0 or 50 µg/ml Kanamycin, respectively. 15 ml BHI medium was inoculated with several colonies from the plate and bacteria were grown for 5 hrs (37°C, 180 rpm). The culture was transferred to 150 ml BHI medium and grown overnight. The following day, the cultures were diluted in 1.5 L BHI

medium and grown at 37°C, 180 rpm for 5 hrs (wild type = negative control) or overnight (*M. catarrhalis* containing pEMCJH04-KAN-Msp22-HIS). The cells were harvested by centrifugation and frozen at -20°C until use.

The pellet was thawed and resuspended in Lysis buffer (50 mM Tris/HCl pH8.0, 500 mM NaCl, 0.1% Tx-100) containing protease inhibitor cocktails I and II (see section 9.3 Buffers and media). Sonication on ice was performed 7x2 min (5 x 10% cycle, 100% power). Small scale Western blot analysis of crude lysate, soluble and insoluble fractions was performed to determine the solubility of the protein. After DN*ase* I (100 µg/ml) digest of the large scale culture, the soluble and insoluble fractions were separated by centrifugation (25,000 x g, 30 min). 1 mM DTT was added to the soluble fraction prior to incubation with Ni-Sepharose beads (GE Healthcare) overnight at 4°C, rotating.

The bead – protein suspension was applied to a column. The flow-through was collected, the beads were washed and the protein was eluted with the buffers shown in Table 4-4.

Table 4-4: Purification of HIS-tagged Msp22. Buffers used for washing and eluting Msp22. WØTx, wash buffer without Tx-100; W20, wash buffer containing 20 mM imidazole; W40, wash buffer containing 40 mM imidazole; EA, eluate A; EE, eluate E.

	Fraction	Buffer	Column volumes
1	Flow-through		
2	W0	50 mM Tris/HCl pH8.0, 500 mM NaCl, 0.1% Tx-100, 0.5 mM DTT	15 CV
3	WØTx	50 mM Tris/HCl pH8.0, 500 mM NaCl, 0.5 mM DTT	10 CV
4	W20	50 mM Tris/HCl pH8.0, 500 mM NaCl, 0.5 mM DTT, 20 mM Imidazole	5 CV
5	W40	50 mM Tris/HCl pH8.0, 500 mM NaCl, 0.5 mM DTT, 40 mM Imidazole	5 CV
6	EA	50 mM Tris/HCl pH8.0, 150 mM NaCl, 250 mM Imidazole	3 CV
7	EE	50 mM Tris/HCl pH8.0, 500 mM NaCl, 250 mM Imidazole, 8 M Urea	3 CV

4.13.3 Determination of heme-dependent peroxidase activity

SDS-PAGE was performed as described in section 4.2.1. 5x Lane marker non-reducing sample buffer (Pierce) without DTT was added to the sample (1x final concentration) and the samples were not heat treated. The proteins were subsequently blotted onto a nitrocellulose membrane (iBlot, Invitrogen) and the membrane was washed with 1x PBS and incubated with substrate (SuperSignal West Femto Maximum Sensitivity Substrate Trial Kit, Pierce). For that purpose, Luminol/Enhancer solution and Stable Peroxidase Buffer were mixed at a 1:1 ratio and added to the membrane. Subsequent exposure to a film allowed the detection of proteins with heme-dependent peroxidase activity.

4.14 Generation of NTHI gene deletion mutant *hxuA*Δ

The *hxuA* gene deletion mutant was obtained from Jeroen Langereis, RUNMC (Radboud University Nijmegen Medical Centre). Briefly, NTHI was grown to mid-log phase, harvested and washed with M-IV medium (78) for rendering the cells competent. DNA fragments of ~1500 bp up- and downstream of *hxuA* were amplified by PCR of genomic DNA and the primers listed in Appendix II. Megaprimer PCR with a Spectinomycin resistance cassette was performed prior to transformation into competent NTHI cells and shaking at 37°C for 60 min. Subsequent plating on Spectinomycin-containing BHI^+ plates and incubation overnight at 37°C (5% CO_2) allowed the selection of mutants lacking the *hxuA* gene.

4.15 Protection studies

Mouse experiments for testing the protective effect of recombinant proteins were performed in collaboration with the Karolinska Institutet, Sweden.

4.15.1 Intranasal immunization

Five to seven-week-old female C57/BL6 bom (inbred wild type) mice were kept under specific-pathogen-free conditions. Groups of 10 mice were immunized intranasally with recombinant protein on days 0, 21 and 42. Control groups received either PBS or adjuvant (IC31®) alone. For vaccination, 17.5 µl protein solution was mixed with 2.5 µl IC31® (2000/80), and incubated for 30 min at RT. Adjuvant control mice received 17.5 µl 50 mM Tris/HCl pH8.0, mixed with 2.5 µl IC31®.

4.15.2 Mouse challenge

M. catarrhalis cells were grown to exponential phase, harvested and resuspended in PBS. Mice were inoculated intranasally with 40 µl (20 µl per nostril) live *M. catarrhalis* cells (~$5x10^6$ CFU). For that purpose, mice were held in a head-up vertical position during the procedure and kept in that position for at least ten seconds after the inoculation.

4.15.3 Euthanasia, tissue collection and bacterial culture

Mice were euthanized six hours post-infection. Both lungs were removed, homogenized in 1 ml PBS (+ protease inhibitor, Roche) using cell strainers (100 µm, Becton Dickinson and Company), and used for serial plating in order to quantify CFU in the lung. Independent experiments were compared, and the CFU data were corrected for the infectious dose to $5x10^6$ CFU bacteria and analyzed with nonparametric Kruskal-Wallis tests (173) and Dunn´s post testing.

4.16 Microarray analysis

RNA was isolated as described in section 4.2.6. Gene expression profiles of the *M. catarrhalis* wild type (0 µM Desferal® and 1.25 µM Desferal®) and *msp22* gene deletion mutant (0 µM Desferal® and 1.25 µM Desferal®) were analyzed by Microarray analysis. 4 replicates per culture / culture condition were examined.

4.16.1 NimbleGen 4x72K array design

4x72K arrays for *M. catarrhalis* strain RH4 were designed by Roche NimbleGen. The arrays contained eight probes per target gene and four technical replicates (16312 experimental probes per replicate). Additionally, the arrays contained 7298 random control probes. The average probe length amounted to 59 base pairs.

4.16.2 cDNA synthesis and labeling

First and second strand cDNA synthesis were performed as described in Table 4-5 using SuperScript® One-Cycle cDNA Kit (Invitrogen). Following cDNA synthesis, RN*ase* A cleanup and cDNA precipitation was performed according to the protocol provided by Roche NimbleGen. cDNA quality was analyzed before sample labeling ($A_{260/280}$, $A_{260/230}$, cDNA concentration). Samples were labeled using NimbleGen One-Color DNA Labeling Kit. Cy3-Random nonamers and nuclease-free water were added to 1 µg cDNA (80 µl total volume), as recommended by the manufacturer. After incubation at 98°C for 10 min, cooling on an ice-water mix was done for over 2 min. Klenow mastermix (100 U Klenow fragment 3´ > 5´ exo, dNTP 1 mM final conc., nuclease-free water) was added to a total

volume of 100 µl. The mix was incubated at 37°C for 2 hours, protected from light. 10 µl 0.5 M EDTA and 11.5 µl 5 M NaCl were added (brief vortexing) before transfer to a 1.5 ml tube containing 110 µl isopropanol. After vortexing and 10 min incubation at RT, a pink pellet was obtained by centrifugation and washed with ice-cold 80% EtOH. The pellet was dried and rehydrated.

Table 4-5: First and second strand cDNA synthesis. Reagents from SuperScript® One-Cycle cDNA Kit (Invitrogen) were used. RT, Reverse transcriptase.

Step	First strand synthesis	Step	Second strand synthesis
1	10 µg RNA First strand reaction mix (1x final conc.) 10 mM DTT (final conc.) 1 µl dNTPs (10 mM) 1 µl Random hexamer primers (3 µg/µl) Aqua destillata ad 18 µl	5	Second strand reaction mix (1x final conc.) 3 µl dNTPs (10 mM) 1 µl DNA ligase (10 U/µl) 4 µl DNA polymerase I (10 U/µl) 1 µl RN*ase* H (2 U/µl) 91 µl DEPC water
2	42°C, 2 min	6	Addition to first strand, final volume: 150 µl
3	2 µl SuperScript II RT (200 U/µl) Final volume: 20 µl	7	16°C, 2 hrs
		8	Addition of 2 µl T4 DNA polymerase (5 U/µl)
4	42°C, 60 min	9	16°C, 5 min
		10	Addition of 10 µl EDTA (0.5 M)

4.16.3 Hybridization of labeled cDNA with 4x72K array and array scanning

Prior to hybridization of the cDNA to the microarrays, the hybridization system was set to 42°C. 2 µg cDNA (in 3.3 µl nuclease-free water) were added to 8.7 µl hybridization solution master mix (hybridization buffer, hybridization component A and alignment oligo provided by the manufacturer), incubated at 95°C for 5 min (protected from light) and adjusted to a temperature of 42°C. Mixers were prepared as described in the NimbleGen Array User´s Guide before hybridization to a 4x72K array. Washing of the slides was performed according to manufacturer´s instructions using Wash buffers I, II and III.

The 4x72K arrays were scanned and images were processed using NimbleScan software (RMA algorithm).

4.16.4 Evaluation of Microarray data

Raw probe signal intensities were loaded into ANAIS, a web-based tool for the analysis of NimbleGen expression data (165). Normalization of the data (interarray analysis) and background correction (intraarray analysis) of probe signal intensities was performed. The signal-to-noise threshold value was calculated, and the averages of the technical

replicates (threshold-corrected data) were determined. Values were converted to $\log_2$ scale and all average probe signal intensities were averaged to analyze expression per gene. Paired analysis of bacteria grown in iron-rich (0 μM Desferal®) and iron-depleted (1.25 μM Desferal®) medium was performed for the purpose of identifying genes which are up- or downregulated during iron starvation. A statistical T-test was performed to determine differences in gene expression between the wild type and *msp22* gene deletion mutant (unpaired).

4.16.5 Quantitative RT-PCR

Quantitative RT-PCR (qRT-PCR) was performed using 500 ng RNA, 250 ng random hexamers and 1 μl 10 mM dNTPs (13 μl total volume). 7 μl SuperScript™ III Reverse transcriptase mastermix (200 U SuperScript RT, First-strand buffer, 1 μl 0.1 M DTT and water) were added to a final volume of 20 μl. For testing of efficiency of genomic DNA removal, each RNA sample was also tested without the addition of SuperScript™ III Reverse transcriptase. The mix was incubated at 25°C for 5 min, 50°C for 60 min and 70°C for 5 min. 5 μl of a 1:50 dilution of the samples was pipetted into a 96-well plate with 15 μl PCR mastermix (Fw and Rev primers, PCR mastermix). Primer sequences are listed in Appendix II. Primer binding efficiency was tested using decreasing concentrations (10 ng – 0.001 ng) of *M. catarrhalis* RH4 genomic DNA.

4.17 Primer order and sequencing

Primers were ordered from MWG. All sequencing of all DNA constructs was done by MWG.

5 Results *M. catarrhalis*

5.1 The membrane proteome of *M. catarrhalis* shows overlap with the antigenome

In order to identify novel vaccine candidates, the antigenome technology was used for *M. catarrhalis* and led to the identification of 214 candidate antigens in previous studies. Biotinylated human IgGs from patients and healthy individuals were coupled to magnetic streptavidin beads and used for the screening of *E. coli* surface display libraries expressing all *M. catarrhalis* proteins via FhuA or LamB platforms. Approximately 20 antigens were selected for subsequent testing in animal models and for further evaluation and characterization of their potential as vaccine candidates based on the number of AIP® screen hits and gene distribution data as well as *in vitro* assays. Out of these antigens, six proteins were hypothetical proteins found between two and eight times by AIP®. The identification of antigens using the antigenome approach provided evidence that these proteins are expressed *in vivo* during infection and/or colonization due to the presence of human antibodies.

In parallel to the selection of potential vaccine antigens by the antigenome technology, the membrane proteome of *M. catarrhalis* was determined. This was done for the purpose of supporting the antigenome approach. Membrane preparations including outer membrane vesicles (OMVs) isolated from *M. catarrhalis* cultures grown in iron-depleted and iron-rich medium and whole membrane preparations were isolated from *M. catarrhalis* by the methods described in Materials and methods, and subjected to mass spectrometric analyses (performed by the University of Graz), to identify membrane proteins. 1D gel electrophoresis was followed by proteolytic digest (trypsin) of the proteins, and LC MS/MS as well as 2D nano-HPLC MS/MS was performed. The resulting protein list was mapped with Intercell´s antigenome, and the overlaps were determined (for the complete list see Appendix I). Table 5-1 lists the 23 AIP® antigens selected for further characterization and indicates the overlap with the proteins identified by mass spectrometry of membrane preparations. Additionally, the presence of the respective genes in 47 selected strains as well as the total number of hits obtained in all screens (FhuA and LamB screens using four different IgG pools) are shown. In fact, all of the genes were present in > 90% of all strains.

Table 5-1: Comparison of the *M. catarrhalis* membrane proteome and antigenome. 23 antigens identified by AIP® and selected for further evaluation are listed. ORF, open reading frame; GD, gene distribution (47 strains tested, a list of all strains is represented in section 9.2); Hits, AIP® screen hits. 1 = Proteins identified in the whole membrane preparation; 2 = Proteins identified in OMVs; 3 = Proteins identified in OMVs (iron-depleted growth conditions).

ORF	Protein name	GD	Hits	1	2	3
MCR_0063	Hypothetical protein	47/47	8	x	x	
MCR_0076	TonB-dependent receptor	44/47	13			
MCR_0136	Hypothetical protein	47/47	2			
MCR_0186	Outer membrane lipoprotein LolB	46/47	6	x		
MCR_0196	Lytic murein transglycosylase MltB	47/47	12	x		
MCR_0439	Penicillin-binding protein 1A	47/47	5			
MCR_0560	Hypothetical protein	44/47	5			
MCR_0681	Putative lytic transglycosylase	47/47	7			
MCR_0686	Peptide methionine sulfoxide reductase MsrA/MsrB	47/47	3	x	x	x
MCR_0691	Hypothetical protein	46/47	4	x	x	
MCR_0692	Hypothetical protein	45/47	7	x	x	
MCR_0739	Hemoglobin utilization protein MhuA	46/47	15	x	x	x
MCR_0918	M16-like peptidase	46/47	5	x	x	x
MCR_0996	Hypothetical protein	47/47	3		x	
MCR_1003	LysM domain protein	47/47	9	x		
MCR_1010	D-alanyl-D-alanine carboxypeptidase DacC	47/47	48			
MCR_1228	D15 surface antigen family protein	47/47	4	x		
MCR_1303	Oligopeptide ABC transport system substrate binding protein OppA	47/47	6	x	x	x
MCR_1357	Cytochrome c1 family protein	47/47	22			
MCR_1416	Cytochrome c class II Msp22	47/47	2			
MCR_1690	Extracellular solute-binding protein family 3	44/47	6		x	
MCR_1742	Outer membrane protein	46/47	24			
MCR_1761	OPA-like protein A OlpA	47/47	7	x		

The proteins MsrAB (MCR_0686), a methionine sulfoxide reductase, MhuA (MCR_0739), a hemoglobin utilization protein as well as an M16-like peptidase (MCR_0918) and OppA (MCR_1303), an oligopeptide-binding protein, were detected in all membrane preparations and showed overlap with candidates identified by AIP®. A detailed illustration of the total number of all overlaps is shown in Figure 5-1.

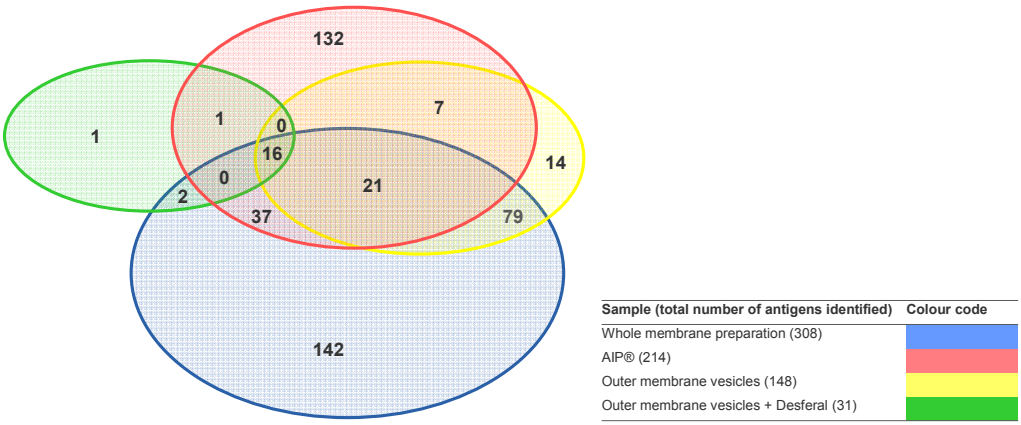

Figure 5-1: *M. catarrhalis* proteins common to antigenome and proteomic analyses. OMV = outer membrane vesicles; AIP® = proteins identified by the antigenome approach. Overlaps not shown in the figure: OMVs/OMVs Desferal®/whole membrane: 11; OMVs,/OMVs Desferal®: 0.

In effect, not all proteins identified by mass spectrometry were predicted to be membrane proteins. Some of the proteins were predicted to have a cytoplasmic localization according to the genome annotation. However, a considerable enrichment of outer membrane proteins could be achieved by this approach, indicating that the methods used for isolating OMVs and whole membranes followed by subsequent mass spectrometry were suitable for determining the membrane proteome of a bacterial species.

In total, 16 proteins were identified independently in each of the three *M. catarrhalis* preparations as well as by the antigenome approach, providing good evidence that these proteins are membrane localized. At least six of these 16 proteins are involved in iron acquisition as shown in Table 5-2 (e.g. lactoferrin- and transferrin-binding proteins).

Table 5-2: 16 common proteins identified by all proteome approaches and AIP®. Iron-regulated proteins are **bold**. ORF, open reading frame.

ORF	Protein name
MCR_0217	**Lactoferrin binding protein B LbpB**
MCR_0219	**Lactoferrin binding protein A LbpA**
MCR_0264	C-terminal processing peptidase-1
MCR_0476	RND system membrane channel OprM
MCR_0492	**Outer membrane protein CopB**
MCR_0546	Outer membrane protein assembly complex protein YaeT
MCR_0686	Peptide methionine sulfoxide reductase MsrA/MsrB
MCR_0690	**Transferrin binding protein A TbpA**
MCR_0694	**Transferrin binding protein B TbpB**
MCR_0739	**Hemoglobin utilization protein MhuA**
MCR_0917	M16-like peptidase
MCR_0918	M16-like peptidase
MCR_1303	Oligopeptide ABC transport system substrate binding protein OppA
MCR_1366	ABC transporter substrate binding protein
MCR_1698	Outer membrane protein CD
MCR_1863	Hypothetical protein

The purpose of the proteomic analyses was to confirm the antigenome approach as a powerful method to identify interesting vaccine candidates and to supplement this approach by potentially identifying additional candidate antigens. Further, the data obtained by the proteomic approach were considered as experimental evidence for the localization of the identified proteins. An important observation of the combined approach was that the data obtained by the antigenome approach in combination with the data generated by mass spectrometric analysis of membrane preparations from cultures grown in the presence of different iron concentrations strongly supported the hypothesis that iron transporters play a crucial role during infection due to the presence of antibodies against the respective proteins.

5.2 *M. catarrhalis* growth is significantly diminished during iron-limiting conditions and can be restored by iron repletion

In order to further evaluate the importance of iron for *M. catarrhalis in vitro* growth, growth experiments were performed using Desferal® to specifically remove iron from the medium. Growth experiments were carried out in both, BHI medium as well as chemically defined medium which contains $FeSO_4$ as the sole iron source, and varying Desferal® concentrations were tested. In BHI medium, a Desferal® concentration of about 30 μM was necessary to affect bacterial growth (data not shown). For the purpose of performing growth experiments in chemically defined medium, the bacteria were initially grown in BHI medium, as direct inoculation of chemically defined medium failed. Subsequently, the bacteria were transferred to chemically defined medium (0.1 mg/L $FeSO_4*7H_2O$) followed by the transfer to Desferal®-containing medium. In order to determine the appropriate concentration of Desferal®, an initial experiment was carried out by adding Desferal® concentrations of 0 μM – 50 μM to the medium. The resulting low concentration of free iron in the medium caused an inhibition of bacterial growth, as expected (4). Whereas the presence of as little as 2 μM Desferal® could inhibit bacterial growth, the addition of 2.5 μM Desferal® essentially abolished bacterial multiplication when *M. catarrhalis* was grown in a chemically defined medium with 0.5 mg/L $FeSO_4*7H_2O$ (Figure 5-2). This observation was not unexpected as the growth in chemically defined medium already represented a stress condition with only limited amounts of nutrients available compared to BHI medium.

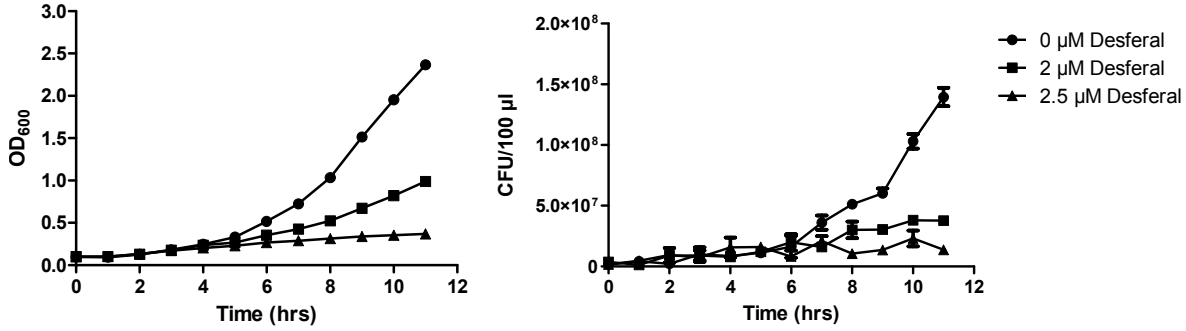

Figure 5-2: Growth inhibition of *M. catarrhalis* by the addition of Desferal®. Growth in the presence of 0.5 mg/L $FeSO_4*7H_2O$ and 0 μM, 2 μM or 2.5 μM Desferal®. A Desferal® concentration of 2 μM reduced growth considerably. 2.5 μM Desferal® completely inhibited bacterial growth in chemically defined medium. OD_{600}, Optical density 600 nm. CFU, colony forming units. CFUs corresponding to the respective OD_{600} are represented in the right graph. CFU counts of 3 plates per culture were used for calculation (standard error of the mean (SEM)).

In a separate experiment, *M. catarrhalis* cultures grown under iron-limiting conditions were resupplemented with $FeSO_4*7H_2O$ after 8 and 12 hours growth in order to rule out possible toxic effects of Desferal®. Bacterial growth could be resumed upon the readdition of iron, indicating that the decrease in bacterial growth was due to iron starvation (Figure 5-3).

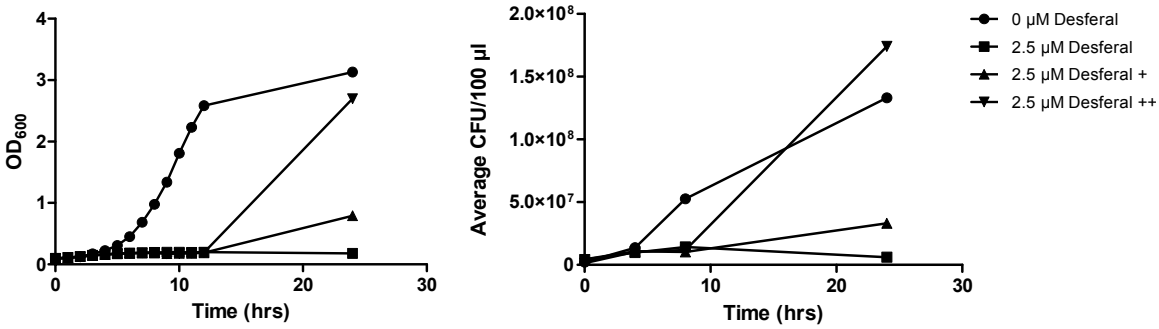

Figure 5-3: Iron repletion of *M. catarrhalis* cultures. Bacteria were grown in chemically defined medium in the presence of 0.5 mg/L $FeSO_4*7H_2O$ and 0 µM or 2.5 µM Desferal®. OD_{600}, Optical density 600 nm. Two cultures grown with 2.5 µM Desferal® were resupplemented with iron. + and ++ indicate the readdition of $FeSO_4*7H_2O$ to the cultures after 8 hours (+, 5 µM; ++, 10 µM) and 12 hours (+, 7 µM; ++, 14 µM). CFUs corresponding to the respective OD_{600} are represented in the right graph.

Excess amounts of $FeSO_4*7H_2O$ were added to cultures grown in iron-depleted medium in order to allow bacterial multiplication and due to the fact that the exact amounts of iron that are chelated by Desferal were not known. CFU counts generally corresponded to OD_{600} measurements. However, whereas OD_{600} measurements were higher for the culture grown without Desferal® compared to the resupplemented culture, CFU counts were lower for the culture grown without Desferal®. This was possibly due to the fact that bacteria grown without Desferal® had already reached stationary phase probably resulting in many dead cells in the medium.

5.3 Outer membrane vesicles isolated from *M. catarrhalis* cultures contain iron-repressible and iron-inducible proteins

OMVs contain outer membrane proteins, periplasmic proteins and other surface structures of bacteria such as LPS. They are formed by many gram-negative bacteria, are involved in host-pathogen interactions and might play an essential role in virulence (48).

They mediate adherence (45), serve as transport vehicles for virulence factors and modify the host immune response such as by stimulating B-cells (96, 186). OMVs were studied for the purpose of analyzing outer membrane proteins involved in pathogenesis. To achieve this, the expression profile of proteins on OMVs that were isolated from *M. catarrhalis* cultures grown under iron-rich (no addition of the iron chelator Desferal®) and iron-depleted conditions, was assessed. Cultures grown in the presence of the iron-chelating agent Desferal® showed a considerable reduction in growth due to the low levels of iron present. Moreover, SDS-PAGE of these preparations revealed that distinct proteins, especially between a molecular weight of 70 and 130 kDa, were overexpressed under iron-limiting conditions using 2 µM Desferal® (Figure 5-4).

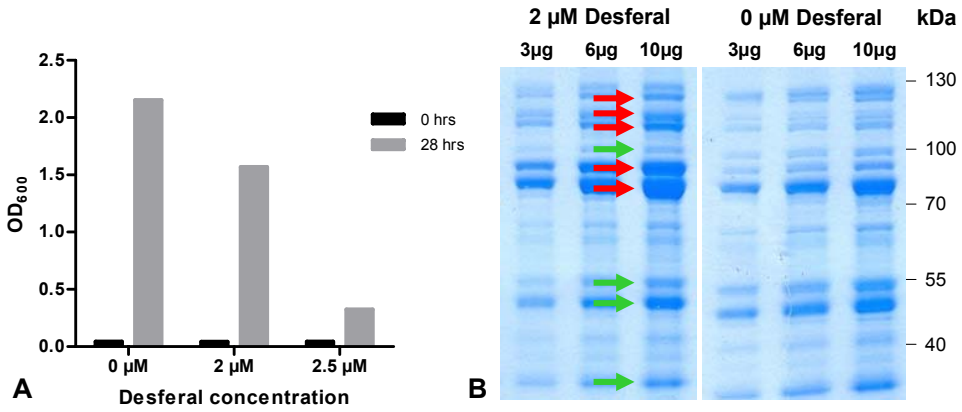

Figure 5-4: Differential expression of iron-inducible and iron-repressible proteins on *M. catarrhalis* OMVs. A: Overnight increase in OD_{600} of cultures grown in the presence (2 µM, 2.5 µM) or absence (0 µM) of Desferal®. **B**: SDS-PAGE (4-12% gel, 200 V, 50 min) of OMVs. OD_{600}, Optical density 600 nm. Red arrows indicate upregulation during iron starvation, green arrows indicate downregulation during iron limitation. OMV preparations were normalized and equal amounts of protein (as measured by BCA) were loaded.

Due to the low optical density obtained when *M. catarrhalis* was grown in the presence of 2.5 µM Desferal®, the protein concentration of the membrane preparation was too low and the preparation obtained from this culture was not further analyzed.

To further examine which proteins were present in the OMVs, mass spectrometry was performed. 148 proteins were identified from OMVs isolated from cultures grown under iron-rich conditions (see Appendix I). In total, 31 proteins were detected in OMVs isolated during iron-limiting conditions (Table 5-3).

Table 5-3: Proteins identified in OMVs isolated from cultures grown in the presence of the iron chelator Desferal®. 31 proteins were identified. Dark grey boxes represent proteins involved in iron metabolism (Fe). Light grey boxes show antigens which have previously been identified as potential vaccine candidates (V) plus the relevant reference. ORF, open reading frame.

ORF	Protein name	Fe	V	Reference
MCR_0078	Hypothetical protein	-	-	
MCR_0079	Hypothetical protein	-	-	
MCR_0135	Nitrite reductase AniA/Msp78	-	+	(151)
MCR_0217	Lactoferrin binding protein B LbpB	+	+	(111)
MCR_0219	Lactoferrin binding protein A LbpA	+	-	
MCR_0228	Translation elongation factor G	-	-	
MCR_0264	C-terminal processing peptidase-1	-	-	
MCR_0295	Iron (III) ABC transporter iron binding protein FbpA	+	-	
MCR_0419	Moraxella catarrhalis adherence protein McaP	-	+	(104)
MCR_0476	RND system membrane channel OprM	-	-	
MCR_0492	Outer membrane protein CopB	+	+	(76, 77)
MCR_0546	Outer membrane protein assembly complex protein YaeT	-	-	
MCR_0686	Peptide methionine sulfoxide reductase MsrA/MsrB	-	-	
MCR_0690	Transferrin binding protein A TbpA	+	+	(111)
MCR_0694	Transferrin binding protein B TbpB	+	+	(29)
MCR_0739	Hemoglobin utilization protein MhuA	+	+	(60)
MCR_0797	TonB-like protein	+	-	
MCR_0860	ErfK/YbiS/YcfS/YnhG family protein	-	-	
MCR_0917	M16-like peptidase	-	-	
MCR_0918	M16-like peptidase	-	-	
MCR_1053	DNA uptake lipoprotein-like protein	-	-	
MCR_1063	C-terminal processing peptidase	-	-	
MCR_1168	Outer membrane assembly lipoprotein YfgL	-	-	
MCR_1247	Outer membrane porin M35	-	+	(47)
MCR_1303	Oligopeptide ABC transport system substrate binding protein OppA	-	+	(198)
MCR_1366	ABC transporter substrate binding protein	-	-	
MCR_1367	ABC transporter substrate binding protein	-	-	
MCR_1393	Putative lipoprotein	-	-	
MCR_1446	Malate dehydrogenase	-	-	
MCR_1698	Outer membrane protein CD	-	+	(5)
MCR_1863	Hypothetical protein	-	-	

26% of the 31 proteins are involved in iron metabolism, including lactoferrin- and transferrin-binding proteins A and B (Lbp, Tbp), MhuA, CopB and FbpA. Moreover, over 20% of the proteins identified in OMVs isolated during iron limitation have been shown to be potential vaccine candidates. These proteins include CopB, Msp78, TbpB and LbpB (29, 76, 77, 111, 151).

It was assumed that one band on the SDS-gel shown in Figure 5-4 represented more than one single protein. Therefore, the bands representing proteins which appeared to be significantly upregulated during iron depletion were excised and subjected separately to mass spectrometric analysis. Thus, iron-repressible proteins could be analyzed. Table 5-4 represents exclusively outer membrane proteins and proteins with a molecular weight of more than 70 kDa that were isolated from the gel.

Table 5-4: Iron-repressible proteins detected in OMVs isolated from a culture grown in iron-depleted medium. Only cell outer membrane proteins with a molecular weight of > 70 kDa are represented. The figure (right) represents the corresponding Coomassie-stained protein gel. SDS-PAGE: 4-12% gel, 200 V, 50 min. Black arrows indicate the proteins identified from the respective bands. Molecular weights were determined using sequence manipulation suite, version 2 (sequence analysis tool). ORF, open reading frame.

ORF	Protein name	Molecular weight (kDa)
MCR_0217	Lactoferrin binding protein B LbpB	95.9
MCR_0219	Lactoferrin binding protein A LbpA	110.9
MCR_0492	Outer membrane protein CopB	83.1
MCR_0690	Transferrin binding protein A TbpA	119.4
MCR_0694	Transferrin binding protein B TbpB	75.8
MCR_0739	Hemoglobin utilization protein MhuA	106.4

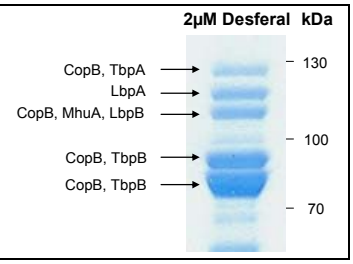

The proteins CopB and TbpB with a molecular weight of approximately 80 kDa or 75 kDa respectively were present in more than one band. Most probably, these proteins were trapped in the gel due to the relatively high protein amount loaded.

These data suggest that a number of proteins are upregulated in response to changing environments. In this case, iron functions as a regulator of gene expression.

5.4 *In vivo* and *in vitro* evaluation of *M. catarrhalis* candidate antigens

5.4.1 Recombinant expression of *M. catarrhalis* proteins in *E. coli*

In total, 12 proteins (Table 5-5) were expressed in *E. coli* for subsequent *in vivo* testing in an animal model and/or the generation of hyperimmune sera in mice for *in vitro* analysis. Figure 5-5 shows a protein gel demonstrating the different fractions of the purification of one soluble *M. catarrhalis* hypothetical protein (MCR_0560).

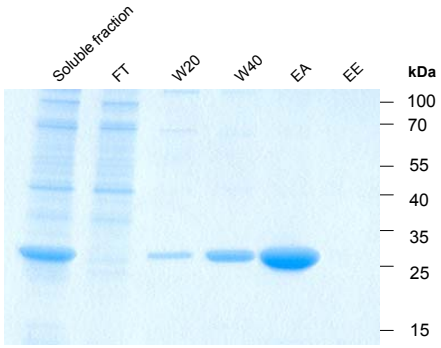

Figure 5-5: Purification of MCR_0560. SDS-PAGE of purification steps. 4-20% gel, Molecular weight: 24.9 kDa (protein fragment). FT, flow-through; W20, wash buffer containing 20 mM imidazole; W40, wash buffer containing 40 mM imidazole; EA, eluate A (protein in Tris/NaCl buffer pH8.0 containing 250 mM imidazole); EE, eluate E (see Materials and methods for details).

All proteins showed LPS values of less than 5000 EU/mg protein. Eight proteins expressed in *E. coli* were soluble, however, four proteins – MCR_0136, MltB (MCR_0196), DacC (MCR_1010) and Msp22 (MCR_1416) could not be purified from the soluble fraction. Thus, inclusion bodies (insoluble fraction after cell lysis) were solubilized in 6 M Guanidine/HCl buffer (MltB, DacC and Msp22) or 8 M urea (MCR_0136), and finally the recombinant proteins were stored in Tris/NaCl buffer containing 100 mM Arginine (MltB, DacC, Msp22) or in PBS (pH7.4) containing 0.2% N-lauroylsarcosine (MCR_0136).

Table 5-5: Recombinant *M. catarrhalis* proteins expressed in *E. coli*. ORF, open reading frame; * proteins were expressed in fragments; *in vivo*, proteins tested in a mouse model; *in vitro*, proteins used for the generation of hyperimmune sera in mice and for *in vitro* assays; Δ, deletion mutants lacking the respective genes were generated; pI, isoelectric point; Cys, number of cysteines in recombinant protein; aa, amino acid; MW, molecular weight; rec, recombinant protein; nat, native protein; S, solubility; sol, soluble; ins, insoluble.

ORF	Protein name (abbreviated)	*in vivo*	*in vitro*	Δ	MW rec.	pI	Cys	aa start-stop	aa rec.	aa nat.	MW nat.	S
MCR_0076*	MCR_0076	+	+	+	15.7	6.03	0	21-160	149	913	102.5	sol
MCR_0136	MCR_0136	-	-	+	28.1	8.95	3	40-278	249	278	31.0	ins
MCR_0196	MltB	+	-	-	50.8	9.1	2	36-485	460	485	53.4	ins
MCR_0560*	MCR_0560	-	-	+	24.9	4.69	0	37-255	229	359	37.6	sol
MCR_0686	MsrAB	+	-	+	60.3	5.88	6	28-558	540	558	62.1	sol
MCR_0739*	MhuA	-	+	+	13.6	6.31	0	47-192	155	961	107.2	sol
MCR_0996	MCR_0996	+	-	+	14.7	5.36	2	27-148	132	148	16.4	sol
MCR_1003*	LysM	+	-	-	39.3	6.59	0	30-375	356	819	87.7	sol
MCR_1010	DacC	+	-	-	41.0	7.29	2	27-386	370	386	42.6	ins
MCR_1303nHIS	OppA	+	+	+	74.1	4.82	0	24-679	669	679	74.8	sol
MCR_1416	Msp22	+	+	+	15.7	5.62	2	21-152	142	152	16.5	ins
MCR_1698	OmpCD	+	-	-	47.0	5.32	2	27-453	436	453	48.3	sol

Some of the proteins were expressed in full-length, other proteins, usually with a high molecular weight, had to be expressed in fragments. For these proteins, distinct domains (e.g. "plug" domain of MCR_0076) were chosen for expression. The signal peptide and lipidation sequences were not included in the constructs because of their high content of hydrophobic amino acids, which hampers protein purification. In the following sections, abbreviated protein names will be utilized (as indicated in Table 5-5). For the corresponding full protein names refer to Table 5-1.

5.4.2 Identification of three protective candidates

It is a major challenge to develop an adequate mouse model for *M. catarrhalis* infection as the bacterium is readily cleared from the murine lung. Therefore, efforts were made in these studies to set up an appropriate mouse model in order to evaluate a set of new

vaccine candidates that were identified by AIP®. In these studies, eight novel selected candidate antigens were tested in a mouse pulmonary clearance model. Figure 5-6 represents the structural domains and immunogenic regions of these proteins.

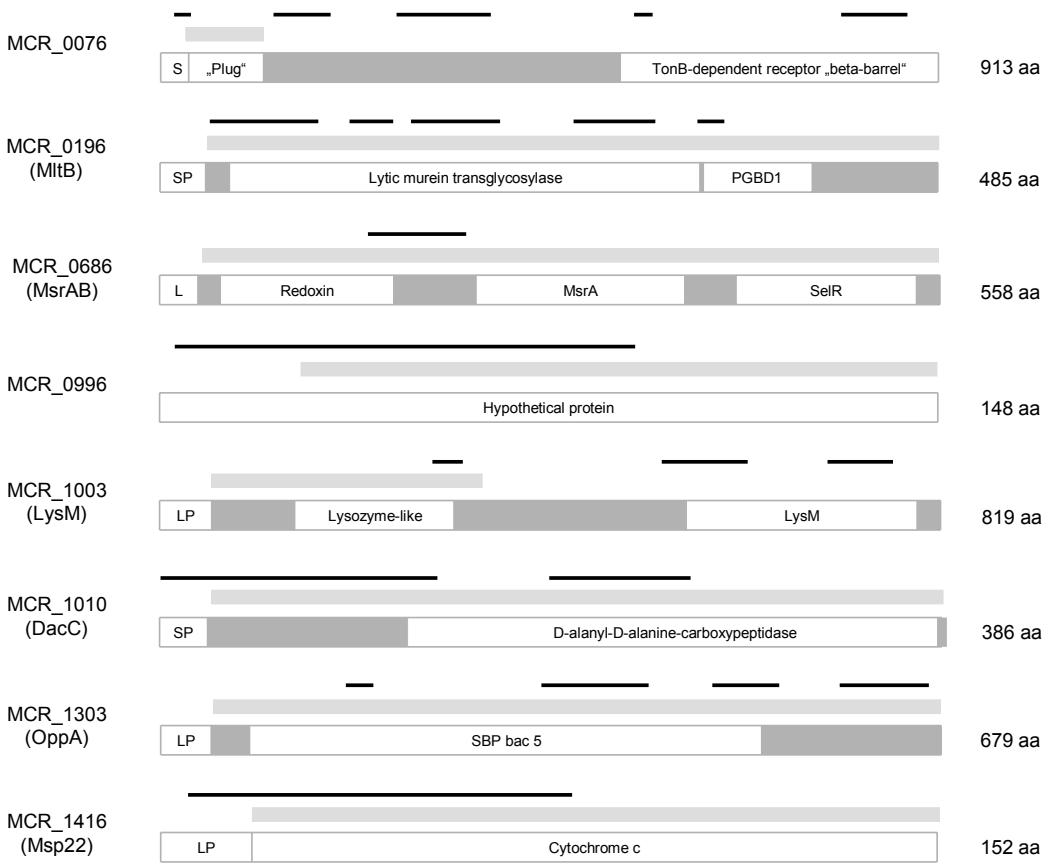

Figure 5-6: Structural features and domains of eight potential *M. catarrhalis* vaccine candidates. MCR_0076, TonB-dependent receptor; MCR_0196, Lytic murein transglycosylase MltB; MCR_0686, peptide methionine sulfoxide reductase MsrAB; MCR_0996, Hypothetical protein; MCR_1003, LysM domain protein; MCR_1010, D-alanyl-D-alanine carboxypeptidase; MCR_1303, Oligopeptide ABC transport system substrate binding protein; MCR_1416, Cytochrome c class II Msp22. S(P), Signal peptide; L(P), Lipidation site; PGBD1, Peptidoglycan binding-like domain; MsrA, Methionine sulfoxide reductase A; SelR, Selenoprotein R; LysM, Lysine motif; SBP bac 5, Bacterial extracellular solute-binding protein family 5. Light grey bars represent recombinant proteins (fragments). Thin black bars demonstrate epitope regions covered by clones selected by the antigenome technology with human IgGs.

MCR_0076 shows homology with TonB-dependent receptors and contains an N-terminal "plug" domain which was expressed recombinantly (MCR_0076) and used for the vaccination studies. Moreover, MCR_0076 was predicted to be involved in iron metabolism. For LysM (MCR_1003), the lysozyme-like domain was utilized for immunization. MCR_0996 is a hypothetical protein to which no function has been attributed so far. It was selected three times by AIP® and was also detected in OMVs,

indicating that this protein might be localized in the membrane. For MltB (MCR_0196), MsrAB (MCR_0686), DacC (MCR_1010), OppA (MCR_1303) as well as Msp22 (MCR_1416), the full-length proteins were expressed, only lacking the lipidation sites or signal peptide sequences. OppA, an oligopeptide-binding protein with a "solute-binding-protein" domain may exhibit diverse functions. This protein was expressed with an N-terminal HIS-tag compared to all other proteins which were expressed with C-terminal HIS-tags. The proteins chosen for immunization were thus predicted to play various different roles in metabolism.

In order to test if immunization with purified recombinant proteins enhances pulmonary clearance of *M. catarrhalis*, mice were immunized three times intranasally with recombinant protein and subsequently challenged with live *M. catarrhalis* cells three weeks after the final vaccination. Six hours post infection the mice were sacrificed and lung CFU counts were determined.

Groups of mice that were immunized with recombinant proteins MCR_0076, OppA and Msp22 showed an increased clearance of bacteria from lungs compared to the negative control (PBS), but also to the positive control protein OmpCD (MCR_1698). The effect was significant for Msp22 with one log reduced bacterial recovery compared to the mice immunized with adjuvant alone (IC31®) ($p<0.01$). For OppA and MCR_0076, there was also a significant reduction ($p<0.05$) compared to IC31® alone. However, sterile lung cultures were neglected in these analyses as they seemed to be a technical artefact and also appeared in the PBS groups (Figure 5-7).

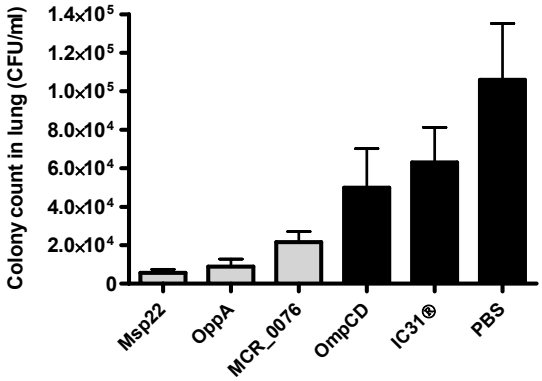

Figure 5-7: Identification of three protective *M. catarrhalis* candidates. Immunization with recombinant proteins MCR_0076 (TonB-dependent receptor, "plug" domain), Msp22 and OppA lead to enhanced bacterial clearance upon challenge with *M. catarrhalis*. Groups of ten mice were immunized intranasally on days 0, 21 and 42. Intranasal challenge with ~$5x10^6$ live *M. catarrhalis* was performed three weeks after the last immunization. Mean CFU values of the combined and normalized results from two to six experiments are represented. The standard error of the mean is shown. IC31®, Intercell´s adjuvant. OmpCD, positive control protein.

Immunization with IC31® (adjuvant control) alone also showed a reduction in CFU counts in the lung. However, this was not surprising as adjuvants are known to stimulate immune responses.

In summary, mice clear *M. catarrhalis* infection very quickly. However, immunization with three novel vaccine candidates (Msp22, OppA and MCR_0076) significantly increased bacterial clearance from the mouse lung after infection with *M. catarrhalis*, suggesting that these candidates are promising vaccine antigens. For that reason, these antigens were further evaluated by *in vitro* analysis.

5.4.3 *In vitro* expression of *M. catarrhalis* candidate antigens

In this section, the *in vitro* expression of selected *M. catarrhalis* antigens is examined. In order to study the vaccine antigens in *in vitro* assays, hyperimmune sera were generated against the respective recombinant proteins. Pre- and hyperimmune sera were analyzed by ELISA to determine antibody titers (data not shown). All hyperimmune sera showed high antibody titers (when incubated with 50 ng recombinant protein), whereas preimmune sera did not (incubation with 500 ng bacterial lysate).

In order to examine whether hyperimmune sera raised against recombinant protein react with the recombinant proteins and the respective native protein in *M. catarrhalis* lysate, Western blot analyses were performed. Figure 5-8 represents the analysis for four selected proteins, the three protective candidates Msp22, OppA and MCR_0076 as well as MhuA, due to its involvement in iron metabolism.

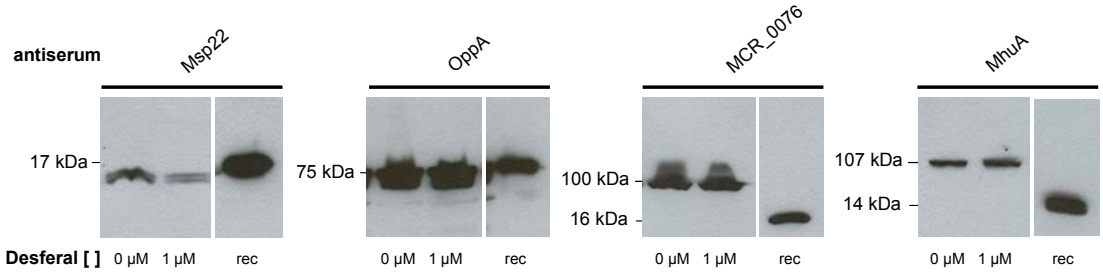

Figure 5-8: *In vitro* expression of selected *M. catarrhalis* proteins. Recombinant MCR_0076 and MhuA were expressed in fragments, therefore the signal of the recombinant protein is visible at a lower molecular weight compared to the wild type protein in the bacterial lysate (MCR_0076, 15.7 kDa; MhuA fragment, 13.6 kDa). Rec, recombinant protein (100 ng). First two lanes each: 25 µg lysate of cultures grown in iron-rich (0 µM Desferal®) and iron-depleted medium (1 µM Desferal®). Msp22, MCR_1416; OppA, MCR_1303; MCR_0076, TonB-dependent receptor; MhuA, MCR_0739.

Lysates were prepared from bacteria grown under iron-rich conditions. In order to test whether the expression of these proteins is regulated by iron, lysates from bacteria grown in iron-depleted medium (1 μM Desferal®) were analyzed in parallel.

Hyperimmune sera did recognize the recombinant protein as well as the native protein in bacterial lysate at the expected size. The two proteins involved in iron transport were expressed as fragments and thus the recombinant proteins showed a lower molecular weight than the respective native proteins (MCR_0076, 15.7 kDa; MhuA fragment, 13.6 kDa). Moreover, the differences in expression of the four proteins Msp22, OppA, MCR_0076 and MhuA between cultures grown under iron-limiting conditions (1 μM Desferal®) and cultures grown under iron-rich conditions (no Desferal®) were compared. Bacteria grown under iron-depleted conditions did not show up- or downregulation of the four tested proteins. This observation was surprising for MhuA as well as the TonB-dependent receptor – two proteins which are predicted to be involved in iron metabolism.

5.5 Characterization of *M. catarrhalis* gene deletion mutants

5.5.1 Generation and confirmation of gene deletion mutants in *M. catarrhalis*

M. catarrhalis gene deletion mutants were generated for the purpose of examining the essentiality of selected genes for bacterial survival as well as involvement in virulence. Table 5-6 lists the eight genes which were successfully deleted in *M. catarrhalis*. The generation of *M. catarrhalis* gene deletion mutants was done in parallel to the protection studies, therefore, gene deletion mutants were not only generated in MCR_0076, *msp22* and *oppA* (the protective candidates), but also additional candidate antigens were chosen. Three of the genes that were deleted encode hypothetical proteins (MCR_0136, MCR_0560 and MCR_0996), two code for proteins involved in iron metabolism, a TonB-dependent receptor (MCR_0076), and MhuA, a hemoglobin utilization protein (MCR_0739). Additionally, the essentiality of the three genes *msp22*, *oppA* and *msrAB* which play diverse roles in metabolism were examined with regard to survival.

Table 5-6: Eight *M. catarrhalis* genes selected for the generation of gene deletion mutants. ORF, open reading frame. The genome location refers to the annotated genome sequence of *M. catarrhalis* strain RH4 (40).

ORF	Protein name	Genome location
MCR_0076	TonB-dependent receptor	85410-88151
MCR_0136	Hypothetical protein	151016-151852
MCR_0560	Hypothetical protein	576162-577229
MCR_0686	Peptide methionine sulfoxide reductase MsrAB	691816-693492
MCR_0739	Hemoglobin utilization protein MhuA	745210-748074
MCR_0996	Hypothetical protein	994910-995350
MCR_1303	Oligopeptide ABC transport system substrate binding protein OppA	1298180-1300219
MCR_1416	Cytochrome c class II Msp22	1409310-1409768

The steps that were required for the generation of gene deletion mutants in *M. catarrhalis* are represented for the *msp22* gene and apply to all other seven candidates as well (Figure 5-9). Homologous recombination of the megaprimer PCR product (flanking regions of the gene to be deleted ligated with a Spectinomycin resistance cassette) with the genomic DNA resulted in Spectinomycin-resistant clones lacking the respective gene.

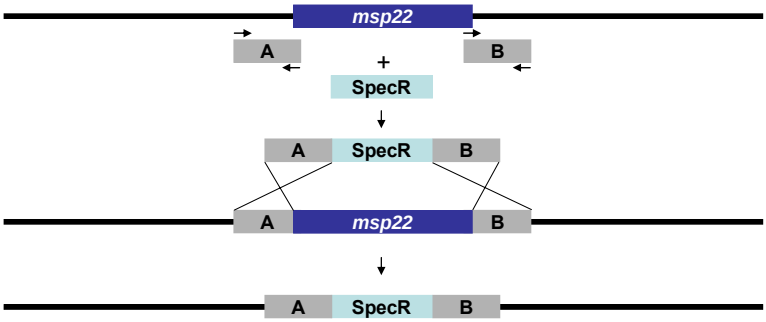

Figure 5-9: Generation of the *M. catarrhalis msp22* gene-deletion mutant. Approximately 500 bp regions up- and downstream of the gene to be deleted were PCR amplified from *M. catarrhalis* strain RH4 genomic DNA. These flanking regions were fused by overlap-extension PCR with a Spectinomycin resistance cassette (amplified from pR412T7). *M. catarrhalis* strain RH4 was transformed with these PCR products as described in Materials and methods and plated on selective medium (Spectinomycin). Clones were tested by colony PCR.

The verification of the gene deletions was initially done by colony PCR of Spectinomycin-resistant clones. In total, four primer pairs per gene were selected for the confirmation of the gene deletions. PCR with a primer (primer A) located within the Spectinomycin resistance cassette resulted in the lack of a PCR product for the wild type, whereas PCR with a gene-specific primer (primer C) did not give a product for the gene deletion mutant. As can be seen in Figure 5-10, both clones for the *msp22* gene deletion mutant contained the required deletion, and the expected fragment sizes were obtained in the wild type bacteria as well as in the gene deletion mutant.

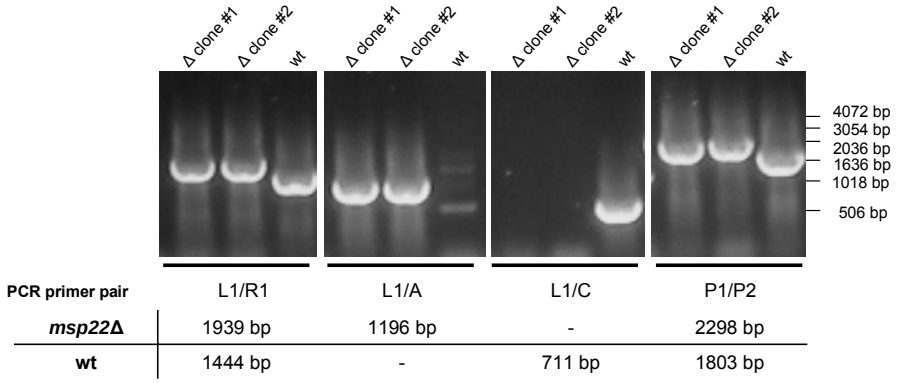

Figure 5-10: Confirmation of *M. catarrhalis msp22* gene deletion mutant by colony PCR. A: Primers L1/R1, B: Primers L1/C, C: Primers L1/A, D: Primers P1/P2 (see Appendix II for primer sequences); wt, wild type; *msp22*Δ, *msp22* gene deletion mutant; Δ clone #1 and #2, two *msp22*Δ clones; Primer C is gene-specific, primer A is specific for the Spectinomycin resistance cassette. Expected fragment sizes are shown above. 0.8% agarose gel; 120 V; 30 min.

As an additional control, Western blot analysis using bacterial lysate of the wild type and the gene deletion mutant was performed in order to verify the absence of expression of the deleted genes at protein level. This is shown for four candidates in Figure 5-11 (remaining four candidates not shown).

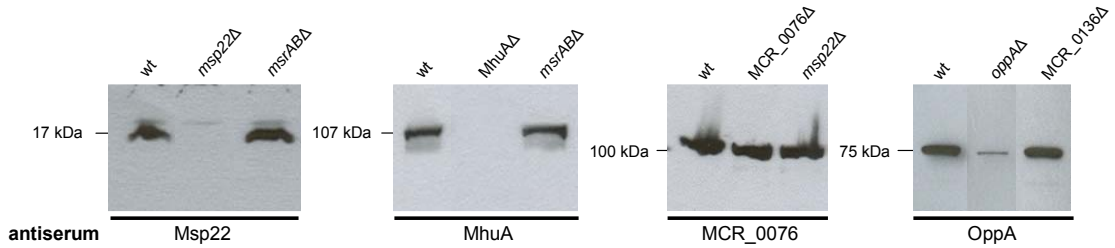

Figure 5-11: Confirmation of gene deletion mutants at protein level. Western blot analysis of 4 proteins is shown. wt, wild type; antiserum, hyperimmune serum against the respective recombinant protein. Bacterial lysates of the *msp22*Δ, *mhuA*Δ, MCR_0076Δ and *oppA*Δ were analyzed. The wt, *msrAB*Δ and MCR_0136Δ served as controls. An unexpected signal was observed in the MCR_0076 gene deletion mutant. A weak signal was present in the *oppA* gene deletion mutant.

The deletion of the eight genes was successful according to PCR and sequence analysis. Western blot analysis confirmed the lack of protein expression for six of the eight candidates, however, the immunoblot showed controversial results for two genes, namely MCR_0076 and *oppA*. Antibodies raised against the recombinant proteins MCR_0076 and OppA reacted with bacterial lysates of the respective gene deletion mutants. Therefore, *M. catarrhalis* gene deletion mutants that showed a signal in Western

blot as well as the *msp22* knock-out (all candidates which showed protection in the mouse pulmonary clearance model) were further validated by Southern blot analysis using probes for the Spectinomycin resistance cassette as well as for the respective deleted genes (Figure 5-12). For the remaining five gene deletion mutants, PCR, sequence analysis as well as Western blot was considered sufficient for the confirmation of the lacking genes.

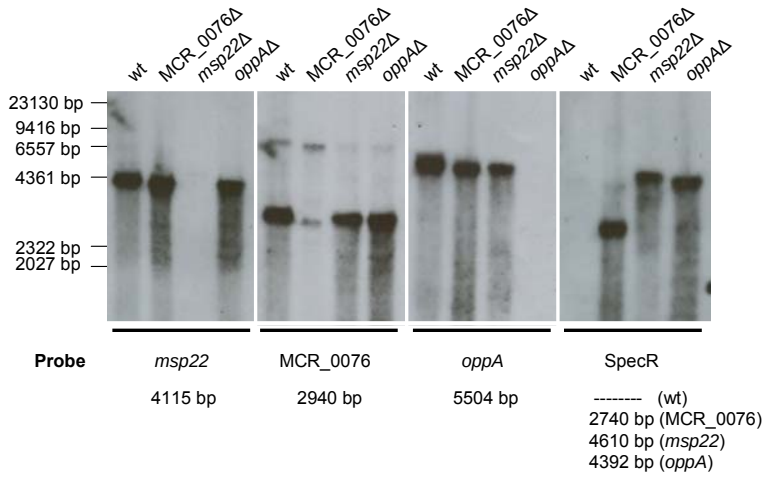

Figure 5-12: Confirmation of gene deletion mutants by Southern blot analysis. SpecR, Spectinomycin resistance cassette. DIG-labeled probes against *msp22*, MCR_0076, *oppA* and the Spectinomycin resistance cassette were used. Expected fragment sizes are indicated. Probe lengths: 368 bp (*msp22*), 832 bp (MCR_0076), 749 bp (*oppA*) and 503 bp (SpecR). The probe for MCR_0076 weakly reacted with DNA from the MCR_0076 gene deletion mutant.

Southern blot analysis confirmed the deletion of *oppA* and *msp22*. However, a weak band could still be observed in the MCR_0076 gene deletion mutant using a probe specific for this gene. Possibly, the probe for MCR_0076 crossreacted with a homologous gene of *M. catarrhalis*.

In summary, all eight genes were successfully replaced by a Spectinomycin resistance cassette as confirmed by PCR, sequencing and Western blot. For three candidates, Southern blot was performed as a confirmatory method in order to verify the gene deletions at DNA level.

5.5.2 *M. catarrhalis* gene deletion mutants do not show increased sensitivity to selected antibiotics

It has frequently been published that there is a rise in antibiotic resistance among *M. catarrhalis* strains (21, 38). In order to examine whether *M. catarrhalis* wild type RH4 strain and the 8 gene deletion mutants are resistant to selected antibiotics, these strains were tested for growth inhibition using different antibiotic discs: Vancomycin, Rifampin, Penicillin, Kanamycin and Colistin. Table 5-7 represents the inhibition zones in mm around the antibiotic discs for all candidates.

Table 5-7: Antibiotic sensitivity of *M. catarrhalis* wild type and eight gene deletion mutants. The radius of the inhibition zone is represented in mm. A volume of bacteria corresponding to 100 µl of an OD_{600} = 2 was plated on blood agar. Antibiotic discs were placed on the plate prior to incubation overnight at 37°C. *M. catarrhalis* was resistant to Vancomycin and Penicillin, slightly sensitive to Colistin, and sensitive to Rifampin and Kanamycin.

Strain	Vancomycin	Rifampin	Penicillin	Kanamycin	Colistin
wild type	0	11	0	12	4
***msp22*Δ**	0	10	0	10	4
***mhuA*Δ**	0	11	0	12	3
***msrAB*Δ**	0	10	0	11	3
oppAΔ	0	8	0	9	3
MCR_0136Δ	0	10	0	10	3
MCR_0076Δ	0	11	0	13	4
MCR_0996Δ	0	10	0	12	3
MCR_0560Δ	0	11	0	12	3

In summary, wild type *M. catarrhalis* was resistant to Vancomycin and Penicillin. Minor differences of the inhibition zones caused by Kanamycin could be observed, the inhibition zones ranging from 9 mm (*oppA* gene deletion mutant) to 12 mm (wild type and *mhuA*, MCR_0996 and MCR_0560 gene deletion mutants). Moreover, the *oppA* gene deletion mutant seemed to be slightly more resistant to Rifampin (8 mm inhibition zone) compared to the wild type and seven other gene deletion mutants (10 – 11 mm inhibition zone).

5.5.3 *M. catarrhalis* gene deletion mutants are not deficient in growth

To examine possible differences in fitness between the wild type and the gene deletion mutants, *M. catarrhalis* was grown in two different media, BHI broth and a chemically defined medium. When grown in the iron-rich BHI medium, no differences in the growth rate between the wild type and all eight gene deletion mutants could be observed. Similar observations were made when the bacteria were cultivated in chemically defined

medium with 0.5 mg/L $FeSO_4*7H_2O$. Figure 5-13 represents growth experiments performed with four out of eight gene deletion mutants in chemically defined medium. Similar observations were made in the remaining four gene deletion mutants *msp22*Δ, MCR_0076Δ, *msrAB*Δ and *mhuA*Δ (data not shown).

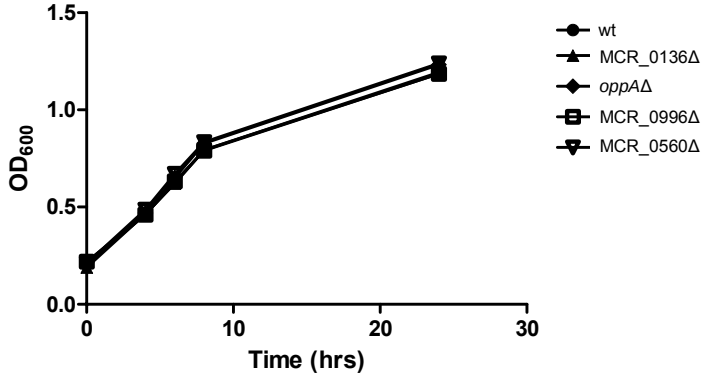

Figure 5-13: Growth of *M. catarrhalis* RH4 wild type and four gene deletion mutants in chemically defined medium. The 4 gene deletion mutants represented in the graph were not deficient in growth compared to the wild type. Growth in the presence of 0.5 mg/L $FeSO_4*7H_2O$ in chemically defined medium. OD_{600}, Optical density 600 nm.

In summary, the eight genes selected for the generation of *M. catarrhalis* gene deletion mutants did not appear essential for bacterial survival. Even in a chemically defined medium which itself represents a stressful condition for the bacteria, the gene deletion mutants did not show any deficiencies in growth compared to the wild type. However, even though these genes are not essential for survival, these observations do not indicate that these genes are not involved in virulence or pathogenesis.

5.5.4 The *msp22* gene deletion mutant shows increased sensitivity to low iron concentrations

The eight *M. catarrhalis* gene deletion mutants did not show a reduction in multiplication rate in BHI medium as well as in chemically defined medium. As it was earlier shown that Desferal® reduced bacterial growth by the specific elimination of iron from the medium (section 5.2) and since some of the deleted genes were suspected to be involved in iron metabolism, growth of *M. catarrhalis* wild type RH4 strain and all eight gene deletion mutants was analyzed under iron-limiting conditions using the chelating agent Desferal®. Seven gene deletion mutants were not negatively affected by the lower iron

concentration compared to the wild type. However, the *msp22* gene deletion mutant showed an elevated sensitivity to iron starvation (Figure 5-14).

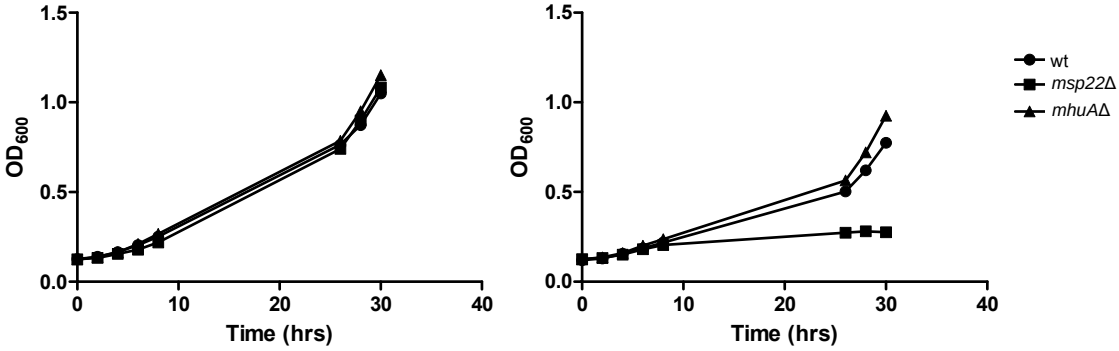

Figure 5-14: Sensitivity of the *msp22* gene deletion mutant to iron limitation. Left: 0 μM Desferal®; Right: 2 μM Desferal®. Bacteria were grown in chemically defined medium (0.5 mg/L $FeSO_4*7H_2O$). The *msp22* gene deletion mutant was more sensitive to iron-limiting conditions (2 μM Desferal®) compared to the wild type and the *mhuA* gene deletion mutant (internal control). OD_{600}, Optical density 600 nm.

These results indicated, that the *msp22* gene deletion mutant exhibited reduced fitness to augmented stress conditions, in this case a low iron concentration. Whether these observations mean that Msp22 is directly involved in iron transport remains unclear. This protein may also be indirectly involved in iron metabolism or it may require iron to fulfill its function.

5.5.5 The *msp22* gene deletion mutant does not show increased autoagglutination

The ability of *M. catarrhalis* to autoagglutinate is commonly known (135, 185), however, the degree of clumping is different from strain to strain (97). The *msp22* gene deletion mutant was shown to be more dependent on free iron than the other gene deletion mutants and wild type *M. catarrhalis*. In this experiment only the *msp22* gene deletion mutant was analyzed and compared to the wild type in order to exclude the possibility that the reduction in growth rate of this mutant was due to increased autoagglutination. Microscopy of overnight cultures was performed as shown in Figure 5-15.

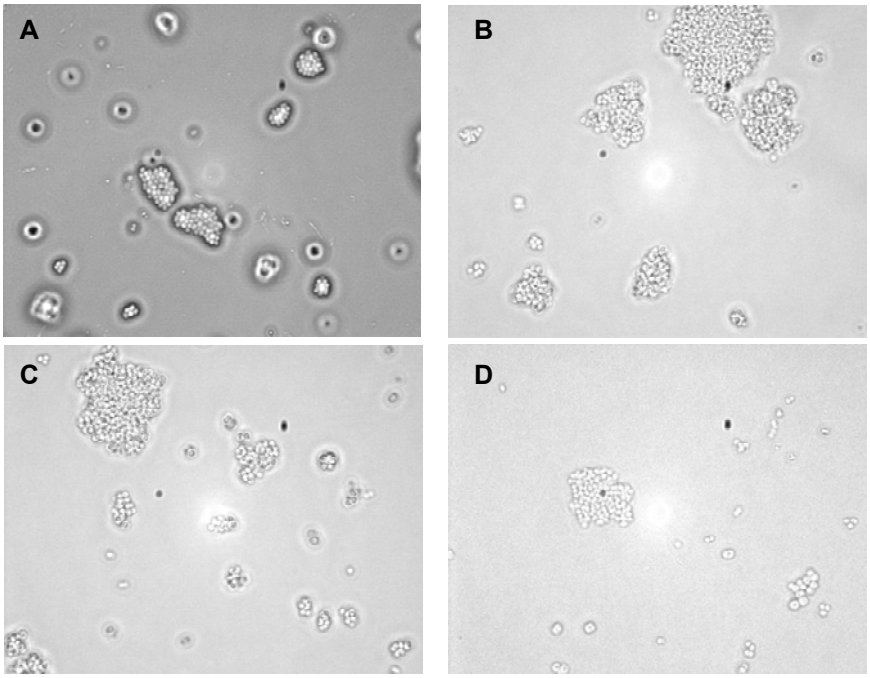

Figure 5-15: Autoagglutination of *M. catarrhalis* RH4 wild type and *msp22* gene deletion mutant. A) wild type *M. catarrhalis* RH4, 0 μM Desferal®; B) wild type *M. catarrhalis* RH4, 2.5 μM Desferal®; C) *msp22* gene deletion mutant, 0 μM Desferal®; D) *msp22* gene deletion mutant, 2.5 μM Desferal®. Cultures were grown in chemically defined medium in the presence of 0.5 mg/L $FeSO_4*7H_2O$ and analyzed with Axioskop 2 plus (Zeiss, Germany) after 24 hrs growth (100x magnification).

M. catarrhalis strain RH4 exhibited medium autoagglutination and microscopy did not reveal a significant difference in clumping between the wild type and the *msp22* gene deletion mutant. Moreover, the addition of Desferal® to the medium did not influence autoagglutination. Thus, the growth deficiency of the *msp22* gene deletion mutant in chemically defined medium with Desferal® could not be attributed to elevated autoagglutination of the respective gene deletion mutant.

5.5.6 Complementation of the *msp22* gene deletion mutant

In order to demonstrate that the *msp22* mutant phenotype was due only to the deletion of *msp22* and can be restored, a potential complementation plasmid containing a gene conferring Kanamycin resistance (pEMCJH04-KAN) derived from *M. catarrhalis* (72) was used. As this plasmid does not contain a universal *M. catarrhalis* promoter, the *msp22* gene was amplified from genomic DNA including a 213 bp region upstream. This upstream region contained 8 potential promoters which were predicted using an online tool for the prediction of prokaryotic promoters (www.fruitfly.org). The gene was cloned

into the plasmid using restriction enzymes *Bam*HI/*Pst*I and transformed into *M. catarrhalis* wild type and *msp22* gene deletion mutant cells. Kanamycin/Spectinomycin (gene deletion mutant) or Kanamycin (wild type) resistant clones were selected and grown in BHI medium. In order to test whether Msp22 is expressed in the complemented strains, bacterial lysates were prepared and Western blot analysis using hyperimmune serum against Msp22 was performed (Figure 5-16).

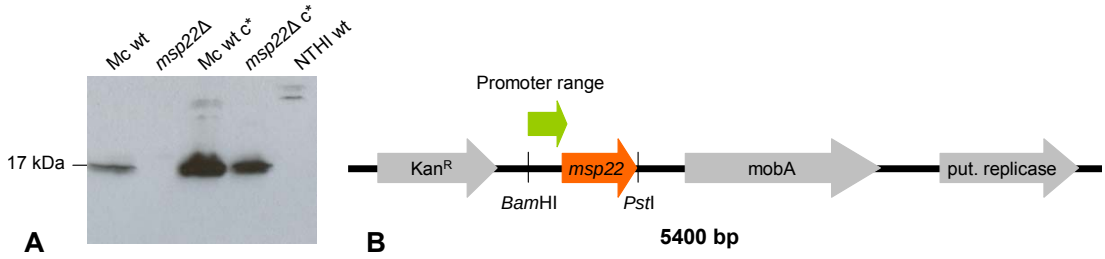

Figure 5-16: Expression of Msp22 in complemented *M. catarrhalis* strains (A). Mc wt, wild type RH4; *msp22*Δ, *msp22* gene deletion mutant; Mc wt c*, wild type RH4 transformed with pEMCJH04-KAN-Msp22; *msp22*Δ c*, *msp22* gene deletion mutant transformed with pEMCJH04-KAN-Msp22; NTHI wt, nontypeable *H. influenzae* wild type strain 86-028NP (negative control). B: schematic drawing of linearized complementation plasmid. Grey arrows represent genes present on the vector. The orange arrow demonstrates the *msp22* gene with its promoter sequence (promoter range: green) that was inserted in the vector using restriction sites *Bam*HI and *Pst*I.

M. catarrhalis (wild type and *msp22* gene deletion mutant) transformed with pEMCJH04-KAN-Msp22 showed overexpression of Msp22 compared to the wild type strain.

In order to verify that the increased sensitivity of the *msp22* gene deletion mutant to iron starvation is due to the absence of *msp22* expression, growth experiments were carried out. An initial experiment revealed that bacteria transformed with the plasmid did not grow in chemically defined medium. Therefore, I switched to BHI medium. However, an extended lag-phase was observed for all cultures carrying the plasmid with or without the *msp22* gene as can be seen in Figure 5-17.

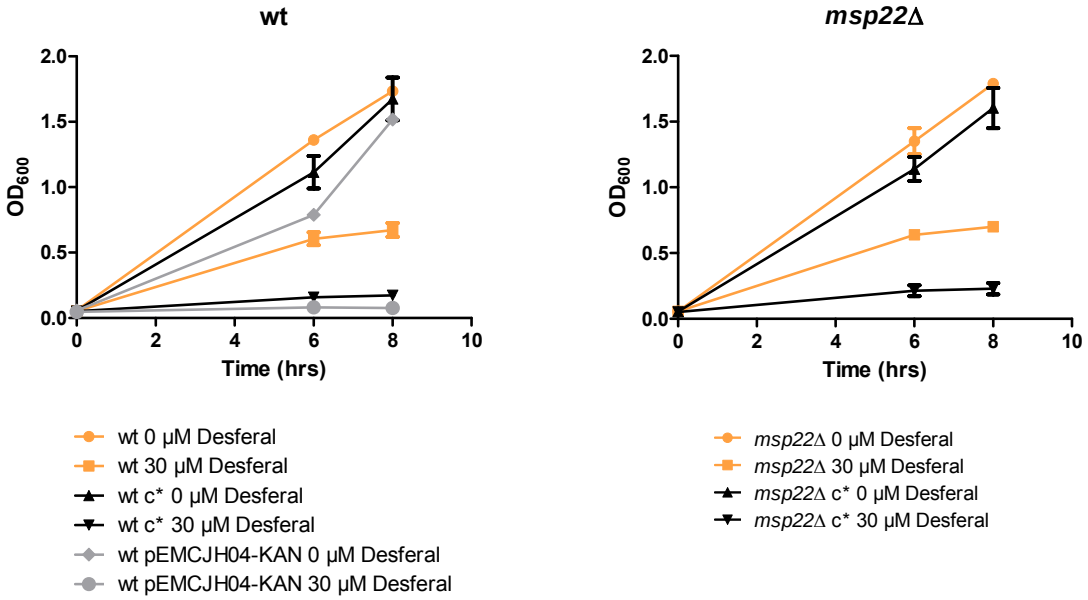

Figure 5-17: Transformation of *M. catarrhalis* with pEMCJH04-KAN or pEMCJH04-KAN-Msp22 leads to growth inhibition. Bacteria transformed with plasmid pEMCJH04-KAN or pEMCJH04-KAN-Msp22 showed an extended lag-phase. Two independent experiments are represented (wild type and *msp22* gene deletion mutant, orange and black curves). One experiment using empty vector transformed into wild type as negative control was performed (grey curves). OD_{600}, Optical density 600 nm.

The fact that also transformation of *M. catarrhalis* with empty vector pEMCJH04-KAN alone resulted in a prolonged lag-phase indicated that it was the vector itself rather than the recombinant *msp22* gene that led to this phenomenon. However, this represented an obstacle for complementation studies. Without the addition of Desferal®, transformed bacteria reached a comparable growth rate after the extended lag-phase. However, *M. catarrhalis* containing the plasmid pEMCJH04-KAN or pEMCJH04-KAN-Msp22 were completely inhibited in growth in the presence of Desferal® compared to non-transformed bacteria. Therefore, it was tested whether strains transformed with complementation plasmid pEMCJH04-KAN-Msp22 show a difference in autoagglutination compared to non-transformed strains in order to examine a possible effect of the plasmid on autoagglutination (Figure 5-18). No significant difference in clumping between transformed and non-transformed bacteria was observed.

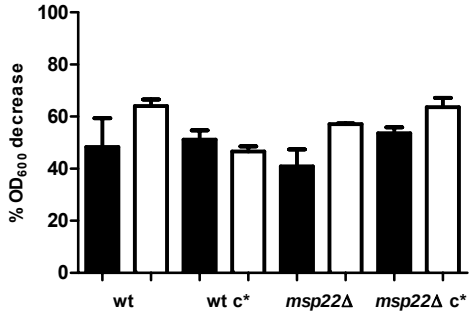

Figure 5-18: *M. catarrhalis* transformed with pEMCJH04-KAN-Msp22 does not show enhanced autoagglutination compared to non-transformed bacteria. OD_{600}, Optical density 600 nm. wt, wild type RH4; *msp22*Δ, *msp22* gene deletion mutant; wt c*, wild type RH4 transformed with pEMCJH04-KAN-Msp22; *msp22*Δ c*, *msp22* gene deletion mutant transformed with pEMCJH04-KAN-Msp22. SEM (standard error of the mean) of two independent experiments is shown. Black columns, 0 µM Desferal®; white columns, 30 µM Desferal®; % OD_{600} decrease, % decrease in OD_{600} overnight (start OD_{600} from log-phase cultures).

An alternative option for *M. catarrhalis* complementation would be the reintroduction of the deleted gene into the *M. catarrhalis* genome at a different locus which is known to fulfill no function. Due to the availability of the complete genome sequence of *M. catarrhalis* RH4 (40), this complementation approach would be a suitable alternative, but was not possible during this work.

5.6 Characterization of *Moraxella* surface protein 22 (Msp22)

5.6.1 Recombinant Msp22 can be purified from its host *M. catarrhalis*

The experiments described in the previous chapter analyzed the effect of the *msp22* and other gene deletions on *M. catarrhalis* growth and fitness. In order to be able to attribute a function to Msp22, *in vitro* experiments were performed with this protein. Figure 5-19 demonstrates the structural features of the full-length protein.

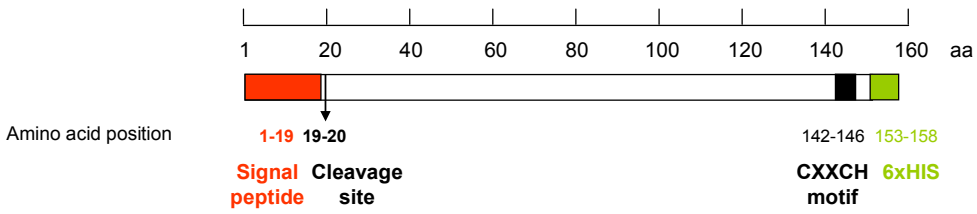

Figure 5-19: Structural features of HIS-tagged Msp22. Msp22 is a lipoprotein of 152 amino acids. It contains a signal peptide of 19 amino acids. The CXXCH motif close to the C terminus is characteristic for hemoproteins. For purification purposes, the protein was expressed with a C-terminal HIS-tag.

Msp22 was previously expressed in *E. coli* (section 5.4.1) for immunization purposes. Msp22 expressed in *E. coli* served as control protein for the subsequent functional analysis of this protein. For the purpose of obtaining the native and correctly folded protein, the full-length protein was additionally expressed heterologously with a C-terminal HIS-tag in *M. catarrhalis*. The plasmid pEMCJH04-KAN was used to recombinantly express HIS-tagged Msp22 (pEMCJH04-KAN-Msp22-HIS).

Western blot analysis of the soluble and insoluble fractions of the bacterial cells expressing HIS-tagged Msp22 using anti-HIS-tag antibody revealed that the protein is highly soluble (data not shown). Due to the presence of four cysteines, DTT was added to the soluble fraction as well as to the washing buffers. Figure 5-20 demonstrates the purification of Msp22. Non-transformed wild type *M. catarrhalis* lacking HIS-tagged Msp22 expression served as negative control.

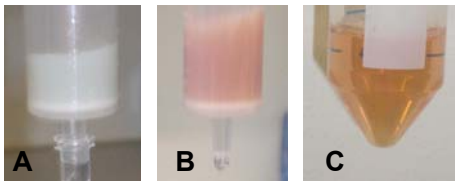

Figure 5-20: Msp22 is a highly soluble protein when heterologously expressed in *M. catarrhalis*. The soluble fraction was applied to the Ni-sepharose beads. A: Negative control = wild type *M. catarrhalis*; B: *M. catarrhalis* transformed with pEMCJH04-KAN-Msp22-HIS. C: Eluate A of bacteria transformed with pEMCJH04-KAN-Msp22-HIS containing purified HIS-tagged Msp22.

The pink coloration of the eluate from HIS-tagged Msp22 expressing cells indicated the presence of iron. In order to verify that indeed Msp22 was purified and eluted, Western blot analysis was performed using hyperimmune serum against recombinant Msp22 (expressed in *E. coli*) as well as an antibody against the HIS-tag (Figure 5-21).

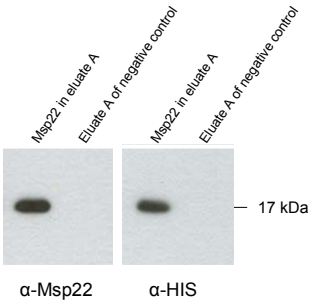

Figure 5-21: Detection of HIS-tagged Msp22 purified from *M. catarrhalis*. Recombinant Msp22 expressed in *M. catarrhalis* detected by hyperimmune serum against recombinant Msp22 (left) and against the HIS-tag (right). Negative control = eluate A of wild type (no expression of HIS-tagged Msp22).

HIS-tagged Msp22 was indeed detected in eluate A from transformed bacteria, but not in the negative control (wild type bacteria not transformed with pEMCJH04-KAN-Msp22-HIS). In summary, Msp22 is a highly soluble protein which could be purified recombinantly from its host by using a vector derived from *M. catarrhalis*.

5.6.2 Msp22 exhibits heme-dependent peroxidase activity

Msp22 is a highly conserved protein that has homology to cytochrome *c* (150, 151). Purification of this protein indicated the presence of iron due to the pink coloration of the eluate containing the protein. *c* type cytochromes indeed show heme-dependent peroxidase activity. Therefore, this enzymatic activity was assessed for Msp22 by performing a heme stain (Figure 5-22). The method applied was previously described by Feissner *et al*. (55). Three different concentrations of the purified, HIS-tagged protein were applied to the SDS-gel. In order to show that the heme stain gives specific signals, hemoglobin was used as a positive control, and BSA as negative control. Bacterial lysates of wild type, complemented wild type (containing pEMCJH04-KAN-Msp22), *msp22* gene deletion mutant and complemented *msp22* gene deletion mutant (containing pEMCJH04-KAN-Msp22) were also analyzed for the purpose of verifying that indeed Msp22 was detected.

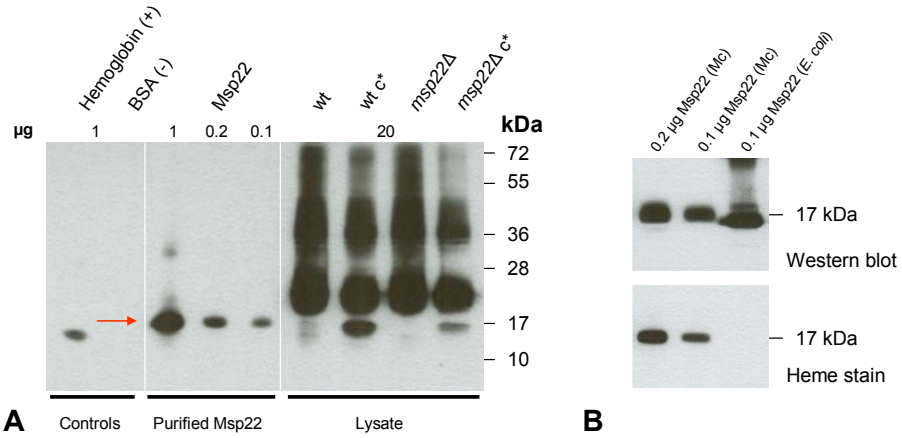

Figure 5-22: Heme-dependent peroxidase activity of Msp22. Heme stain of *M. catarrhalis* Msp22 and bacterial lysates (A) and Western blot (above)/Heme stain (below) of Msp22 expressed in *M. catarrhalis* and *E. coli* (B). Hemoglobin = positive control, BSA = negative control, Msp22 = HIS-tagged protein isolated from *M. catarrhalis*, wt = wild type, wt c* = wild type transformed with pEMCJH04-KAN-Msp22, *msp22*Δ = *msp22* gene deletion mutant, *msp22*Δ c* = *msp22* gene deletion mutant transformed with pEMCJH04-KAN-Msp22. Mc, *M. catarrhalis*. No DTT was added to the samples prior to SDS-PAGE (denaturing conditions).

Signals were obtained in all samples but the negative control BSA. In wild type lysate, the signal attributed to Msp22 was rather weak. In complemented bacteria, the signal was considerably stronger. This was expected, due to the fact that Msp22 was overexpressed in these cultures. Thus, peroxidase activity could be detected for the recombinant protein expressed in *M. catarrhalis* as well as in *M. catarrhalis* lysates. However, no heme-dependent peroxidase activity could be observed for the recombinant protein expressed in *E. coli*. This might be due to incomplete folding of the protein as the protein was not expressed in the full-length version in *E. coli*, but without the signal peptide sequence. Perhaps this was associated with a lack of heme attachment.

In summary, Msp22 is a protein with covalently attached heme and peroxidase activity associated with the heme molecule. Furthermore, Msp22 is highly soluble when expressed in its host *M. catarrhalis*.

5.6.3 Msp22 can be detected in outer membrane vesicles (OMVs) and is not iron-regulated

Mass spectrometric analysis of whole membrane preparations and OMVs allowed the identification of a number of membrane proteins. Proteomic analyses of OMVs isolated from cultures grown under iron-rich conditions (without the addition of Desferal®) and cultures grown in the presence of Desferal® did not identify Msp22. However, this method is prone to missing certain proteins, especially if they are not abundant on the cell surface. In order to obtain evidence for the localization of Msp22, OMVs were examined by Western blot using serum specific for Msp22 (Figure 5-23).

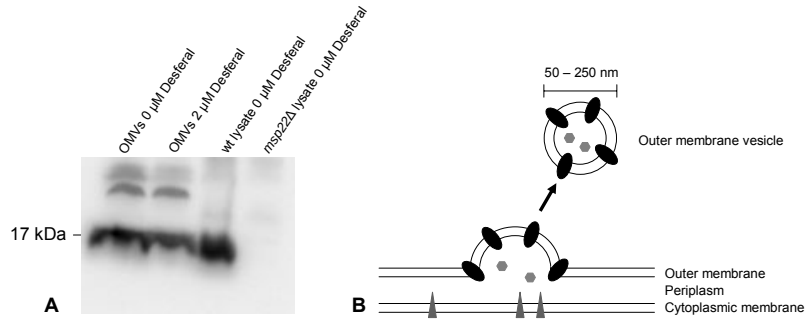

Figure 5-23: Detection of Msp22 in outer membrane vesicles. A: 25 µg protein was analyzed and detected with anti-Msp22 hyperimmune serum at a 1:4,000 dilution. Msp22 was present in outer membrane vesicles from bacteria grown under iron-rich (0 µM Desferal®) and iron-depleted (2 µM Desferal) conditions as well as in the lysate. Msp22 expression was absent in bacterial lysate of the *msp22* gene deletion mutant. B: Schematic drawing of the formation of OMVs.

Msp22 was found in OMVs isolated from *M. catarrhalis* cultures (iron-rich and iron-depleted culture conditions). Furthermore, the expression of this protein remained stable upon the addition of the iron chelator Desferal® to the medium and thus did not appear to be iron-regulated.

5.6.4 Model of the potential mechanism of Msp22 maturation and localization

Surface exposure is an important criterion of promising vaccine candidates of extracellular bacteria. Msp22 is a putative surface protein (151) with a molecular weight of approximately 17 kDa. It was shown to be a highly soluble protein (section 5.6.1) and is present in OMVs (section 5.6.3). In this section, a possible mechanism of Msp22 maturation and localization is described (Figure 5-24).

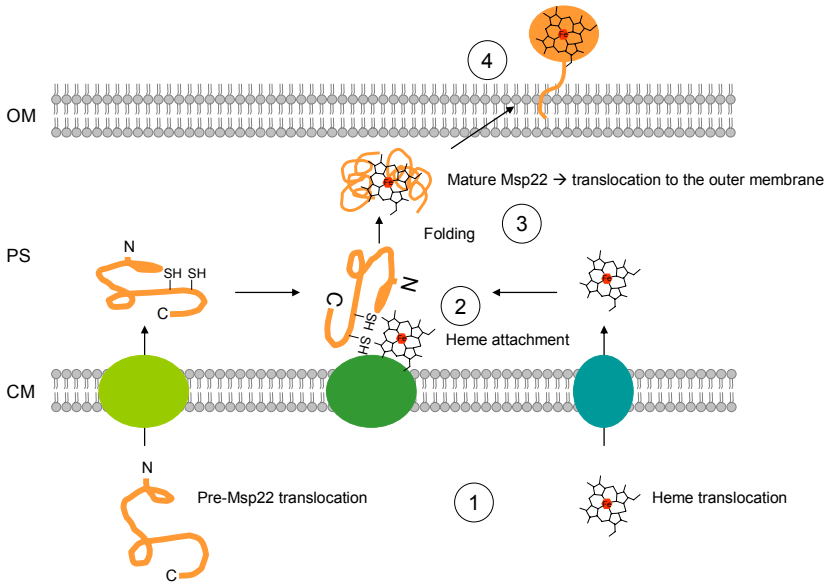

Figure 5-24: Possible mechanism of Msp22 maturation. OM, outer membrane; PS, periplasmic space; CM, cytoplasmic membrane. Adapted from Sanders *et al*. (153). 1) Pre-Msp22 and heme are transported independently across the inner membrane to the periplasmic space. 2) Heme attachment and 3) correct folding of Msp22 occurs in the periplasm. 4) The presence of an asparagine at position "+2" next to the lipidated cysteine is a sign that sorting to the outer membrane occurs.

The attachment of heme to the immature protein might take place in the periplasmic space after separate transport of heme and pre-Msp22 (immature protein) to the periplasm. The presence of an aspartate at position "+2" would indicate that the protein is anchored to the inner membrane (162). However, in the case of Msp22, the amino acid at position "+2" is an asparagine which possibly results in anchoring of the protein to the

outer membrane via the lipid attached to the cysteine. In fact, the "+2" rule does not apply to all lipoproteins of all gram-negative species (128, 158). Furthermore, surface staining of *M. catarrhalis* bacteria resulted in low signal intensities when using antibodies directed against Msp22 (data not shown). This phenomenon could be due to the fact that the protein is weakly expressed in wild type *M. catarrhalis* as observed by Western blot. However, bacteria overexpressing Msp22 (transformed with pEMCJH04-KAN-Msp22) showed a comparable, low signal. Possibly, this protein is not very abundant on the surface or not surface-exposed at all.

5.7 Identification of iron-regulated proteins at mRNA level

Many of the candidate antigens selected by AIP® are involved in iron transport and were shown to be differentially expressed at protein level in the presence of varying iron concentrations. In order to evaluate differences in gene expression under iron-rich and iron-depleted conditions at RNA level, Microarray analyses were performed. Additionally, the effect of the *msp22* gene deletion on the expression of neighbouring genes as well as other genes was determined by this method. In total, 16 cultures (four replicates per culture and culture condition) were grown in chemically defined medium with 1.25 μM or without Desferal®. Lysates of these cultures (four replicates combined) were analyzed by Western blot using antisera against Msp22 and the two proteins involved in iron transport, MCR_0076 and MhuA, in order to examine expression levels at protein level for these specific cultures (Figure 5-25 A). It was observed previously that expression of *M. catarrhalis* proteins selected by the antigenome technology did not respond strongly to varying iron concentrations *in vitro* (section 5.4.3). In order to determine the global effect of iron limitation on *M. catarrhalis* gene expression, RNA was isolated from mid-log and late-log cultures grown in the presence of 0 μM Desferal® and 1.25 μM Desferal® (Figure 5-25 B) for the purpose of examination by Microarray analysis.

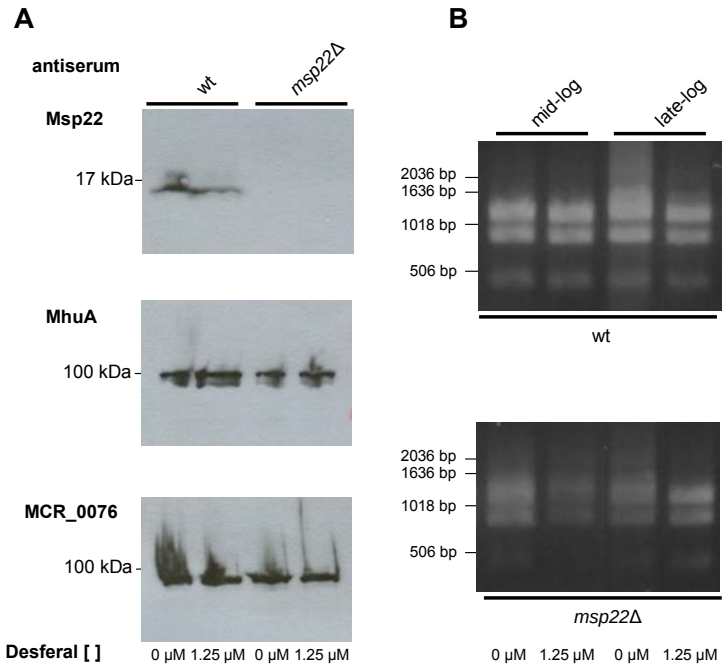

Figure 5-25: Expression of Msp22, MCR_0076 and MhuA (A) in bacterial cultures used for RNA isolation (B). wt, wild type; *msp22*Δ, *msp22* gene deletion mutant. A: Western blot analysis of *M. catarrhalis* cultures (wild type and *msp22* gene deletion mutant, 0 µM and 1.25 µM Desferal®); 20 µg lysate (4 replicates combined) per lane. B: RNA isolated with RNeasy mini kit (Qiagen). mid-log, RNA isolated from mid-log cultures; late-log, RNA isolated from late-log cultures.

The RNA was transcribed in cDNA, labeled, and hybridized to the arrays for the subsequent analysis of differential gene expression. Due to the high numbers of outliers for one wild type replicate, and one *msp22*Δ replicate, these were removed from the analysis. The expression analysis revealed that at least 35 genes were significantly upregulated ($\log_2$ ratio iron-depleted vs. iron-rich ≥ 1 in the wild type) in the presence of 1.25 µM Desferal® and at least 31 genes were downregulated ($\log_2$ ratio iron-depleted vs. iron-rich ≤ -0.9 in the wild type) under these conditions. Table 5-8 lists the genes that appeared to be the most interesting candidates and were chosen for additional qRT-PCR analysis. See Appendix I for the extended list.

Table 5-8: Differentially expressed genes identified by Microarray analysis and selected for testing in qRT-PCR. Numbers highlighted in red represent genes that were upregulated during iron depletion; numbers in green show genes that were downregulated during iron depletion. Overlaps with 214 proteins identified by AIP® are indicated in the column on the very right; ORF, open reading frame; nd, not detected; Sign. Pr., number of significant probes (out of 8); Log_2, fold increase / decrease in expression due to iron starvation represented as log_2 values.

#	ORF	Protein name	Log_2 wt	Sign. pr.	Log_2 *msp22* Δ	Sign. pr.	Overlap AIP® (214)
1	MCR_0159	Membrane protein	2.0	8	1.5	8	
2	MCR_0218	Hypothetical protein	2.9	8	2.3	8	
3	MCR_0219	Lactoferrin binding protein A LbpA	2.1	8	1.6	8	x
4	MCR_0492	Outer membrane protein CopB	0.8	4	0.4	7	x
5	MCR_0694	Transferrin binding protein B TbpB	1.2	7	1.0	8	x
6	MCR_0798	MotA/TolQ/ExbB proton channel	1.3	8	1.3	8	
7	MCR_0810	Heme oxygenase	1.2	8	0.8	8	
8	MCR_1040	Putative bacterioferritin-associated ferredoxin	1.1	6	0.7	8	
9	MCR_1868	Chelated iron ABC transporter ATPase subunit AfeB	1.6	8	0.8	8	
10	MCR_0056	TraR/DksA family transcriptional regulator	-1.1	8	-0.3	8	
11	MCR_0593	Hypothetical protein	-1.8	8	-0.5	8	
12	MCR_0760	Molybdenum cofactor biosynthesis protein B	-1.2	8	-0.9	7	
13	MCR_0858	Outer membrane protein E	-1.5	8	nd	nd	
14	MCR_1039	Bacterioferritin A	-2.2	8	-1.3	8	

Interestingly, one hypothetical gene (MCR_0218) was overexpressed almost eight-fold in the wild type and five-fold in the *msp22* gene deletion mutant during iron-limiting conditions. MCR_0218, a protein of only 41 amino acids, is situated between the Lbps (lactoferrin-binding proteins), but transcribed in reverse orientation (Figure 5-26). The function of this protein in iron metabolism is unclear. Also, *lbpA* expression was considerably affected by low iron concentrations (four-fold upregulation in the wild type and ~ three-fold upregulation in the *msp22* gene deletion mutant).

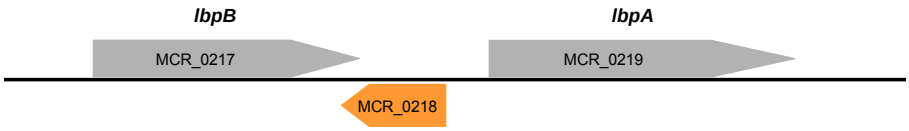

Figure 5-26: Location of the MCR_0218 gene and Lbps in the *M. catarrhalis* genome. MCR_0218 is a hypothetical protein of 41 amino acids and is situated between the Lbps in reverse orientation. Genome locations: MCR_0218: 229520 – 229645 (complement); LbpA: 229717 – 232719; LbpB: 226918 – 229533.

It remains to be elucidated whether MCR_0218 expression is related to the Lbps. Moreover, the requirement of this protein for the uptake of specific iron sources will have to be further examined e.g. by the generation of a MCR_0218 gene deletion mutant. Further, *copB* and *tbpB* expression was shown to be increased at RNA level during iron

limitation in these studies and confirmed previous studies conducted by Wang *et al*. (189) who performed similar experiments, but with *M. catarrhalis* grown in BHI medium in the presence of 30 µM or no Desferal®. Additionally, bacterioferritin A (MCR_1039), an iron storage protein (24) was downregulated during iron starvation in these studies. Further, the expression of OmpE (MCR_0858), a conserved outer membrane protein (125), was diminished during iron limitation. qRT-PCR analysis was performed in order to verify the expression data obtained by Microarray analysis. Gene-specific primers were designed for that purpose (Appendix II). Figure 5-27 represents both Microarray and qRT-PCR data of mid-log cultures of 14 selected candidates which were strongly influenced by iron depletion as identified by Microarray analysis and qRT-PCR. Late-log cultures were tested by qRT-PCR as well, but did not reveal any more interesting candidates and were thus not further analyzed. Both methods, Microarray analysis and qRT-PCR, showed a good correlation (the house keeping gene *gyrA* was used as reference gene).

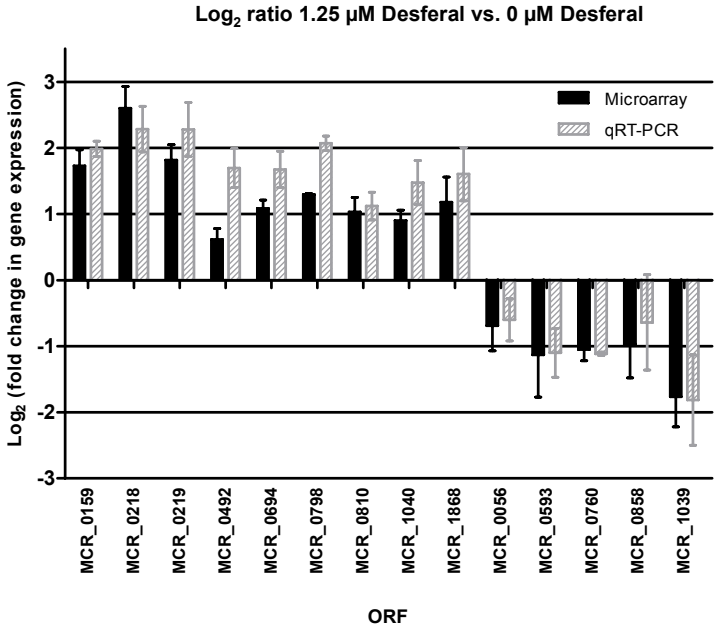

Figure 5-27: Detection of up- and downregulated genes during iron depletion by Microarray analysis and qRT-PCR. Log_2 ratio, fold change in gene expression during iron-depleted (1.25 µM Desferal®) versus iron-rich culture conditions (no Desferal®). ORF, open reading frame; Mean with standard error of the mean represented (wt + *msp22*Δ combined); *gyrA* was used as reference gene.

In addition to the effect of iron on the global gene expression of *M. catarrhalis*, the effect of the deletion of the *msp22* gene on the expression of other genes was examined. The

difference in gene expression between the wild type and the *msp22* gene deletion mutant was minor (Table 5-9). A hypothetical protein (MCR_0920), as well as PstB, a phosphate ABC transporter ATPase were upregulated in the *msp22* gene deletion mutant, whereas CysD, a sulphate adenylate transferase and a type III restriction-modification system endonuclease were downregulated in the mutant.

Table 5-9: Genes influenced by the deletion of *msp22* and selected for testing in qRT-PCR. Numbers highlighted in red were upregulated in the *msp22* gene deletion mutant; numbers in green were downregulated in the *msp22* gene deletion mutant; Overlaps with 214 proteins identified by AIP® are indicated in the column on the very right; ORF, open reading frame. Sign. Pr., number of significant probes (out of 8); Log_2 ratio, fold increase (red) / decrease (green) in expression in the *msp22* gene deletion mutant.

#	ORF	Annotation	Log_2 ratio wt vs. *msp22Δ*	Sign. pr.	Overlap AIP® (214)
1a	MCR_0920	Hypothetical protein	1.12	6	
2a	MCR_1731	Phosphate ABC transporter ATPase subunit PstB	1.16	6	x
3a	MCR_0096	Sulfate adenylate transferase subunit 2 CysD	-0.94	7	
4a	MCR_0361	Type III restriction-modification system restriction endonuclease	-3.55	5	

Due to these observations, the *msp22* gene or its gene product does not seem to play a central role in metabolism. Moreover, Microarray analysis revealed that it is neither up- nor downregulated during iron depletion. Additionally, there was no influence on the expression of neighbouring genes, indicating that the deletion of *msp22* did not have any polar effects.

In summary, the global gene expression of *M. catarrhalis* during iron depletion was examined at RNA level by Microarray analysis. The expression of a number of genes in both, the wild type and the *msp22* gene deletion mutant, responded to changes in the iron concentration. However, the overall effect of iron starvation on gene expression was stronger in the wild type compared to the *msp22* gene deletion mutant in these analyses and the effect of the *msp22* gene deletion on the global gene expression of *M. catarrhalis* was minor.

6 Results NTHI

6.1 Comparison of the membrane proteome and the antigenome of NTHI

In previous studies, the antigenome technology was applied to NTHI for the identification and selection of novel vaccine candidates for this pathogen. In the present studies, an additional proteomic approach was used for the purpose of complementing the antigenome approach. The combination of these two approaches was performed in order to obtain additional evidence for the surface localization of the proteins selected by AIP® and to potentially identify new candidates.

In total, 156 antigens were identified after applying the antigenome technology to NTHI. Three IgG pools of healthy individuals and young patients were used for the screening of surface display libraries as previously described for *M. catarrhalis* (section 5.1). Eventually, 23 lead vaccine candidates were selected for further analysis based on the number of antigenome screen hits, peptide ELISA and gene distribution among 47 strains (including the library strain NTHI86-028NP). At least 8 of the 23 candidates play a role in iron metabolism (Figure 6-1) and all of the candidates were present in at least 80% of 47 tested isolates (Table 6-1). The entire *hxu* gene cluster (HxuA, HxuB and HxuC) was selected and was present in 100% of all clinical isolates. Further, a hemoglobin-haptoglobin-binding protein (HgpB), a hemin receptor (HemR), a heme utilization protein (Hup), a transferrin-binding protein (TbpB) as well as a protein that is indirectly involved in iron metabolism (TonB), were identified.

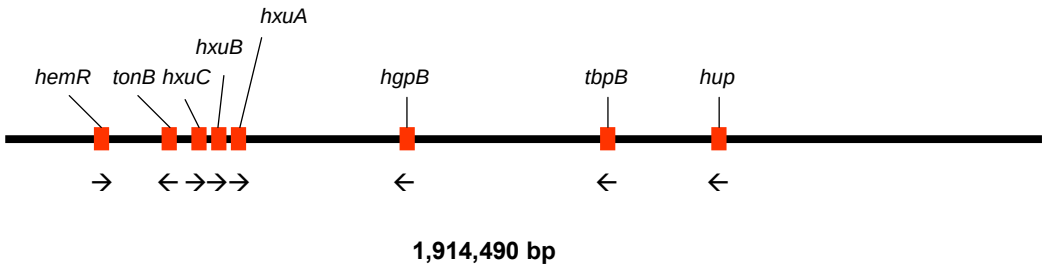

Figure 6-1: Distribution of 8 NTHI iron-regulated genes (identified by AIP®) on the NTHI86-028NP genome. *hemR* (186076-188313), hemin receptor; tonB (346174-346968, complement); (*hxuC* (355249-357378), *hxuB* (357454-359151), *hxuA* (359163-361928), heme-hemopexin-binding proteins; *hgpB* (735591-738569, complement), hemoglobin-haptoglobin-binding protein B; *tbpB* (1117519-1119411, complement), transferrin-binding protein B; *hup* (1317594-1320341, complement), heme utilization protein. Arrows indicate the direction of transcription.

In addition to iron transporters, proteins carrying out various functions in metabolism were selected by AIP®. This includes a multidrug resistance protein (NTHI1063), a cell cycle protein (NTHI0525), an IgA protease (NTHI1164) and other proteins with enzymatic activity. For pneumococcus it was shown that a protein involved in cell division (PcsB) is a promising vaccine candidate (63) suggesting that cell cycle proteins are not only important for bacterial growth, but also have the capability to elicit protective immune responses. Furthermore, IgA protease activity is linked to pathogenesis as could be shown for different *Neisseria* species (120). The NTHI IgA protease was frequently selected by AIP® (52 hits). For the lipoprotein LppB (NTHI0830), 45 clones were picked by AIP® with human antibodies. Bioinformatic analysis revealed that this protein is a putative metalloprotease that might contain zinc as a cofactor due to its similarity with the zinc binding center of a *Vibrio cholerae* zinc peptidase (protein data base 2GU1). A hypothetical protein (NTHI1667) of 191 amino acids was selected 27 times. So far, no function could be attributed to this protein.

In parallel to the antigenome approach, the membrane proteome of NTHI was determined by isolating whole and outer membranes from NTHI cultures grown exclusively in iron-rich BHI medium containing hemin. The outer membrane was obtained by sarcosyl extraction and the whole membrane was isolated by carbonate extraction. SDS-PAGE of the membrane preparations was performed, the protein spots were excised from the gel, proteolytically digested and subjected to LC-MS/MS analysis or 2D nano-HPLC MS/MS. The complete protein list resulting from these two membrane preparations is shown in Appendix I. Table 6-1 represents Intercell´s NTHI lead antigens from the antigenome and the overlaps with proteins detected by the proteomic approaches.

Table 6-1: NTHI overlaps between the membrane proteome and the antigenome approach. ORF, open reading frame; GD, gene distribution; genes were present in 80 – 100% of all tested strains (strains are listed in section 9.2). Hits, antigenome screen hits. 1 = Proteins identified in the whole membrane preparation. 2 = Proteins identified in the outer membrane preparation.

ORF	Protein name	GD	Hits	1	2
NTHI0007	Formate dehydrogenase major subunit	47/47	10		x
NTHI0202	Hemin receptor	45/47	3		
NTHI0334	Polynucleotide phosphorylase/polyadenylase	46/47	7	x	x
NTHI0358	TonB	47/47	6		
NTHI0369	Heme-hemopexin-binding protein C	47/47	5	x	x
NTHI0370	Heme-hemopexin-binding protein B	47/47	9		
NTHI0371	Heme-hemopexin-binding protein A	47/47	35		
NTHI0525	Putative cell cycle protein MesJ	47/47	8		
NTHI0716	Sigma-E factor regulatory protein RseB	46/47	5		
NTHI0782	Hemoglobin-haptoglobin binding protein B	47/47	17	x	x
NTHI0830	Lipoprotein LppB	41/47	45		
NTHI0921	Murein transglycosylase C	47/47	4		
NTHI1059	Putative membrane-fusion protein	47/47	14		
NTHI1063	Multidrug resistance protein A	46/47	2		
NTHI1164	IgA-specific serine endopeptidase IgA protease	41/47	52		
NTHI1169	Transferrin-binding protein 2 precursor	42/47	19		
NTHI1342	Opacity protein	46/47	8		
NTHI1390	Heme utilization protein	47/47	22	x	x
NTHI1449	HMW2B, OMP-85-like protein required for HMW1A and HMW2A secretion	38/47	17	x	
NTHI1638	Serine/threonine protein phosphatase family protein	44/47	5		
NTHI1667	Hypothetical protein	47/47	27		x
NTHI1707	ABC transporter periplasmic protein	45/47	1		
NTHI1915	ABC transporter permease	47/47	3		

The total numbers of overlaps between the proteomic and the antigenome approaches are demonstrated in Figure 6-2. The overlap between these two completely different methods suggested that the proteomic data supported and complemented the antigenome approach.

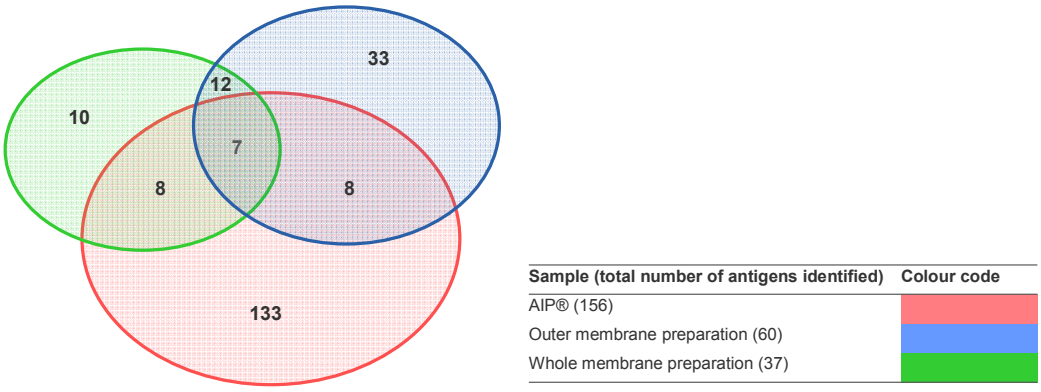

Figure 6-2: NTHI overlaps between antigenome approach and proteomic analyses. AIP® = proteins identified by the antigenome approach. 7 proteins were detected independently by all three approaches. Red, number of proteins identified by AIP®; blue, number of proteins identified in the outer membrane (sarcosyl extraction); green, number of proteins identified in the whole membrane (carbonate extraction).

Seven proteins were identified independently by the antigenome, the outer membrane as well as the whole membrane proteomic approach. Three of these proteins are involved in iron transport, namely HxuC, HgpB and Hup. HxuC and HgpB seem to play a crucial role in virulence (159) and are important for iron uptake from heme-hemopexin (HxuC, (34)) and hemoglobin-haptoglobin (HgpB, (119)). Furthermore, six out of these seven proteins are located in the outer membrane (Table 6-2). Outer membrane proteins OmpP2 (133), OmpP4 (85) and OmpP5 (191) were shown to be promising vaccine candidates. Moreover, the enrichment of (outer) membrane proteins that could be achieved by the proteomic approach as well as the combination with the antigenome approach indicated that the proteins found by both approaches are surface-exposed, which is an important characteristic of vaccine candidates.

Table 6-2: Seven common proteins identified by AIP® and two proteomic approaches. Proteins involved in iron transport are **bold**. ORF, open reading frame.

ORF	Protein name
NTHI0225	Outer membrane protein P2 precursor
NTHI0334	Polynucleotide phosphorylase/polyadenylase
NTHI0369	**Heme-hemopexin utilization protein C, HxuC**
NTHI0782	**Hemoglobin-haptoglobin binding protein B, HgpB**
NTHI0816	Outer membrane protein P4, NADP phosphatase, Hel
NTHI1332	Outer membrane protein P5
NTHI1390	**Heme utilization protein, Hup**

These studies mainly focussed on proteins associated with iron transport, due to the fact that eight NTHI iron transporters were selected by the antigenome approach, and some of them were also identified by proteomic analyses. In addition, the following aim was to shed light on the importance of iron and the availability of an iron source for NTHI *in vitro* growth.

Functional analyses of the other vaccine candidates found by AIP® are being pursued in separate studies and are therefore not described here.

6.2 NTHI growth is slightly inhibited in the presence of an iron chelator

Iron is essential for the growth and survival for virtually all bacteria, with only very few exceptions. NTHI requires iron for survival and a heme source under aerobic growth conditions (202). In order to examine the effect of iron starvation on NTHI growth, growth experiments were performed in iron-rich and iron-depleted medium. For *M.*

catarrhalis it could be shown that bacterial growth was significantly affected in the presence of an iron chelator (section 5.2). In order to analyze NTHI growth in the presence of different Desferal® concentrations, NTHI was grown in BHI medium containing NAD, hemin as well as different Desferal® concentrations ranging from 30 – 150 μM. Figure 6-3 demonstrates that high Desferal® concentrations were required in order to decrease NTHI growth slightly.

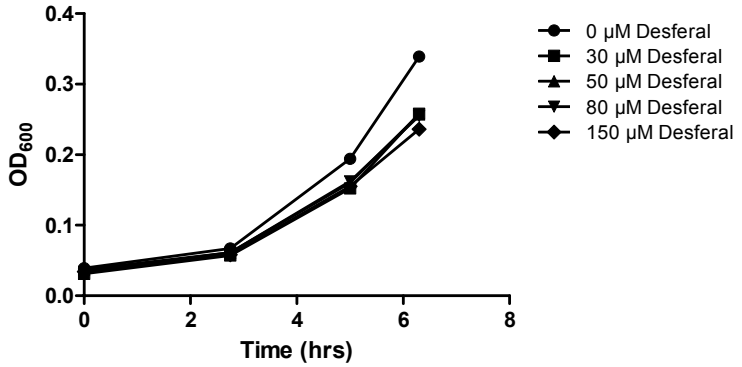

Figure 6-3: NTHI growth is slightly inhibited in the presence of the iron chelator Desferal®. BHI medium containing 1 μg/ml hemin and 10 μg/ml NAD was used. This experiment is representative for independently performed experiments. OD_{600}, Optical density 600 nm.

No major differences in bacterial multiplication could be observed upon iron starvation. This could be due to the fact that the Desferal® concentrations chosen for the growth studies were too low as BHI is a nutrient-rich medium and was additionally supplied with an extra iron source, namely hemin. In order to test whether protein expression was affected by iron limitation, subsequent analysis of the *in vitro* expression of antigens selected by AIP® was performed.

6.3 Analysis of NTHI iron-regulated proteins

6.3.1 *In vitro* analysis of NTHI protein expression

The NTHI growth rate was not strongly affected in the presence of up to 150 μM Desferal®. However, these observations did not provide any information about the expression profiles of the vaccine antigens involved in iron transport. Therefore, the aim was to examine the *in vitro* expression of NTHI vaccine candidates under iron-rich and iron-limiting conditions using hyperimmune sera against the respective recombinant proteins expressed in *E. coli* (Table 6-3).

Table 6-3: Recombinant expression of NTHI proteins in *E. coli*. ORF, open reading frame; * proteins were expressed in fragments; Cys, number of cysteines in recombinant protein. aa, amino acid; MW, molecular weight; rec., recombinant protein; nat., native; S, solubility; sol, soluble; ins, insoluble;

ORF	Protein name (abbreviated)	MW rec.	pI	Cys	aa start-stop	aa rec.	aa nat.	MW nat.	S
NTHI0811	Protein D	40.4	6.40	0	28-364	347	364	41.8	sol
NTHI0358	TonB	27.5	6.23	0	26-264	252	264	28.7	sol
NTHI0370	HxuB	61.2	9.16	0	27-565	549	565	62.7	ins
NTHI0371*	HxuA	31.0	5.76	0	23-299	287	921	100.5	sol
NTHI1169*	TbpB	43.1	6.69	2	252-630	389	630	69.3	sol

The NTHI genome encodes a large number of iron transporters and iron-containing proteins. In order to assess whether some of the proteins identified by AIP® are iron-regulated proteins, bacterial lysates were prepared after growth in iron-rich (no addition of Desferal® to the medium) and iron-depleted medium (80 µM Desferal®). Protein D is not predicted to be involved in iron metabolism and thus its expression was not expected to be affected by different iron levels. Therefore, protein D was used as a negative control. It did in fact not exhibit differences in expression following iron depletion. HxuA and TbpB were strongly upregulated by iron depletion, whereas protein TonB was only weakly upregulated by iron depletion. Figure 6-4 shows this analysis for the four selected NTHI proteins.

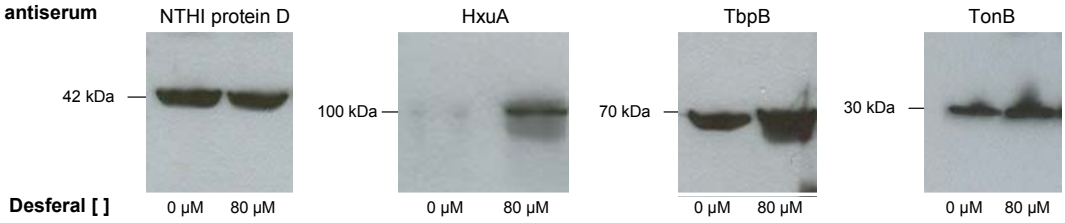

Figure 6-4: *In vitro* expression of of four selected NTHI proteins under iron-rich and iron-depleted culture conditions. Immunoblot using hyperimmune sera against the respective recombinant proteins. Negative control: NTHI protein D. 25 µg lysate (protein D, HxuA, TbpB), 15 µg lysate (TonB). HxuA was strongly upregulated, TbpB showed about two-fold increase in expression and TonB was slightly upregulated during iron depletion.

In order to verify these data and to examine whether these proteins are exposed to the bacterial surface, surface staining of the bacteria was performed under iron-rich and iron-depleted conditions (Figure 6-5). The data shown for one experiment are representative for independently performed experiments. For TbpB and HxuA, a strong shift could be observed for bacteria grown in the presence of an iron chelator, suggesting that the protein is surface-exposed and overexpressed during iron limitation. Flow cytometry

confirmed thus the results obtained by Western blot. In particular, TbpB as well as HxuA were overexpressed on the cell surface in the presence of Desferal®.

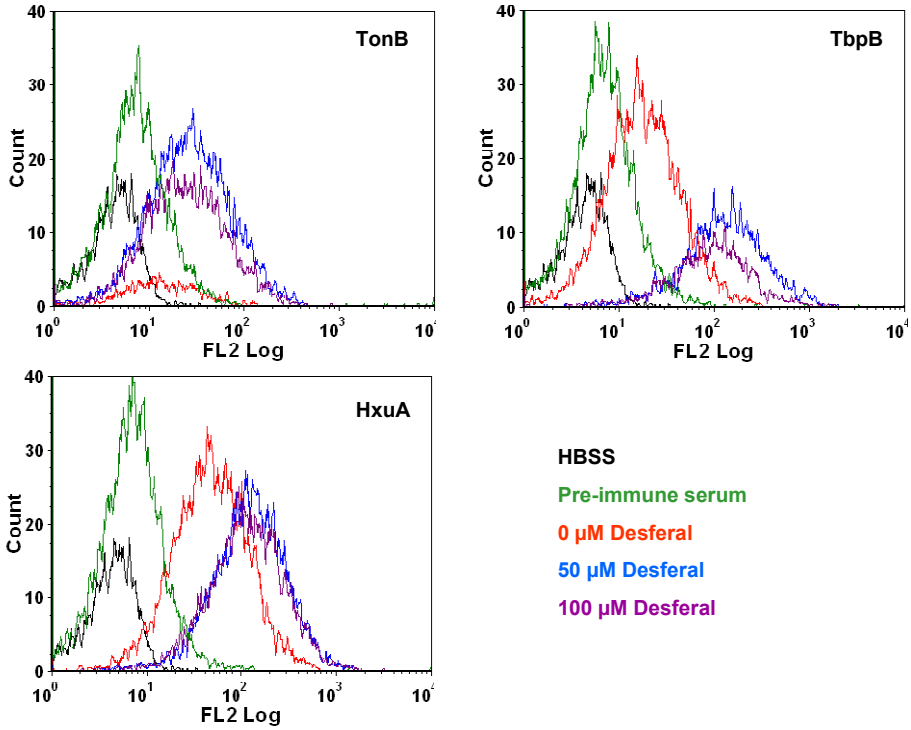

	HxuA (NTHI0371)	TbpB (NTHI1169)	TonB (NTHI0358)
Hyperimmune serum	NTHI0371-1	NTHI1169-2	NTHI0358
Median HBSS	4.07	4.07	4.07
Median Preimmune serum	6.73	6.55	6.76
Positives Preimmune serum	32.09%	30.74%	32.52%
Median 0 µM Desferal®	46.56	17.00	12.86
Positives 0 µM Desferal®	91.69%	71.48%	61.09%
Median 50 µM Desferal®	124.09	129.80	26.42
Positives 50 µM Desferal®	97.06%	96.12%	80.34%
Median 100 µM Desferal®	113.42	95.60	23.50
Positives 100 µM Desferal®	97.03%	94.26%	78.61%

Figure 6-5: Surface exposure of three NTHI antigens. NTHI was grown in BHI+ medium under iron-rich (without Desferal®) and iron-depleted (50 µM and 100 µM Desferal®) conditions. The table lists median values of fluorescence intensity and percentage of events. Black, HBSS negative control; green, preimmune serum control; red, bacterial population grown in iron-rich medium (without Desferal®); blue, bacterial population grown in the presence of 50 µM Desferal®; purple, bacterial population grown in the presence of 100 µM Desferal®. x-axis, fluorescence intensity; y-axis, bacterial counts; histogram created by FCS express. Results of one representative experiment are shown. Bacteria were stained with SYTO® 60 (red fluorescent nucleic acid stain); Flow cytometer, Cell Lab Quanta™ SC Flow Cytometer (Beckman Coulter, U.S.A).

The fact that these proteins were not only upregulated during iron starvation, but also expressed on the surface makes them valuable candidate antigens. These data thus support the hypothesis that iron transporters may play a crucial role during infection.

6.3.2 Two NTHI iron transport proteins selected by AIP® are secreted

Many virulence factors as well as some proteins involved in iron metabolism are secreted (15, 33, 67, 87, 181). In order to test whether proteins identified by AIP® are secreted and released to the culture supernatant, cultures were grown in iron-rich and iron-depleted medium for subsequent examination of the culture supernatant. Culture supernatants were obtained by centrifugation and subsequent concentration to ~ 1/12 of the original volume. For comparison, bacterial lysates were analyzed in parallel, also by Western blot analysis (Figure 6-6). HxuA was found to be present in the lysate as well as in the supernatant. Under iron-limiting conditions, HxuA is not only upregulated, but also higher concentrations of HxuA were secreted *in vitro*. Interestingly, low amounts of TbpB were also released to the medium. However, protein D, TonB and HxuB could not be detected in the culture supernatant.

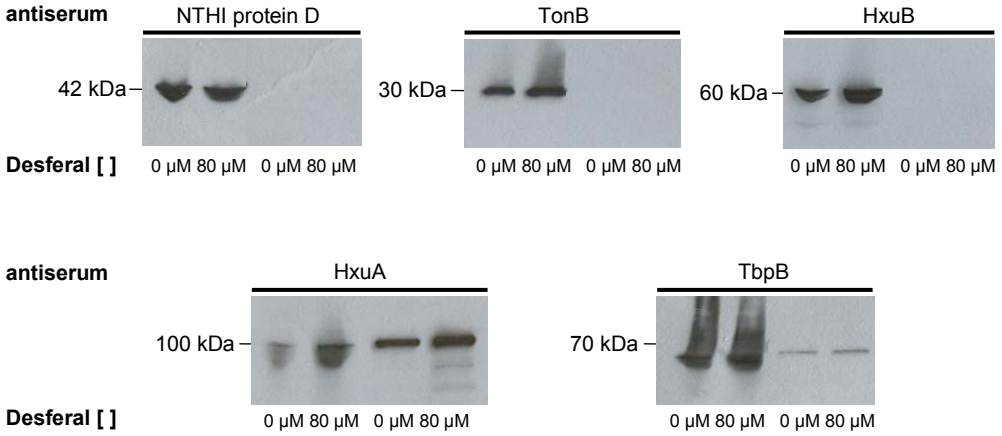

Figure 6-6: The two NTHI antigens HxuA and TbpB are secreted. The two left lanes of each blot show bacterial lysates, two right lanes represent culture supernatants. Cultures used for lysate preparation and supernatant were grown in the presence of 0 µM or 80 µM Desferal®. Protein D served as control protein (not iron-regulated). Antiserum generated against the respective recombinant proteins was used as primary antibody. Proteins HxuA and TbpB were detected in bacterial lysate (25 µg) as well as in the culture supernatant. Protein D, TonB and HxuB were not secreted.

The secretion of HxuA to the culture supernatant was expected (33), however, for TbpB this observation is new. Therefore, the following section focuses on this transferrin receptor.

6.3.3 Comparison of NTHI and *M. catarrhalis* TbpB

TbpB, one of the transferrin-binding proteins was shown to be overexpressed in NTHI during iron limitation, exposed to the bacterial surface and to be secreted (sections 6.3.1 and 6.3.2). Tbps are present in both, NTHI and *M. catarrhalis* and bioinformatic analysis of *M. catarrhalis* and NTHI Tbps revealed that *tbpA* precedes *tbpB* in *M. catarrhalis*, whereas the opposite is true for NTHI. In addition, the two *M. catarrhalis tbp* genes are segregated by an additional ORF encoding a hypothetical protein of 503 amino acids (MCR_0692). In NTHI, no such intervening ORF is present between the *tbp* genes (Figure 6-7).

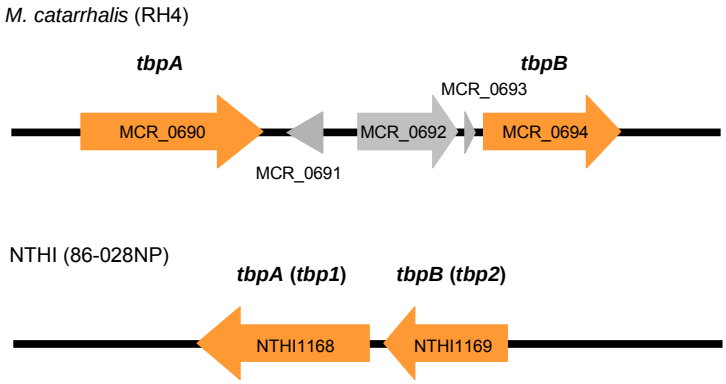

Figure 6-7: Organizational arrangement of tranferrin-binding proteins of *M. catarrhalis* and NTHI. *M. catarrhalis* Tbps are separated by a hypothetical protein. Genome locations: NTHI1168: 1114736-1117474 (complement); NTHI1169: 1117519-1119411 (complement); MCR_0690: 695767-698991; MCR_0691: 699144-699461 (complement); MCR_0692: 700051-701562; MCR_0693: 701664-701780; MCR_0694: 701826-703952. Orange arrows, Tbps; Grey arrows, hypothetical proteins.

Further, similarities of the two TbpBs were analyzed at amino acid level in order to identify conserved sequences. The *M. catarrhalis* RH4 TbpB and the NTHI 86-028NP TbpB show approximately 30% identity in amino acid sequence (Figure 6-8). Short identical peptide segments (up to 13 amino acids) are distributed across the entire protein. Moreover, the molecular weight of the *Moraxella* TbpB is slightly higher (75.8 kDa) than that of NTHI (69.3 kDa).

```
M.catarrhalis_TbpB      MKHIPLTTLCVAISAVLLTACGGSGGSNPPAPTPIPNAGGAGNAGSGTGGAGSTDNAANA
NTHI_TbpB               ---MKSVPLITGGLSFLLSACSGGGGSFDVDDVSNP-----------------------

M.catarrhalis_TbpB      GSTGGASSGTGSASTPEPKYQDVPTDKNEKAEVSDIQKPAMGYGMALSKINLYEQKDISL
NTHI_TbpB               ------------SSSKPRYQDDTSSSRTKSNLEKLSIPSLGGGMKLVAQNLSGNKEPSF

M.catarrhalis_TbpB      DANNIITLDGKKQVAEGKKSPLPFSLDVENKLLDGYMAKMDKADKNAIGDRIKKDNKDKS
NTHI_TbpB               LNE------------NGYISYFSSPSTIEDDVKN--VKTENKIHTNPIGLEPNRALQD--

M.catarrhalis_TbpB      LSEAELAEKIKEDVRKSPDFQKVLSSIKAKTFHSNDGTTKATTRDLKYVDYGYYLVNDAN
NTHI_TbpB               ----------------PNLQKYVYSG-----------------------LYYIENWKD

M.catarrhalis_TbpB      YLTVKTDKLWNSGPVGGVFYNGSTTAKELPTQDAVKYKGHWDFMTDVANKRNRFSEVKEN
NTHI_TbpB               FSKLATEKKAYSGHYGYAFYYGNKTATDLPVSGVATYKGTWDFITATKYGQNYSLFSNAR

M.catarrhalis_TbpB      PQAGRYYGASSKDEYNRLLTKEDSAPDGHSGEYGHSSEFTVNFKEKKLTGELSSNLQDSR
NTHI_TbpB               GQAYFRRSATRG--------DIDLENNSKNGDIGLISEFSADFGTKKLTGQLSYTKRKTD

M.catarrhalis_TbpB      KGNVTKTKRYDIDANIDGNRFRGSATASNKNDTSKHPFTSDAKNSLEGGFYGPNAEELAG
NTHI_TbpB               IQQYEKEKLYDIDAHIYSNRFRGKVTP-TKSTSDEHPFTSEG--TLEGGFYGPNAEELGG

M.catarrhalis_TbpB      KFLTNDKKLFGVFGAKRDKVEKTEAILDAYALG----TFNTKGATTFTP-----------
NTHI_TbpB               KFLARDKRVFGVFSAKETPETEKEKLSKETLIDGKLITFSTKTADATTSTTASTTADVKT

M.catarrhalis_TbpB      ----FTKKQLDNFGNAKKLVLGSTVINLVSTDATKNEFTKEFTKNKPKSATNEAGETLMV
NTHI_TbpB               DEKNFTTKDISSFGEADYLLIDNYPVPLFPEGDTD-----DFVTSKHHDIGNKTYKVEAC

M.catarrhalis_TbpB      NDKVSVKTYGKNFEYLKFGELSVGGSHSVFLQGERTATTGEKAVPTEGTAKYLGNWVGYI
NTHI_TbpB               CKNLSYVKFGMYYEDKEKKNTNQTGQYHQFLLGLRTPSS---QIPVTGNVKYLGSWFGYI

M.catarrhalis_TbpB      TG-ADTGASTGKSFNEAQDIADFDIDFKNKTVKGKLTTKGRTDPVFNITGDITGNGWKGK
NTHI_TbpB               GDDKTSYSTTGNKQQDKNAPAEFDVNFDNKTLTGKLKRADSQNTVFNIEATFKNG---SN

M.catarrhalis_TbpB      ASTAKADAGGYNIDSNGTNKSIVIENAEVTGGFYGPNANEMGGSFTHNTND---------
NTHI_TbpB               AFEGKATANVVIDPKNTQATSKVNFTTTVNGAFYGPHATELGGYFTYNGNNPTATNSESS

M.catarrhalis_TbpB      -----------SKASVVFGTKRQEEVKQ-
NTHI_TbpB               STVPSPPNSPNARAAVVFGAKRQVEKTNK
```

Figure 6-8: Sequence alignment (ClustalW) of *M. catarrhalis* RH4 TbpB (MCR_0694) and NTHI 86-028NP TbpB (NTHI1169). Identical positions are highlighted in yellow.

In order to test whether TbpB is expressed *in vitro* in *M. catarrhalis* and upregulated during iron limitation as well, hyperimmune serum against NTHI recombinant TbpB (NTHI1169) was utilized for immunoblot analysis of *M. catarrhalis* lysates grown under iron-depleted conditions. TbpB was indeed expressed in *M. catarrhalis* as could be shown by Western blot analysis. As a control, NTHI lysate was used and antibodies raised against recombinant NTHI TbpB reacted with *M. catarrhalis* lysate as well as NTHI lysate (Figure 6-9). That indeed TbpB was recognized and not another protein in the *M. catarrhalis* lysate was supported by the fact that the antiserum crossreacted with the band of the expected size (75.8 kDa) and the *M. catarrhalis* protein was also upregulated under iron-limiting conditions. Moreover, the expression of TbpB was not affected by either of the four selected gene deletions (3 hypothetical proteins and *oppA*Δ) in *M. catarrhalis* indicating that these genes or gene products did not have an influence on TbpB expression.

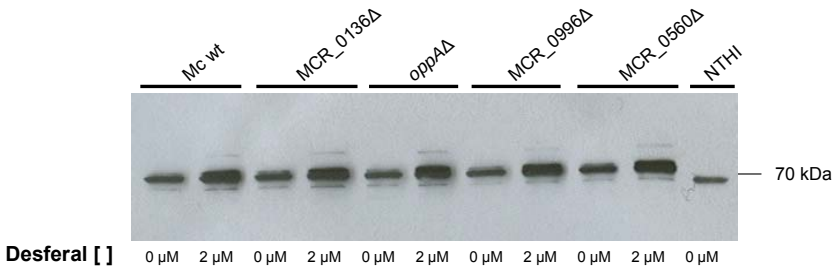

Figure 6-9: Hyperimmune serum against NTHI rTbpB crossreacts with *M. catarrhalis* TbpB. TbpB is upregulated in *M. catarrhalis* when grown in iron-depleted medium (2 µM Desferal). TbpB expression is not affected in 4 selected *M. catarrhalis* gene deletions mutants. MCR_0136, MCR_0996, MCR_0560, hypothetical proteins; Mc wt, *M. catarrhalis* RH4 wild type; NTHI, NTHI 86-028NP wild type.

In summary, TbpB appears to be a promising vaccine antigen. It was approximately two-fold upregulated during iron depletion and expressed on the surface. Furthermore, antibodies raised against the NTHI recombinant TbpB crossreacted with native *M. catarrhalis* TbpB in bacterial lysate suggesting that linear as well as conformational epitopes were recognized.

6.4 Characterization of the *hxuA* mutant

6.4.1 Generation and confirmation of the *hxuA* gene deletion mutant

The *hxuA* gene encodes a heme-hemopexin-binding protein that is highly conserved among NTHI strains and was frequently found by the antigenome technology (35 hits). Although this protein was hardly expressed under iron-rich conditions *in vitro*, it was shown to be strongly upregulated during iron starvation. Moreover, it was secreted to the culture supernatant and surface-exposed (sections 6.3.1 and 6.3.2). In order to further characterize this protein, a gene deletion mutant was generated and obtained from the Radboud University Nijmegen Medical Centre, The Netherlands (RUNMC). The gene deletion was confirmed by PCR and Western blot (Figure 6-10). Western blot of cultures grown under iron-rich and iron-depleted conditions was carried out, due to the weak expression of this protein in the wild type in the presence of high iron concentrations.

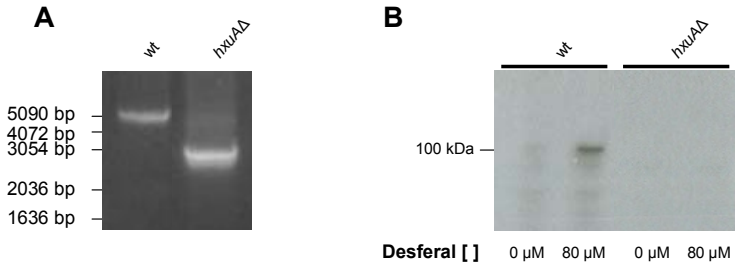

Figure 6-10: Confirmation of the *hxuA* gene deletion by PCR (A) and Western blot (B). wt, wild type; *hxuA*Δ, *hxuA* gene deletion mutant. A: Primers 8030 and 7956 (see Appendix II) were used for the confirmation of the gene deletion by colony PCR. B: Western blot analysis of NTHI lysates. Due to the low expression levels of HxuA in iron-rich medium, bacterial lysates from cultures grown in iron-depleted medium (80 µM Desferal®) were prepared in addition.

The *hxuA* ORF was successfully deleted by replacing the gene with a Spectinomycin resistance cassette, as clones transformed with the mutant construct (flanking regions of *hxuA* and the Spectinomycin resistance cassette) were rendered resistant to the antibiotic Spectinomycin. Moreover, the lack of *hxuA* could be confirmed at DNA level by colony PCR, and the absence of HxuA expression could be verified by Western blot.

6.4.2 NTHI growth is not affected by the deletion of *hxuA*

For the purpose of analyzing potential characteristics and possible growth defects of an *hxuA* gene deletion mutant, growth experiments were performed in iron-rich and iron-depleted medium. BHI medium supplemented with NAD and hemin as well as varying Desferal® concentrations was utilized (Figure 6-11).

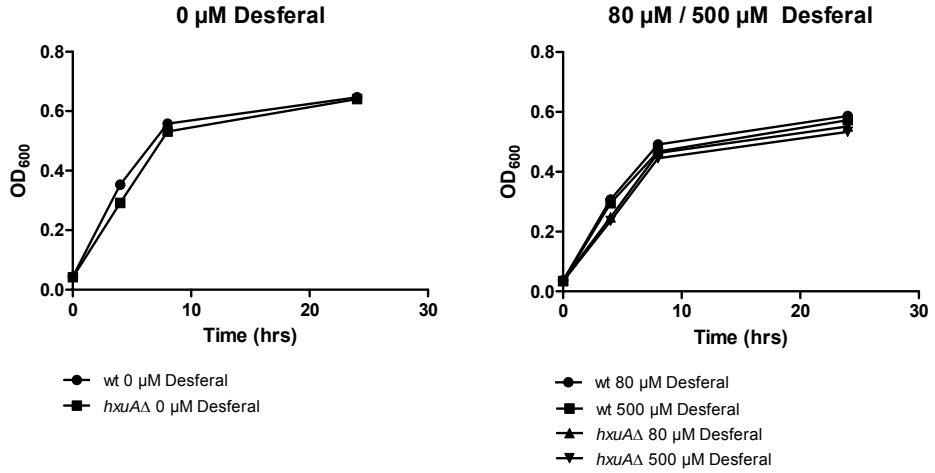

Figure 6-11: Growth of NTHI wild type and *hxuA* gene deletion mutant. The *hxuA* gene deletion mutant was not restricted in growth and not affected by lower iron levels (in the presence of 80 µM or 500 µM Desferal) compared to the wild type. OD_{600}, Optical density 600 nm.

The growth rate of the NTHI mutant lacking the *hxuA* gene was not affected under these growth conditions. Moreover, the addition of either 80 μM or 500 μM Desferal to the medium did not have a major impact on NTHI growth (wild type and *hxuA* gene deletion mutant). Most probably, the upregulation of iron transporters during iron-limiting conditions compensates the lack of freely available iron and prevents growth inhibition.

6.4.3 The deletion of *hxu*A does not have an effect on the expression of three selected proteins

In order to analyze the effect of the *hxuA* gene deletion on the expression of other genes, bacterial lysates of the wild type and the *hxuA* gene deletion mutant were prepared and examined by Western blot using hyperimmune sera against the recombinant proteins HxuB, TonB and protein D (Figure 6-12).

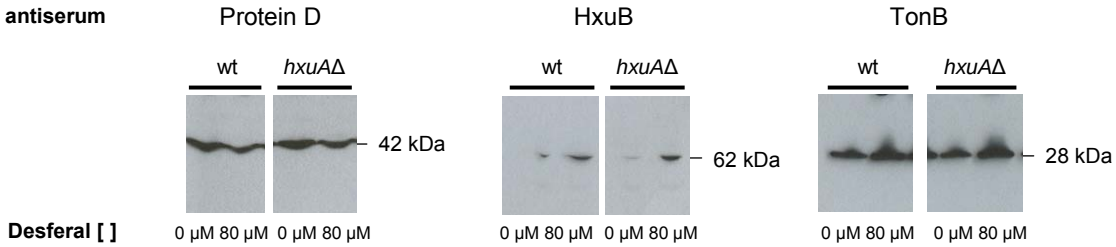

Figure 6-12: The expression of three selected genes is not affected in an *hxuA* gene deletion mutant compared to the wild type. wt, wild type; *hxuA*Δ, *hxuA* gene deletion mutant. Protein D was expressed at equal levels during iron-rich (0 μM Desferal®) and iron-depleted (80 μM Desferal®) conditions. HxuB and TonB were upregulated during iron starvation in the wild type as well as in the *hxuA* gene deletion mutant. 15 μg lysate was analyzed.

The deletion of *hxuA* did not have an impact on the expression levels of HxuB, protein D and TonB, compared to the wild type. As also observed for the wild type, the two genes involved in iron metabolism (HxuB and TonB) were upregulated during iron starvation, whereas the expression of protein D remained stable in the *hxuA* gene deletion mutant. These findings suggest that HxuA expression is not required for HxuB, TonB and protein D expression.

6.4.4 The NTHI *hxuA* gene deletion mutant does not show increased sensitivity to five selected antibiotics

Antibiotic resistance is a major issue with regard to fighting diseases. In order to examine whether an *hxuA* gene deletion mutant shows augmented sensitivity to antibiotics, NTHI wild type as well as the *hxuA* gene deletion mutant were tested for their antibiotic sensitivity/resistance using five selected antibiotics: Kanamycin, Rifampin, Colistin, Penicillin and Vancomycin. No significant difference in antibiotic sensitivity between the wild type and the *hxuA* gene deletion mutant could be observed (Figure 6-13). Both, the wild type and the mutant strain were resistant to Penicillin and Vancomycin. Furthermore, Kanamycin caused an inhibition zone of 9 – 10 mm, indicating that the bacteria were sensitive to this antibiotic. Rifampin also had a bactericidal effect with an inhibition zone of 5 mm. Moreover, a weak sensitivity (2 mm inhibition zone) to Colistin was observed.

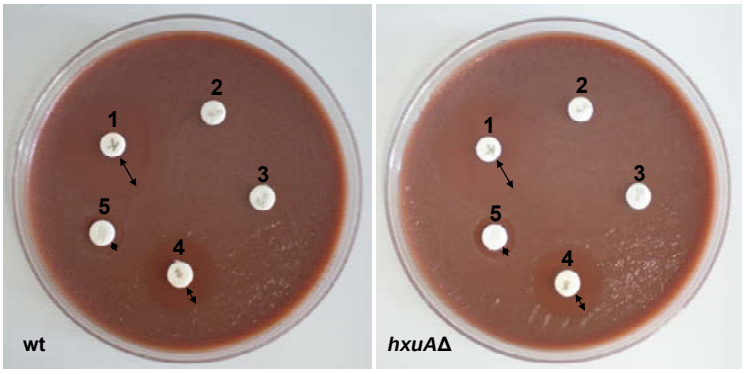

Figure 6-13: Antibiotic sensitivity of the *hxuA* gene deletion mutant. Bacteria (100 µl of OD_{600} ~ 0.55) were plated on chocolate agar. wt, wild type; *hxuA*Δ, *hxuA* gene deletion mutant. Antibiotic discs were placed on the plate prior to incubation at 37°C overnight. The *hxuA* gene deletion was not associated with an increased sensitivity to five selected antibiotics compared to the wild type. Both strains were sensitive to (1) Kanamycin (9-10 mm) and (4) Rifampin (5 mm). A slight sensitivity to (5) Colistin (2 mm) could be observed. There was resistance against (2) Penicillin (0 mm) and (3) Vancomycin (0 mm). mm, inhibition zones; black arrows indicate inhibition zones.

Overall, the deletion of *hxuA* did not seem to have an effect on the antibiotic resistance or sensitivity of NTHI.

In summary, the *hxuA* gene deletion mutant was not inhibited in growth in iron-rich or iron-depleted medium. This led to the conclusion that this protein is not essential for bacterial survival. However, it might play an important role in virulence due to its frequent selection by AIP® and therefore the indirect evidence for *in vivo* expression, its surface exposure and overexpression during iron limitation.

7 Discussion

The overall aim of this study was to characterize potential novel vaccine antigen targets of *M. catarrhalis* and NTHI following the identification by the antigenome technology developed by Intercell, which was previously also applied to other pathogens such as *S. pneumoniae*, group A streptococcus, and several other bacterial targets (58, 114). These studies therefore strongly supported efforts to develop a vaccine against a polymicrobial disease, namely otitis media. The antigenome approach selected 214 *M. catarrhalis* and 156 NTHI antigens, and after careful evaluation of these proteins, a set of about 20 novel candidate antigens per pathogen was chosen for detailed analysis.

7.1 Complementation of the antigenome technology by a proteomic approach for the identification of novel vaccine candidates

The antigenome approach was supported and complemented by a proteomic approach that was performed as part of this work to identify potential surface-exposed vaccine candidates. The proteomic approach provided a list of mainly membrane proteins derived from the analysis of the membrane proteomes of *M. catarrhalis* and NTHI. In combination with the antigenome approach, the selection of potential vaccine candidates was facilitated, and the overlap was a good indication for the surface exposure of the selected proteins. Furthermore, the fact that both methods identified proteins which have previously been described in the literature to be immunogenic and promising vaccine candidates suggested, that the combination of the antigenome approach and the proteomic approach was a suitable tool for the identification and priorization of candidate antigens. For example, *M. catarrhalis* proteins CopB, transferrin-binding proteins (Tbp) and lactoferrin-binding proteins (Lbp) were detected by AIP® as well as by the proteomic approach. Hag (MID), UspA1 and UspA2H were predominantly identified by the antigenome technology, and these proteins were also found in outer membrane vesicles (OMVs) as well as in the whole membrane preparation (Hag, UspA2H). Hag (MID) is known to be expressed on OMVs *in vivo* as well and expression of this protein on the bacterial surface is dense (186). The outer membrane protein CD (OmpCD) was found in all preparations and served as positive control for the *M. catarrhalis* vaccination studies. Out of the three protective *M. catarrhalis* candidates

identified by animal studies, one, namely OppA was independently identified by the antigenome approach, in OMVs isolated from bacteria grown under iron-rich and iron-depleted conditions as well as in the whole membrane preparation. Msp22 and a TonB-dependent receptor were exclusively selected by the antigenome approach, but not detected by proteomics. As Msp22 did not show high expression levels in the *M. catarrhalis* wild type, this was not surprising. More detailed conclusions for these three proteins are provided in section 7.4.

Furthermore, the HMW (high molecular weight) proteins of NTHI were predominantly identified by screening bacterial surface display libraries, but only HMW1A was found in membrane preparations. Yet, the overlap between AIP® and the proteomic approach was considerable. Whereas the entire HxuCBA gene cluster was selected by the antigenome approach, only HxuC was detected by proteomics. In the case of NTHI, only membrane preparations of bacteria grown under iron-rich conditions were analyzed by mass spectrometry. As Western blot and surface staining gave evidence that HxuA is only very weakly expressed in the presence of high iron concentrations, it might have been missed due to its low abundance. Moreover, this protein was also secreted to the culture supernatant which was discarded prior to the isolation of the outer and whole membranes.

The membrane proteome revealed (outer) membrane proteins which are expressed *in vitro* in the presence or absence of an iron chelator. Especially the iron-limiting environment imitated the situation in the human body with its scarce free iron concentration. Yet, it need be kept in mind that this method did not present quantitative results. Moreover, proteomic analyses did not provide information about the immunogenicity of proteins. However, the selection of proteins by the antigenome technology provided indirect proof that the antigens are immunogenic and expressed *in vivo* during infection and/or colonization due to the presence of IgGs in patients and healthy individuals (antibody pools used for library screening). This method is in contrast not specific for outer membrane proteins, as bacterial surface display libraries statistically express every single protein of a pathogen including membrane proteins as well as cytoplasmic proteins. The combination of the antigenome approach and the proteomic approach therefore improved and facilitated the evaluation of the selected candidate antigens. Thus, proteomics was not performed for the purpose of replacing the antigenome technology, but rather for supporting and confirming this method.

7.2 Outer membrane vesicles – key players of *M. catarrhalis* infection?

Outer membrane vesicles, small particles of 50 – 250 nm in size released from the bacterial surface of many gram-negative bacteria, carry outer membrane proteins of which many are potential virulence factors and immunogenic (96). OMVs from *M. catarrhalis* grown under iron-rich and iron-depleted conditions were examined and compared, and indeed a large number of outer membrane proteins were identified. Moreover, many proteins detected in OMVs from iron-starved bacteria are involved in iron transport such as the Tbps A and B and the Lbps A and B. Previously described candidate antigens including Msp78 as well as MhuA were also detected in OMVs isolated from bacteria grown in iron-depleted medium. Msp78, a nitrite reductase, was examined by Ruckdeschel *et al*. (151) and it was shown to be conserved, expressed *in vivo* in the human respiratory tract and to elicit antibody responses in humans. MhuA, a hemoglobin utilization protein is a well conserved protein capable of binding hemoglobin (60). There is indirect evidence that the protein is also expressed *in vivo* due to the selection of this protein by the antigenome technology.

OMVs have been shown to interfere with the human immune system by interacting with B-cells and inhibiting complement activity (186). This enables the bacterium to evade the human immune response. The advantage for the bacterium of secreting these vesicles might be that antibodies directed against outer membrane proteins will bind to these proteins on OMVs rather than on bacterial surfaces and thus prevent killing of the bacteria. Moreover, these small particles might be spread to niches which cannot be reached by whole bacterial cells. An indication for the importance of OMVs for the human host is the fact that they do not only stimulate immune responses against *M. catarrhalis*, but they also inhibit killing of NTHI by human serum via UspA-dependent inactivation of the complement system (131, 172).

In conclusion, OMVs are useful for the study of *M. catarrhalis* outer membrane proteins as well as for examining interactions with the host immune system and bacterial co-infections.

7.3 Iron-regulated proteins as potential vaccine candidates

These studies focused mainly on iron metabolism as a considerable number of the antigens selected by the antigenome technology as well as by the proteomic approach are involved in iron transport. This in combination with the literature indicates that these proteins play an important role in pathogenesis and thus might be useful vaccine candidates (82, 148, 174). Iron metabolism in bacteria is extremely complex, and due to the abundance of iron transport proteins, some of the mechanisms appear redundant. However, the human host represents a very hostile environment with low concentrations of free iron. Iron is bound by proteins such as transferrin and lactoferrin, therefore, it is a necessity for bacteria to express transporters which allow the uptake of this essential element. *In vitro*, such an iron-limiting environment was mimicked by the addition of Desferal® to the growth medium. Desferal® is an iron-chelating agent that has a very high affinity for iron and originates from the species *Streptomyces pilosus* which produces Deferoxamine, a siderophore. These studies showed that in NTHI proteins involved in iron transport are strongly upregulated during iron depletion. Especially the expression of hxuA was increased upon the addition of Desferal® to the growth medium. Under iron-rich conditions this protein can hardly be detected by Western blot analysis of bacterial lysates. However, during iron depletion, expression levels were drastically increased. This indicated that this protein is repressible by iron. Moreover, considerable amounts of HxuA were found in the culture supernatant of an NTHI culture. This finding verified and supported the mechanism of iron uptake by HxuA described in the literature (33, 192). In many bacteria, the *fur* gene encodes a ferric uptake regulation protein that controls the expression of iron-regulated proteins and thus plays a central role in accomplishing iron homeostasis. This is essential because iron excess is toxic to the bacterial cell as reactive oxygen species may be formed (50). NTHI also encodes a ferric uptake regulation protein (NTHI0284). In *E. coli*, it was shown that Fur complexed with iron negatively affects the expression of certain iron transporters by binding to the so called iron boxes, a DNA sequence consisting of 19 bp, with two hexamers in forward orientation, one in reverse orientation, and one base pair in between (102). The role of *fur* with regard to regulation of *hxuA* expression remains to be elucidated. *M. catarrhalis* strain RH4 also encodes a Fur protein. The expression of the *fur* gene of *M. catarrhalis* strain 7169 complements a *fur* deficient *E. coli* mutant, showing that this protein is indeed

functional. Moreover, a *fur* gene deletion mutant of *M. catarrhalis* was shown to be more susceptible to human serum compared to the wild type. Additionally, the deletion of the *fur* gene led to the constitutive expression of iron transporters (59).

In effect, the expression of the two *M. catarrhalis* antigens involved in iron metabolism, MhuA and a TonB dependent receptor, did not respond strongly to changes in iron concentrations compared to the tested NTHI proteins (TbpB, HxuA, TonB). Furthermore, these studies confirmed that antibodies raised against the recombinant iron-regulated proteins recognized their corresponding native proteins in Western blot and detected the protein on the bacterial surface by surface staining suggesting that these proteins are promising candidate antigens.

7.3.1 Evaluation of TbpB as potential vaccine antigen

TbpB, a protein responsive to varying iron concentrations was shown to be surface-exposed by flow cytometry and was approximately two-fold upregulated by iron starvation in NTHI. Additionally, low amounts of TbpB were detected in NTHI culture supernatant (these studies). In the literature this has not yet been reported. Previous analyses revealed that TbpB is a lipoprotein that independently binds especially the iron-loaded form of transferrin (65, 117). Antibodies raised against the recombinant NTHI protein expressed in *E. coli* were cross-reactive and recognized the respective native protein in *M. catarrhalis* lysate. Both, Western blot analysis and Microarray analysis showed that TbpB is also upregulated in *M. catarrhalis* during iron depletion. Whereas antibodies against *M. catarrhalis* TbpB have been reported to promote bactericidal killing of *M. catarrhalis* (126), it is at present unknown whether antibodies raised against NTHI TbpB also have a bactericidal effect on *M. catarrhalis* or vice versa. If immunization with a single protein could provide protection against *M. catarrhalis* and NTHI, this would mean an enormeous advantage pertaining to vaccine development against this polymicrobial disease. It will be essential to test whether antibodies against this protein are capable of preventing iron uptake from transferrin.

7.4 Protective *M. catarrhalis* antigens

Eight *M. catarrhalis* candidate antigens selected by AIP® were chosen for testing in a mouse pulmonary clearance model. Vaccination with three of eight candidates showed efficacy in this animal model.

In fact, immunization with the N-terminal "plug" domain of the **TonB-dependent receptor (MCR_0076)** enhanced bacterial clearance in this model. TonB-dependent proteins are outer membrane proteins which bind and transport iron. This active process requires energy from the proton motive force as well as the TonB/ExbB/ExbD inner membrane complex. The "plug" domain is a protein fragment of the TonB-dependent receptor that folds independently and, prior to ligand binding, the pore is blocked by this domain (130). Further analyses will be necessary to determine the vaccine potential of this protein fragment. Furthermore, immunization of mice with the recombinant "plug" domain expressed in *E. coli* elicited antibodies that recognize the native protein in bacterial lysate. Interestingly, the antibodies reacted with bacterial lysate of a MCR_0076 gene deletion mutant as well, even though the gene deletion mutant was verified by sequencing and PCR analysis. Therefore, it is unlikely that the generation of the mutant lacking the TonB-dependent receptor gene failed. Analysis of the *M. catarrhalis* RH4 genome revealed the presence of a homologue of MCR_0076, namely MCR_1311. MCR_1311 shows 34.4% amino acid sequence identity with MCR_0076 and encodes the heme utilization protein HumA. In order to provide additional evidence that the correct gene deletion mutant was obtained, Southern blot analysis was performed. A weak signal was obtained with the expected size of the wild type. When genomic wild type DNA is digested with the restriction enzymes *Nco*I and *Afl*II, the probe for MCR_0076 binds a fragment of 2940 bp. If the probe binds MCR_1311, a fragment of 2923 bp would be detected, possibly explaining the weak band in Figure 5-12 (section 5.5.1).

Two further proteins showed protection. Vaccination with an **oligopeptide-binding protein (OppA, MCR_1303)** as well as a ***Moraxella* surface protein 22 (Msp22, MCR_1416)** showed the same effect as MCR_0076, namely enhanced clearance of *M. catarrhalis* from the mouse lung. In parallel, OppA and Msp22 were identified by another research group using a genome mining approach. Ruckdeschel *et al*. (150) examined the potential of Msp22 to elicit a protective immune response in mice. Systemic immunization with the recombinant Msp22 protein resulted in higher IgG levels as

compared to mucosal vaccination. IgA levels were rather poor following mucosal immunization, which was unexpected. Both, systemic and mucosal immunization led to a significant decrease in lung CFU counts mediated by a strong immune response.

Yang *et al*. (198) published protection data on OppA, a highly conserved and immunogenic protein. It is predicted to be located in the periplasm. Possibly, when oligopeptides are bound from the environment, the protein exposes epitopes briefly to the surface prior to transport across the periplasm (198). *M. catarrhalis* encodes five oligopeptide-binding proteins which belong to the ABC transporter family (*oppA*, *oppB*, *oppC*, *oppD*, *oppF*). Oligopeptide-binding proteins play an important role in various mechanisms including nutrient uptake, competence, adherence and the regulation of gene expression (41).

Due to the fact that immunization with Msp22, OppA or MCR_0076 conferred protection in the present studies, these three antigens should be further tested for their suitability as vaccines in an animal model of otitis media. In addition, it will be of great value to test whether the deletion of these genes would have an impact on *M. catarrhalis* virulence.

7.4.1 Msp22, a novel *M. catarrhalis* antigen – part of a future vaccine?

The Msp22 protein was studied in more detail by the generation of a gene deletion mutant as well as functional studies of the recombinant protein expressed in *M. catarrhalis*. HIS-tagged Msp22 could be expressed and purified from *M. catarrhalis* from the soluble fraction using a plasmid derived from *M. catarrhalis* (pEMCJH04-KAN) (72). This allowed the examination of the correctly folded, native protein in the functional assays.

I could show that Msp22 is covalently attached to heme, and the heme exhibits peroxidase activity. In order to explore whether the CXXCH motif is indeed required for heme binding of Msp22, point mutations within the motif will have to be generated. Bingham-Ramos and Hendrixson have analyzed two putative cytochrome *c* peroxidases of *Campylobacter jejuni* (16). They were able to detect heme binding applying the method by Feissner *et al*. (55). However, the creation of point mutations within the CXXCH motif resulted in unstable proteins which could no longer be detected by Western blot analysis of whole bacterial lysates (16). If this holds true for *M. catarrhalis* protein Msp22 as well remains to be elucidated.

It is unknown whether Msp22 functions as cytochrome *c* in *M. catarrhalis*. In general, bacteria extract energy mainly from redox reactions such as the oxidation of sugars (respiration). In an aerobic environment, O_2 serves as terminal receptor for electrons and is thus reduced to water. Cytochrome *c* is part of an electron transport chain and is a highly conserved protein present in a wide variety of species, ranging from unicellular organisms to plants and animals. *c* type cytochromes are heme bound proteins and the heme is attached via two thioether bonds to the CXXCH motif (vinyl group of heme and cysteine residue sulfurs of the CXXCH motif) (6). The heme group and the polypeptide are independently transported across the cytoplasmic membrane to the periplasmic space where posttranslational modification of the apo-cytochrome occurs and the heme is attached to the polypeptide. The heme group accepts electrons from the b-c1 complex and transfers them to the cytochrome oxidase complex. The iron cofactor of the heme group interconverts between the two oxidation states Fe^{2+} (reduced) and Fe^{3+} (oxidized). It can have several functions including heme-dependent peroxidase activity and initiation of apoptosis in more complex organisms. Many bacteria have an alternative electron transport chain which allows aerobic growth independently of cytochrome *c*. Therefore, a mutant lacking cytochrome *c* is still viable (203).

The deletion of eight selected genes in *M. catarrhalis* did not have a major effect on bacterial growth. However, the addition of Desferal® to the chemically defined medium revealed an augmented sensitivity of the *msp22* gene deletion mutant compared to the wild type and the remaining gene deletion mutants. Therefore, the protein Msp22 and the *msp22* gene deletion mutant were examined in most detail in these studies. Microarray analysis revealed that the neighbouring genes of *msp22* were not affected by the gene deletion. This finding excluded possible downstream effects of the gene deletion and therefore confirmed that the phenotype could be attributed to the *msp22* gene deletion. It has recently been shown to be an interesting vaccine candidate and is immunogenic in mice and rabbits. It is expressed in multiple strains and enhanced clearance was shown after immunization with recombinant protein in a mouse pulmonary clearance model ((150), these studies). Msp22 is highly conserved, has homology to cytochrome *c* and may be involved in the transport of divalent cations (151). The annotation Msp22 refers to the molecular weight of this protein which consists of 152 amino acids. However, in fact, its molecular weight amounts to about 17 kDa, and not 22 kDa as published by Ruckdeschel *et al*. (150, 151). This was shown by both, Western blot

analysis and an online tool used for the calculation of the molecular weight (sequence manipulation suite). Moreover, Western blot as well as Microarray analysis revealed that the expression levels of this protein were equal in the presence of varying iron concentrations.

The location of Msp22 has not yet been verified. Surface staining of bacteria did not result in a strong signal. However, this does not mean that the protein is not surface-exposed. Possibly, this protein is not abundant on the surface or not easily accessible for antibodies. In some gram-negative bacteria, different electron transfer mechanisms, which necessitate *c* type cytochromes to be positioned in the outer membrane rather than in the periplasm, are present (164). Even though Msp22 was not identified by the proteomic approach, Western blot analysis confirmed that it was present in OMVs.

In summary, this protein should be considered a potential vaccine antigen due to its conservation among most *M. catarrhalis* strains, immunogenicity and capability to enhance bacterial clearance significantly.

7.4.2 The suitability of the *M. catarrhalis* shuttle vector pEMCJH04-KAN for complementation experiments and recombinant protein expression

So far, two vectors which are potentially suitable for the expression of heterologous genes in *M. catarrhalis* have been identified (72, 188). In these studies, complementation of the *msp22* gene deletion mutant was attempted using vector pEMCJH04-KAN. Due to the fact that the vector pEMCJH04-KAN does not contain a universal *M. catarrhalis* promoter, the promoter sequence of the gene to be heterologously expressed had to be included. For that purpose, an online prediction tool (www.fruitfly.org) which allows the prediction of potential prokaryotic promoters was useful. In practice, more than one potential promoter was identified and therefore, it was necessary to include a reasonably long DNA sequence upstream when amplifying the gene from genomic DNA with the corresponding promoter sequence. These studies showed that *M. catarrhalis* strain RH4 could be transformed with the empty shuttle vector as well as with the plasmid expressing the heterologous gene. Interestingly, it was more difficult to transform the *msp22* gene deletion mutant with the shuttle vector than the wild type strain, with a 10 – 130x decreased transformation efficacy. The heterologous expression of Msp22 was confirmed by Western blot analysis which revealed overexpression of Msp22 in

transformed strains. However, the attempt to rescue the *msp22* gene deletion mutant phenotype failed because bacteria transformed with the shuttle vector showed a prolonged lag-phase in BHI medium. In chemically defined medium, bacteria carrying pEMCJH04-KAN-Msp22 could not grow at all. In order to exclude the possibility that this was due to the heterologous gene, the empty vector was also transformed. It could be shown that the empty vector alone caused the growth inhibition or the prolonged lag-phase respectively.

An alternative approach to overcome this problem would be to reinsert the gene into the *M. catarrhalis* genome at a different location. As the genome sequence of strain RH4 has recently been published (40), it will be possible to discover regions within the genome which are non-functional and suitable for reinsertion of deleted genes (not possible during these studies).

Furthermore, the shuttle vector pEMCJH04-KAN was also appropriate for the heterologous expression of a HIS-tagged *M. catarrhalis* protein. Msp22 was expressed in *M. catarrhalis* with a C-terminal HIS-tag and subsequently purified from the soluble fraction. This approach had the advantage that the protein was significantly overexpressed and could easily be purified using Ni-sepharose beads. In contrast, Msp22 recombinantly expressed in *E. coli* had to be purified from the insoluble fraction which hampered protein purification. Moreover, the expression of Msp22 in its host *M. catarrhalis* potentially increased the likelihood for correct protein folding, and thus the heterologously expressed protein probably corresponded to the native form rather than protein recombinantly expressed in *E.coli*. This method could be applied to literally all *M. catarrhalis* proteins and could facilitate functional studies.

7.5 Broad analysis of *M. catarrhalis* gene expression by Microarray analysis – the global effect of iron

The analysis of gene expression during iron limitation gave a broad overview of genes affected by the specific removal of iron from the growth medium on mRNA basis. Iron is known to play an essential role in several metabolic pathways, enzymatic reactions and the regulation of gene expression (202). The entire genome was analyzed in parallel, and expression levels of all genes could be determined and compared.

The Microarray analysis revealed a number of proteins that are repressed by iron in *M. catarrhalis*. However, no overlap between these proteins and the 23 lead vaccine candidates selected by AIP® was observed. Yet, there was overlap between the 214 candidates initially identified by the antigenome technology and proteins that were found to be upregulated during iron depletion by Microarray analysis and qRT-PCR (CopB, TbpB and LbpA). These observations strongly supported the hypothesis, that iron transporters are (over)expressed during infection *in vivo* under iron-limiting conditions in the human host due to their selection by AIP® with human antibodies. Proteins which were downregulated during iron starvation were not selected by the antigenome approach. Downregulated proteins included outer membrane protein E (OmpE) and bacterioferritin A (BfrA). Therefore, proteins which are downregulated in this specific environment might not be recognized by the human immune system and thus no or only low titers of antibodies are generated. Some of the candidates identified to be up- or down regulated during iron limitation were already known to be regulated by iron, including CopB (4). The identification of these proteins served as suitable control for the experiment. However, in addition to the candidates whose expression was known to be affected by iron limitation, novel canditates could be identified. For example, the expression of the hypothetical protein MCR_0218 was almost eight-fold upregulated in the *M. catarrhalis* wild type upon iron depletion. The gene is situated between the lactoferrin-binding proteins, in reverse orientation. Whether this protein is indeed involved in iron transport remains unclear. Another hypothetical protein (MCR_0593) was significantly downregulated during iron starvation. The generation of gene deletions within these genes would shed light on the essentiality of these proteins. Moreover, the evaluation of different iron sources would provide information about the possible function of these proteins with regard to iron metabolism.

The results obtained by Microarray analysis thus provide the basis for future studies to potentially identify novel mechanisms of iron transport in *M. catarrhalis*.

7.6 Conclusion - The challenge of developing a vaccine against a polymicrobial disease

Otitis media is a very common childhood disease with multiple environmental and genetic factors involved that favour the development of the disease (136, 149). In addition, otitis media is caused by different bacterial pathogens as well as respiratory viruses. It is a major challenge to identify and evaluate potential vaccine candidates as there are a number of requirements that need to be fulfilled in order for a candidate antigen to be included in a vaccine. Preferably, the protein should be conserved among all strains of a species, surface-exposed and thus accessible for antibodies, immunogenic, and elicit a protective immune response (112, 113). It is also of advantage if the protein is not subject to phase variation. An additional challenge for vaccine development is the identification of suitable correlates of protection. For *M. catarrhalis*, no such correlates of protection have been discovered to date. This might be due to the fact that this bacterium has not been considered a pathogen for a long time (26). Moreover, *M. catarrhalis* and NTHI are exclusively human pathogens which do not cause disease in animals naturally. This complicates the setup of animal experiments and might lead to inconclusive data. However, in spite of these problems and challenges, a lot of progress has been made in the field. Several potential antigens are currently being tested, and the identification of novel antigens provides hope that we are a step closer to the development of a vaccine to prevent otitis media disease and a relief of the economic burden associated with it. This present study has confirmed that the antigenome technology is a suitable tool and fair method to discover antigens that might play a crucial role in pathogenesis. In addition to already well known vaccine candidates, novel proteins were detected and analyzed, supported by proteomic analyses. These novel proteins are of special interest, in particular hypothetical proteins to which no function has yet been attributed. Further studies will be essential in order to evaluate the vaccine potential of these antigens. For that purpose, different formulations including various combinations of antigens as well as suitable adjuvants to stimulate protective immune responses need to be examined.

In vitro analysis of the candidates allowed the identification of iron-regulated proteins from *M. catarrhalis* and NTHI. For a future vaccine, the use of such iron-regulated proteins should be taken into consideration as some of these proteins were also shown to be surface-exposed (TbpB and HxuA).

In summary, these studies provided a broad basis for further research related to vaccine development against otitis media. The identification of the three protective *M. catarrhalis* vaccine candidates Msp22, OppA and MCR_0076 as well as the characterization and evaluation of candidate antigens involved in iron transport indicate that future studies should aim at a detailed characterization of these antigens, including their capability to induce serum bactericidal activity. This will require the setup of suitable *in vitro* assays as well as the identification of correlates of protection.

8 References

1. **Adhami, M., and S. Tohme.** 2010. Complications of acute otitis media in children: case reports and review of literature. Le Journal medical libanais **58:**231-237.
2. **Aebi, C., L. D. Cope, J. L. Latimer, S. E. Thomas, C. A. Slaughter, G. H. McCracken, Jr., and E. J. Hansen.** 1998. Mapping of a protective epitope of the CopB outer membrane protein of Moraxella catarrhalis. Infection and immunity **66:**540-548.
3. **Aebi, C., I. Maciver, J. L. Latimer, L. D. Cope, M. K. Stevens, S. E. Thomas, G. H. McCracken, Jr., and E. J. Hansen.** 1997. A protective epitope of Moraxella catarrhalis is encoded by two different genes. Infection and immunity **65:**4367-4377.
4. **Aebi, C., B. Stone, M. Beucher, L. D. Cope, I. Maciver, S. E. Thomas, G. H. McCracken, Jr., P. F. Sparling, and E. J. Hansen.** 1996. Expression of the CopB outer membrane protein by Moraxella catarrhalis is regulated by iron and affects iron acquisition from transferrin and lactoferrin. Infection and immunity **64:**2024-2030.
5. **Akimana, C., and E. R. Lafontaine.** 2007. The Moraxella catarrhalis outer membrane protein CD contains two distinct domains specifying adherence to human lung cells. FEMS microbiology letters **271:**12-19.
6. **Allen, J. W., E. B. Sawyer, M. L. Ginger, P. D. Barker, and S. J. Ferguson.** 2009. Variant c-type cytochromes as probes of the substrate specificity of the E. coli cytochrome c maturation (Ccm) apparatus. The Biochemical journal **419:**177-184, 172 p following 184.
7. **Attia, A. S., E. R. Lafontaine, J. L. Latimer, C. Aebi, G. A. Syrogiannopoulos, and E. J. Hansen.** 2005. The UspA2 protein of Moraxella catarrhalis is directly involved in the expression of serum resistance. Infection and immunity **73:**2400-2410.
8. **Badr, W. H., D. Loghmanee, R. J. Karalus, T. F. Murphy, and Y. Thanavala.** 1999. Immunization of mice with P6 of nontypeable Haemophilus influenzae: kinetics of the antibody response and IgG subclasses. Vaccine **18:**29-37.
9. **Bagg, A., and J. B. Neilands.** 1987. Ferric uptake regulation protein acts as a repressor, employing iron (II) as a cofactor to bind the operator of an iron transport operon in Escherichia coli. Biochemistry **26:**5471-5477.
10. **Bakaletz, L. O.** 2009. Chinchilla as a robust, reproducible and polymicrobial model of otitis media and its prevention. Expert review of vaccines **8:**1063-1082.

11. **Bakaletz, L. O., and S. J. Barenkamp.** 1994. Localization of high-molecular-weight adhesion proteins of nontypeable Haemophilus influenzae by immunoelectron microscopy. Infection and immunity **62:**4460-4468.

12. **Barenkamp, S. J.** 1996. Immunization with high-molecular-weight adhesion proteins of nontypeable Haemophilus influenzae modifies experimental otitis media in chinchillas. Infection and immunity **64:**1246-1251.

13. **Barenkamp, S. J., and F. F. Bodor.** 1990. Development of serum bactericidal activity following nontypable Haemophilus influenzae acute otitis media. The Pediatric infectious disease journal **9:**333-339.

14. **Beddek, A. J., and A. B. Schryvers.** 2010. The lactoferrin receptor complex in Gram negative bacteria. Biometals **23:**377-386.

15. **Benevides-Matos, N., and F. Biville.** 2010. The Hem and Has haem uptake systems in Serratia marcescens. Microbiology (Reading, England) **156:**1749-1757.

16. **Bingham-Ramos, L. K., and D. R. Hendrixson.** 2008. Characterization of two putative cytochrome c peroxidases of Campylobacter jejuni involved in promoting commensal colonization of poultry. Infection and immunity **76:**1105-1114.

17. **Block, S. L., G. V. Doern, and M. A. Pfaller.** 2007. Oral beta-lactams in the treatment of acute otitis media. Diagnostic microbiology and infectious disease **57:**19S-30S.

18. **Bonnah, R. A., R. H. Yu, H. Wong, and A. B. Schryvers.** 1998. Biochemical and immunological properties of lactoferrin binding proteins from Moraxella (Branhamella) catarrhalis. Microbial pathogenesis **24:**89-100.

19. **Britton, J.** 2010. Passive smoking damages children's health. The Practitioner **254:**27-30, 23.

20. **Bryant, K. A., S. L. Block, S. A. Baker, W. C. Gruber, and D. A. Scott.** 2010. Safety and immunogenicity of a 13-valent pneumococcal conjugate vaccine. Pediatrics **125:**866-875.

21. **Budhani, R. K., and J. K. Struthers.** 1998. Interaction of Streptococcus pneumoniae and Moraxella catarrhalis: investigation of the indirect pathogenic role of beta-lactamase-producing moraxellae by use of a continuous-culture biofilm system. Antimicrobial agents and chemotherapy **42:**2521-2526.

22. **Bullard, B., S. L. Lipski, and E. R. Lafontaine.** 2005. Hag directly mediates the adherence of Moraxella catarrhalis to human middle ear cells. Infection and immunity **73:**5127-5136.

23. **Campagnari, A. A., K. L. Shanks, and D. W. Dyer.** 1994. Growth of Moraxella catarrhalis with human transferrin and lactoferrin: expression of iron-repressible proteins without siderophore production. Infection and immunity **62:**4909-4914.

24. **Carrondo, M. A.** 2003. Ferritins, iron uptake and storage from the bacterioferritin viewpoint. The EMBO journal **22:**1959-1968.

25. **Casey, J. R., D. G. Adlowitz, and M. E. Pichichero.** 2010. New patterns in the otopathogens causing acute otitis media six to eight years after introduction of pneumococcal conjugate vaccine. The Pediatric infectious disease journal **29:**304-309.

26. **Catlin, B. W.** 1990. Branhamella catarrhalis: an organism gaining respect as a pathogen. Clinical microbiology reviews **3:**293-320.

27. **Chen, D., V. Barniak, K. R. VanDerMeid, and J. C. McMichael.** 1999. The levels and bactericidal capacity of antibodies directed against the UspA1 and UspA2 outer membrane proteins of Moraxella (Branhamella) catarrhalis in adults and children. Infection and immunity **67:**1310-1316.

28. **Chen, D., J. C. McMichael, K. R. VanDerMeid, D. Hahn, T. Mininni, J. Cowell, and J. Eldridge.** 1996. Evaluation of purified UspA from Moraxella catarrhalis as a vaccine in a murine model after active immunization. Infection and immunity **64:**1900-1905.

29. **Chen, D., J. C. McMichael, K. R. VanDerMeid, A. W. Masi, E. Bortell, J. D. Caplan, D. N. Chakravarti, and V. L. Barniak.** 1999. Evaluation of a 74-kDa transferrin-binding protein from Moraxella (Branhamella) catarrhalis as a vaccine candidate. Vaccine **18:**109-118.

30. **Chu, B. C., R. S. Peacock, and H. J. Vogel.** 2007. Bioinformatic analysis of the TonB protein family. Biometals **20:**467-483.

31. **Coiffier, T., and E. N. Garabedian.** 1998. [Recurrent and long-lasting otitis media in children]. La Revue du praticien **48:**867-870.

32. **Cope, L. D., Z. Hrkal, and E. J. Hansen.** 2000. Detection of phase variation in expression of proteins involved in hemoglobin and hemoglobin-haptoglobin binding by nontypeable Haemophilus influenzae. Infection and immunity **68:**4092-4101.

33. **Cope, L. D., S. E. Thomas, Z. Hrkal, and E. J. Hansen.** 1998. Binding of heme-hemopexin complexes by soluble HxuA protein allows utilization of this complexed heme by Haemophilus influenzae. Infection and immunity **66:**4511-4516.

34. **Cope, L. D., R. Yogev, U. Muller-Eberhard, and E. J. Hansen.** 1995. A gene cluster involved in the utilization of both free heme and heme:hemopexin by Haemophilus influenzae type b. Journal of bacteriology **177:**2644-2653.

35. **Corbeel, L.** 2007. What is new in otitis media? European journal of pediatrics **166:**511-519.

36. **Cripps, A. W., and D. C. Otczyk.** 2006. Prospects for a vaccine against otitis media. Expert review of vaccines **5:**517-534.

37. **Cripps, A. W., D. C. Otczyk, and J. M. Kyd.** 2005. Bacterial otitis media: a vaccine preventable disease? Vaccine **23:**2304-2310.

38. **Damoiseaux, R. A.** 2005. Antibiotic treatment for acute otitis media: time to think again. Cmaj **172:**657-658.

39. **de Vries, S. P., H. J. Bootsma, J. P. Hays, and P. W. Hermans.** 2009. Molecular aspects of Moraxella catarrhalis pathogenesis. Microbiol Mol Biol Rev **73:**389-406.

40. **de Vries, S. P., S. A. van Hijum, W. Schueler, K. Riesbeck, J. P. Hays, P. W. Hermans, and H. J. Bootsma.** 2010. Genome analysis of Moraxella catarrhalis strain RH4, a human respiratory tract pathogen. Journal of bacteriology **192:**3574-3583.

41. **Doeven, M. K., J. Kok, and B. Poolman.** 2005. Specificity and selectivity determinants of peptide transport in Lactococcus lactis and other microorganisms. Molecular microbiology **57:**640-649.

42. **Doherty, C. P.** 2007. Host-pathogen interactions: the role of iron. The Journal of nutrition **137:**1341-1344.

43. **Du, R. P., Q. Wang, Y. P. Yang, A. B. Schryvers, P. Chong, M. H. Klein, and S. M. Loosmore.** 1998. Cloning and expression of the Moraxella catarrhalis lactoferrin receptor genes. Infection and immunity **66:**3656-3665.

44. **Dubreuil, C.** 2001. [Inflammation and acute otitis media]. Presse Med **30:**19-25.

45. **Duchesne, P., D. Grenier, and D. Mayrand.** 1995. Demonstration of adherence properties of Porphyromonas gingivalis outer membrane vesicles using a new microassay. Oral microbiology and immunology **10:**76-80.

46. **Duim, B., P. Ruiter, L. D. Bowler, J. Dankert, and L. van Alphen.** 1997. Sequence variation in the hpd gene of nonencapsulated Haemophilus influenzae isolated from patients with chronic bronchitis. Gene **191:**57-60.

47. **Easton, D. M., A. Smith, S. G. Gallego, A. R. Foxwell, A. W. Cripps, and J. M. Kyd.** 2005. Characterization of a novel porin protein from Moraxella catarrhalis and identification of an immunodominant surface loop. Journal of bacteriology **187:**6528-6535.

48. **Ellis, T. N., and M. J. Kuehn.** 2010. Virulence and immunomodulatory roles of bacterial outer membrane vesicles. Microbiol Mol Biol Rev **74:**81-94.

49. **Erwin, A. L., and A. L. Smith.** 2007. Nontypeable Haemophilus influenzae: understanding virulence and commensal behavior. Trends in microbiology **15:**355-362.

50. **Escolar, L., J. Perez-Martin, and V. de Lorenzo.** 1999. Opening the iron box: transcriptional metalloregulation by the Fur protein. Journal of bacteriology **181:**6223-6229.

51. **Faden, H.** 2001. The microbiologic and immunologic basis for recurrent otitis media in children. European journal of pediatrics **160:**407-413.

52. **Faden, H., J. Bernstein, L. Brodsky, J. Stanievich, D. Krystofik, C. Shuff, J. J. Hong, and P. L. Ogra.** 1989. Otitis media in children. I. The systemic immune response to nontypable Hemophilus influenzae. The Journal of infectious diseases **160:**999-1004.

53. **Faden, H., L. Brodsky, J. Bernstein, J. Stanievich, D. Krystofik, C. Shuff, J. J. Hong, and P. L. Ogra.** 1989. Otitis media in children: local immune response to nontypeable Haemophilus influenzae. Infection and immunity **57:**3555-3559.

54. **Falsone, S. F., B. Gesslbauer, A. Rek, and A. J. Kungl.** 2007. A proteomic approach towards the Hsp90-dependent ubiquitinylated proteome. Proteomics **7:**2375-2383.

55. **Feissner, R., Y. Xiang, and R. G. Kranz.** 2003. Chemiluminescent-based methods to detect subpicomole levels of c-type cytochromes. Analytical biochemistry **315:**90-94.

56. **Forsgren, A., M. Brant, M. Karamehmedovic, and K. Riesbeck.** 2003. The immunoglobulin D-binding protein MID from Moraxella catarrhalis is also an adhesin. Infection and immunity **71:**3302-3309.

57. **Forsgren, A., M. Brant, and K. Riesbeck.** 2004. Immunization with the truncated adhesin moraxella catarrhalis immunoglobulin D-binding protein (MID764-913) is protective against M. catarrhalis in a mouse model of pulmonary clearance. The Journal of infectious diseases **190:**352-355.

58. **Fritzer, A., B. M. Senn, D. B. Minh, M. Hanner, D. Gelbmann, B. Noiges, T. Henics, K. Schulze, C. A. Guzman, J. Goodacre, A. von Gabain, E. Nagy, and A. L. Meinke.** 2010. Novel conserved group A streptococcal proteins identified by the antigenome technology as vaccine candidates for a non-M protein-based vaccine. Infection and immunity **78:**4051-4067.

59. **Furano, K., and A. A. Campagnari.** 2003. Inactivation of the Moraxella catarrhalis 7169 ferric uptake regulator increases susceptibility to the bactericidal activity of normal human sera. Infection and immunity **71:**1843-1848.

60. **Furano, K., N. R. Luke, A. J. Howlett, and A. A. Campagnari.** 2005. Identification of a conserved Moraxella catarrhalis haemoglobin-utilization protein, MhuA. Microbiology (Reading, England) **151:**1151-1158.

61. **Gesslbauer, B., E. Krenn, C. Zenzmaier, K. H. Preisegger, and A. J. Kungl.** 2006. Lessons from the stem cell proteome. Current stem cell research & therapy **1:**395-409.

62. **Giebink, G. S.** 1999. Otitis media: the chinchilla model. Microbial drug resistance (Larchmont, N.Y **5:**57-72.

63. **Giefing, C., A. L. Meinke, M. Hanner, T. Henics, M. D. Bui, D. Gelbmann, U. Lundberg, B. M. Senn, M. Schunn, A. Habel, B. Henriques-Normark, A. Ortqvist, M. Kalin, A. von Gabain, and E. Nagy.** 2008. Discovery of a novel class of highly conserved vaccine antigens using genomic scale antigenic fingerprinting of pneumococcus with human antibodies. The Journal of experimental medicine **205:**117-131.

64. **Goodwin, J. H., and J. C. Post.** 2002. The genetics of otitis media. Current allergy and asthma reports **2:**304-308.

65. **Gray-Owen, S. D., and A. B. Schryvers.** 1995. Characterization of transferrin binding proteins 1 and 2 in invasive type b and nontypeable strains of Haemophilus influenzae. Infection and immunity **63:**3809-3815.

66. **Griffiths, E.** 1991. Iron and bacterial virulence--a brief overview. Biology of metals **4:**7-13.

67. **Guignot, J., C. Chaplais, M. H. Coconnier-Polter, and A. L. Servin.** 2007. The secreted autotransporter toxin, Sat, functions as a virulence factor in Afa/Dr diffusely adhering Escherichia coli by promoting lesions in tight junction of polarized epithelial cells. Cellular microbiology **9:**204-221.

68. **Hallstrom, T., T. Nordstrom, T. T. Tan, T. Manolov, J. D. Lambris, D. E. Isenman, P. F. Zipfel, A. M. Blom, and K. Riesbeck.** 2011. Immune evasion of Moraxella catarrhalis involves ubiquitous surface protein A-dependent C3d binding. J Immunol **186:**3120-3129.

69. **Hallstrom, T., F. Resman, M. Ristovski, and K. Riesbeck.** 2010. Binding of complement regulators to invasive nontypeable Haemophilus influenzae isolates is not increased compared to nasopharyngeal isolates, but serum resistance is linked to disease severity. Journal of clinical microbiology **48:**921-927.

70. **Hanson, M. J.** 1997. Otitis media with effusion. Lippincott's primary care practice **1:**168-171.

71. **Hausdorff, W. P., B. Hoet, and L. Schuerman.** 2010. Do pneumococcal conjugate vaccines provide any cross-protection against serotype 19A? BMC pediatrics **10:**4.

72. **Hays, J. P., K. Eadie, C. M. Verduin, H. Verbrugh, and A. van Belkum.** 2005. A novel plasmid (pEMCJH03) isolated from moraxella catarrhalis possibly useful as a cloning and expression vector within this species. Plasmid **53:**263-268.

73. **Heikkinen, T.** 2000. The role of respiratory viruses in otitis media. Vaccine **19 Suppl 1:**S51-55.

74. **Heikkinen, T., and T. Chonmaitree.** 2003. Importance of respiratory viruses in acute otitis media. Clinical microbiology reviews **16:**230-241.

75. **Helminen, M. E., R. Beach, I. Maciver, G. Jarosik, E. J. Hansen, and M. Leinonen.** 1995. Human immune response against outer membrane proteins of Moraxella (Branhamella) catarrhalis determined by immunoblotting and enzyme immunoassay. Clinical and diagnostic laboratory immunology **2:**35-39.

76. **Helminen, M. E., I. Maciver, J. L. Latimer, L. D. Cope, G. H. McCracken, Jr., and E. J. Hansen.** 1993. A major outer membrane protein of Moraxella catarrhalis is a target for antibodies that enhance pulmonary clearance of the pathogen in an animal model. Infection and immunity **61:**2003-2010.

77. **Helminen, M. E., I. Maciver, M. Paris, J. L. Latimer, S. L. Lumbley, L. D. Cope, G. H. McCracken, Jr., and E. J. Hansen.** 1993. A mutation affecting expression of a major outer membrane protein of Moraxella catarrhalis alters serum resistance and survival in vivo. The Journal of infectious diseases **168:**1194-1201.

78. **Herriott, R. M., E. M. Meyer, and M. Vogt.** 1970. Defined nongrowth media for stage II development of competence in Haemophilus influenzae. Journal of bacteriology **101:**517-524.

79. **Hoberman, A., J. L. Paradise, H. E. Rockette, N. Shaikh, E. R. Wald, D. H. Kearney, D. K. Colborn, M. Kurs-Lasky, S. Bhatnagar, M. A. Haralam, L. M. Zoffel, C. Jenkins, M. A. Pope, T. L. Balentine, and K. A. Barbadora.** 2011. Treatment of acute otitis media in children under 2 years of age. The New England journal of medicine **364:**105-115.

80. **Hol, C., C. M. Verduin, E. E. Van Dijke, J. Verhoef, A. Fleer, and H. van Dijk.** 1995. Complement resistance is a virulence factor of Branhamella (Moraxella) catarrhalis. FEMS immunology and medical microbiology **11:**207-211.

81. **Holland, J., P. R. Langford, K. J. Towner, and P. Williams.** 1992. Evidence for in vivo expression of transferrin-binding proteins in Haemophilus influenzae type b. Infection and immunity **60:**2986-2991.

82. **Holland, J., T. R. Parsons, A. A. Hasan, S. M. Cook, P. Stevenson, E. Griffiths, and P. Williams.** 1996. Conservation and antigenic cross-reactivity of the transferrin-binding proteins of Haemophilus influenzae, Actinobacillus pleuropneumoniae and Neisseria meningitidis. Microbiology (Reading, England) **142 (Pt 12):**3505-3513.

83. **Holm, M. M., S. L. Vanlerberg, I. M. Foley, D. D. Sledjeski, and E. R. Lafontaine.** 2004. The Moraxella catarrhalis porin-like outer membrane protein CD is an adhesin for human lung cells. Infection and immunity **72:**1906-1913.

84. **Hong, W., D. Peng, M. Rivera, and X. X. Gu.** 2010. Protection against nontypeable Haemophilus influenzae challenges by mucosal vaccination with a detoxified lipooligosaccharide conjugate in two chinchilla models. Microbes and infection / Institut Pasteur **12:**11-18.

85. **Hotomi, M., Y. Ikeda, M. Suzumoto, K. Yamauchi, B. A. Green, G. Zlotnick, D. S. Billal, J. Shimada, K. Fujihara, and N. Yamanaka.** 2005. A recombinant P4 protein of Haemophilus influenzae induces specific immune responses biologically active against nasopharyngeal colonization in mice after intranasal immunization. Vaccine **23:**1294-1300.

86. **Hu, W. G., J. Chen, J. F. Battey, and X. X. Gu.** 2000. Enhancement of clearance of bacteria from murine lungs by immunization with detoxified lipooligosaccharide from Moraxella catarrhalis conjugated to proteins. Infection and immunity **68:**4980-4985.

87. **Hytonen, J., S. Haataja, D. Gerlach, A. Podbielski, and J. Finne.** 2001. The SpeB virulence factor of Streptococcus pyogenes, a multifunctional secreted and cell surface molecule with strepadhesin, laminin-binding and cysteine protease activity. Molecular microbiology **39:**512-519.

88. **Ilia, S., G. N. Goulielmos, G. Samonis, and E. Galanakis.** 2008. Host's response in otitis media: understanding genetic susceptibility. The Pediatric infectious disease journal **27:**929-933.

89. **Johnson, R. W., G. McGillivary, P. Denoel, J. Poolman, and L. O. Bakaletz.** 2011. Abrogation of nontypeable Haemophilus influenzae protein D function reduces phosphorylcholine decoration, adherence to airway epithelial cells, and fitness in a chinchilla model of otitis media. Vaccine **29:**1211-1221.

90. **Juni, E., G. A. Heym, and M. Avery.** 1986. Defined medium for Moraxella (Branhamella) catarrhalis. Applied and environmental microbiology **52:**546-551.

91. **Kadioglu, A., J. N. Weiser, J. C. Paton, and P. W. Andrew.** 2008. The role of Streptococcus pneumoniae virulence factors in host respiratory colonization and disease. Nature reviews **6:**288-301.

92. **Kaur, R., J. R. Casey, and M. E. Pichichero.** 2011. Serum antibody response to three non-typeable Haemophilus influenzae outer membrane proteins during acute otitis media and nasopharyngeal colonization in otitis prone and non-otitis prone children. Vaccine **29:**1023-1028.

93. **King, P. T., P. E. Hutchinson, P. D. Johnson, P. W. Holmes, N. J. Freezer, and S. R. Holdsworth.** 2003. Adaptive immunity to nontypeable Haemophilus influenzae. American journal of respiratory and critical care medicine **167:**587-592.

94. **Klein, J. O.** 2011. Is acute otitis media a treatable disease? The New England journal of medicine **364:**168-169.

95. **Kontiokari, T., P. Koivunen, M. Niemela, T. Pokka, and M. Uhari.** 1998. Symptoms of acute otitis media. The Pediatric infectious disease journal **17:**676-679.

96. **Kuehn, M. J., and N. C. Kesty.** 2005. Bacterial outer membrane vesicles and the host-pathogen interaction. Genes & development **19:**2645-2655.

97. **Kyd, J. M., A. W. Cripps, and T. F. Murphy.** 1998. Outer-membrane antigen expression by Moraxella (Branhamella) catarrhalis influences pulmonary clearance. Journal of medical microbiology **47:**159-168.

98. **Lafontaine, E. R., L. D. Cope, C. Aebi, J. L. Latimer, G. H. McCracken, Jr., and E. J. Hansen.** 2000. The UspA1 protein and a second type of UspA2 protein mediate adherence of Moraxella catarrhalis to human epithelial cells in vitro. Journal of bacteriology **182:**1364-1373.

99. **Lafontaine, E. R., N. J. Wagner, and E. J. Hansen.** 2001. Expression of the Moraxella catarrhalis UspA1 protein undergoes phase variation and is regulated at the transcriptional level. Journal of bacteriology **183:**1540-1551.

100. **Lanphear, B. P., R. S. Byrd, P. Auinger, and C. B. Hall.** 1997. Increasing prevalence of recurrent otitis media among children in the United States. Pediatrics **99:**E1.

101. **Lasisi, A. O., O. Olayemi, and A. E. Irabor.** 2008. Early onset otitis media: risk factors and effects on the outcome of chronic suppurative otitis media. Eur Arch Otorhinolaryngol **265:**765-768.

102. **Lavrrar, J. L., and M. A. McIntosh.** 2003. Architecture of a fur binding site: a comparative analysis. Journal of bacteriology **185:**2194-2202.

103. **Li, W. Y., B. N. Wang, F. Q. Zuo, W. Zeng, F. Feng, Y. Kuang, Z. H. Jiang, and M. Y. Li.** 2010. Study on the anti-NTHi infection of Hap recombinant protein in vivo. Xi bao yu fen zi mian yi xue za zhi = Chinese journal of cellular and molecular immunology **26:**635-637, 641.

104. **Lipski, S. L., C. Akimana, J. M. Timpe, R. M. Wooten, and E. R. Lafontaine.** 2007. The Moraxella catarrhalis autotransporter McaP is a conserved surface protein that mediates adherence to human epithelial cells through its N-terminal passenger domain. Infection and immunity **75:**314-324.

105. **Liu, D. F., J. C. McMichael, and S. M. Baker.** 2007. Moraxella catarrhalis outer membrane protein CD elicits antibodies that inhibit CD binding to human mucin and enhance pulmonary clearance of M. catarrhalis in a mouse model. Infection and immunity **75:**2818-2825.

106. **Luke, N. R., and A. A. Campagnari.** 1999. Construction and characterization of Moraxella catarrhalis mutants defective in expression of transferrin receptors. Infection and immunity **67:**5815-5819.

107. **MacArthur, C. J., and D. R. Trune.** 2006. Mouse models of otitis media. Current opinion in otolaryngology & head and neck surgery **14:**341-346.

108. **Maciver, I., M. Unhanand, G. H. McCracken, Jr., and E. J. Hansen.** 1993. Effect of immunization of pulmonary clearance of Moraxella catarrhalis in an animal model. The Journal of infectious diseases **168:**469-472.

109. **Massa, H. M., A. W. Cripps, and D. Lehmann.** 2009. Otitis media: viruses, bacteria, biofilms and vaccines. The Medical journal of Australia **191:**S44-49.

110. **McDonald, S., C. D. Langton Hewer, and D. A. Nunez.** 2008. Grommets (ventilation tubes) for recurrent acute otitis media in children. Cochrane database of systematic reviews (Online)**:**CD004741.

111. **McMichael, J. C.** 2000. Vaccines for Moraxella catarrhalis. Vaccine **19 Suppl 1:**S101-107.

112. **Meinke, A., T. Henics, M. Hanner, D. B. Minh, and E. Nagy.** 2005. Antigenome technology: a novel approach for the selection of bacterial vaccine candidate antigens. Vaccine **23:**2035-2041.

113. **Meinke, A., T. Henics, and E. Nagy.** 2004. Bacterial genomes pave the way to novel vaccines. Current opinion in microbiology **7:**314-320.

114. **Meinke, A., M. Storm, T. Henics, D. Gelbmann, S. Prustomersky, Z. Kovacs, D. B. Minh, B. Noiges, U. Stierschneider, M. Berger, A. von Gabain, L. Engstrand, and E. Nagy.** 2009. Composition of the ANTIGENome of Helicobacter pylori defined by human serum antibodies. Vaccine **27:**3251-3259.

115. **Melhus, A., and A. F. Ryan.** 2000. Expression of cytokine genes during pneumococcal and nontypeable Haemophilus influenzae acute otitis media in the rat. Infection and immunity **68:**4024-4031.

116. **Mollenkvist, A., T. Nordstrom, C. Hallden, J. J. Christensen, A. Forsgren, and K. Riesbeck.** 2003. The Moraxella catarrhalis immunoglobulin D-binding protein MID has conserved sequences and is regulated by a mechanism corresponding to phase variation. Journal of bacteriology **185:**2285-2295.

117. **Moraes, T. F., R. H. Yu, N. C. Strynadka, and A. B. Schryvers.** 2009. Insights into the bacterial transferrin receptor: the structure of transferrin-binding protein B from Actinobacillus pleuropneumoniae. Molecular cell **35:**523-533.

118. **Morton, D. J., T. W. Seale, L. L. Madore, T. M. VanWagoner, P. W. Whitby, and T. L. Stull.** 2007. The haem-haemopexin utilization gene cluster (hxuCBA) as a virulence factor of Haemophilus influenzae. Microbiology (Reading, England) **153:**215-224.

119. **Morton, D. J., P. W. Whitby, H. Jin, Z. Ren, and T. L. Stull.** 1999. Effect of multiple mutations in the hemoglobin- and hemoglobin-haptoglobin-binding proteins, HgpA, HgpB, and HgpC, of Haemophilus influenzae type b. Infection and immunity **67:**2729-2739.

120. **Mulks, M. H., and A. G. Plaut.** 1978. IgA protease production as a characteristic distinguishing pathogenic from harmless neisseriaceae. The New England journal of medicine **299:**973-976.

121. **Murphy, T. F.** 2009. Vaccine development for Moraxella catarrhalis: rationale, approaches and challenges. Expert review of vaccines **8:**655-658.

122. **Murphy, T. F.** 2005. Vaccine development for non-typeable Haemophilus influenzae and Moraxella catarrhalis: progress and challenges. Expert review of vaccines **4:**843-853.

123. **Murphy, T. F., L. O. Bakaletz, J. M. Kyd, B. Watson, and D. L. Klein.** 2005. Vaccines for otitis media: proposals for overcoming obstacles to progress. Vaccine **23:**2696-2702.

124. **Murphy, T. F., A. L. Brauer, N. Yuskiw, and T. J. Hiltke.** 2000. Antigenic structure of outer membrane protein E of Moraxella catarrhalis and construction and characterization of mutants. Infection and immunity **68:**6250-6256.

125. **Murphy, T. F., A. L. Brauer, N. Yuskiw, E. R. McNamara, and C. Kirkham.** 2001. Conservation of outer membrane protein E among strains of Moraxella catarrhalis. Infection and immunity **69:**3576-3580.

126. **Myers, L. E., Y. P. Yang, R. P. Du, Q. Wang, R. E. Harkness, A. B. Schryvers, M. H. Klein, and S. M. Loosmore.** 1998. The transferrin binding protein B of Moraxella catarrhalis elicits bactericidal antibodies and is a potential vaccine antigen. Infection and immunity **66:**4183-4192.

127. **Nakamura, S., M. Shchepetov, A. B. Dalia, S. E. Clark, T. F. Murphy, S. Sethi, J. R. Gilsdorf, A. L. Smith, and J. N. Weiser.** 2011. Molecular basis of increased serum resistance among pulmonary isolates of non-typeable Haemophilus influenzae. PLoS pathogens **7:**e1001247.

128. **Narita, S., and H. Tokuda.** 2007. Amino acids at positions 3 and 4 determine the membrane specificity of Pseudomonas aeruginosa lipoproteins. The Journal of biological chemistry **282:**13372-13378.

129. **Neilands, J. B.** 1995. Siderophores: structure and function of microbial iron transport compounds. The Journal of biological chemistry **270:**26723-26726.

130. **Noinaj, N., M. Guillier, T. J. Barnard, and S. K. Buchanan.** 2010. TonB-dependent transporters: regulation, structure, and function. Annual review of microbiology **64:**43-60.

131. **Nordstrom, T., A. M. Blom, T. T. Tan, A. Forsgren, and K. Riesbeck.** 2005. Ionic binding of C3 to the human pathogen Moraxella catarrhalis is a unique mechanism for combating innate immunity. J Immunol **175:**3628-3636.

132. **Orlova, O. E., and N. P. Vaneeva.** 2007. [Immunity to antigens of nontypeable Haemophilus influenzae strains]. Zhurnal mikrobiologii, epidemiologii, i immunobiologii**:**115-121.

133. **Ostberg, K. L., M. W. Russell, and T. F. Murphy.** 2009. Mucosal immunization of mice with recombinant OMP P2 induces antibodies that bind to surface epitopes of multiple strains of nontypeable Haemophilus influenzae. Mucosal immunology **2:**63-73.

134. **Patel, J. A., S. Nair, K. Revai, J. Grady, K. Saeed, R. Matalon, S. Block, and T. Chonmaitree.** 2006. Association of proinflammatory cytokine gene polymorphisms with susceptibility to otitis media. Pediatrics **118:**2273-2279.

135. **Pearson, M. M., E. R. Lafontaine, N. J. Wagner, J. W. St Geme, 3rd, and E. J. Hansen.** 2002. A hag mutant of Moraxella catarrhalis strain O35E is deficient in hemagglutination, autoagglutination, and immunoglobulin D-binding activities. Infection and immunity **70:**4523-4533.

136. **Pelton, S. I., and E. Leibovitz.** 2009. Recent advances in otitis media. The Pediatric infectious disease journal **28:**S133-137.

137. **Pettersson, A., J. Kortekaas, V. E. Weynants, P. Voet, J. T. Poolman, M. P. Bos, and J. Tommassen.** 2006. Vaccine potential of the Neisseria meningitidis lactoferrin-binding proteins LbpA and LbpB. Vaccine **24:**3545-3557.

138. **Pichichero, M. E., and J. R. Casey.** 2002. Otitis media. Expert opinion on pharmacotherapy **3:**1073-1090.

139. **Pidcock, K. A., J. A. Wooten, B. A. Daley, and T. L. Stull.** 1988. Iron acquisition by Haemophilus influenzae. Infection and immunity **56:**721-725.

140. **Pintor, M., J. A. Gomez, L. Ferron, C. M. Ferreiros, and M. T. Criado.** 1998. Analysis of TbpA and TbpB functionality in defective mutants of Neisseria meningitidis. Journal of medical microbiology **47:**757-760.

141. **Poetker, D. M., D. R. Lindstrom, C. E. Edmiston, C. J. Krepel, T. R. Link, and J. E. Kerschner.** 2005. Microbiology of middle ear effusions from 292 patients undergoing tympanostomy tube placement for middle ear disease. International journal of pediatric otorhinolaryngology **69:**799-804.

142. **Poolman, J. T., L. Bakaletz, A. Cripps, P. A. Denoel, A. Forsgren, J. Kyd, and Y. Lobet.** 2000. Developing a nontypeable Haemophilus influenzae (NTHi) vaccine. Vaccine **19 Suppl 1:**S108-115.

143. **Price, G. A., H. P. Masri, A. M. Hollander, M. W. Russell, and C. N. Cornelissen.** 2007. Gonococcal transferrin binding protein chimeras induce bactericidal and growth inhibitory antibodies in mice. Vaccine **25:**7247-7260.

144. **Prymula, R., P. Peeters, V. Chrobok, P. Kriz, E. Novakova, E. Kaliskova, I. Kohl, P. Lommel, J. Poolman, J. P. Prieels, and L. Schuerman.** 2006. Pneumococcal capsular polysaccharides conjugated to protein D for prevention of acute otitis media caused by both Streptococcus pneumoniae and non-typable Haemophilus influenzae: a randomised double-blind efficacy study. Lancet **367:**740-748.

145. **Prymula, R., and L. Schuerman.** 2009. 10-valent pneumococcal nontypeable Haemophilus influenzae PD conjugate vaccine: Synflorix. Expert review of vaccines **8:**1479-1500.

146. **Ramakrishnan, K., R. A. Sparks, and W. E. Berryhill.** 2007. Diagnosis and treatment of otitis media. American family physician **76:**1650-1658.

147. **Rao, V. K., G. P. Krasan, D. R. Hendrixson, S. Dawid, and J. W. St Geme, 3rd.** 1999. Molecular determinants of the pathogenesis of disease due to non-typable Haemophilus influenzae. FEMS microbiology reviews **23:**99-129.

148. **Rokbi, B., G. Renauld-Mongenie, M. Mignon, B. Danve, D. Poncet, C. Chabanel, D. A. Caugant, and M. J. Quentin-Millet.** 2000. Allelic diversity of the two transferrin binding protein B gene isotypes among a collection of Neisseria meningitidis strains representative of serogroup B disease: implication for the composition of a recombinant TbpB-based vaccine. Infection and immunity **68:**4938-4947.

149. **Rovers, M. M., A. G. Schilder, G. A. Zielhuis, and R. M. Rosenfeld.** 2004. Otitis media. Lancet **363:**465-473.

150. **Ruckdeschel, E. A., A. L. Brauer, A. Johnson, and T. F. Murphy.** 2009. Characterization of proteins Msp22 and Msp75 as vaccine antigens of Moraxella catarrhalis. Vaccine **27:**7065-7072.

151. **Ruckdeschel, E. A., C. Kirkham, A. J. Lesse, Z. Hu, and T. F. Murphy.** 2008. Mining the Moraxella catarrhalis genome: identification of potential vaccine antigens expressed during human infection. Infection and immunity **76:**1599-1607.

152. **Sabirov, A., and D. W. Metzger.** 2008. Mouse models for the study of mucosal vaccination against otitis media. Vaccine **26:**1501-1524.

153. **Sanders, C., S. Turkarslan, D. W. Lee, and F. Daldal.** 2010. Cytochrome c biogenesis: the Ccm system. Trends in microbiology **18:**266-274.

154. **Santolaya de, P. M.** 2007. [Acute otitis media: Diagnosis and treatment]. Rev Chilena Infectol **24:**297-300.

155. **Sassen, M. L., R. Brand, and J. J. Grote.** 1994. Breast-feeding and acute otitis media. American journal of otolaryngology **15:**351-357.

156. **Schaar, V., S. P. de Vries, M. L. Perez Vidakovics, H. J. Bootsma, L. Larsson, P. W. Hermans, A. Bjartell, M. Morgelin, and K. Riesbeck.** 2011. Multicomponent Moraxella catarrhalis outer membrane vesicles induce an inflammatory response and are internalized by human epithelial cells. Cellular microbiology **13:**432-449.

157. **Schryvers, A. B., R. Bonnah, R. H. Yu, H. Wong, and M. Retzer.** 1998. Bacterial lactoferrin receptors. Advances in experimental medicine and biology **443:**123-133.

158. **Schulze, R. J., and W. R. Zuckert.** 2006. Borrelia burgdorferi lipoproteins are secreted to the outer surface by default. Molecular microbiology **59:**1473-1484.

159. **Seale, T. W., D. J. Morton, P. W. Whitby, R. Wolf, S. D. Kosanke, T. M. VanWagoner, and T. L. Stull.** 2006. Complex role of hemoglobin and hemoglobin-haptoglobin binding proteins in Haemophilus influenzae virulence in the infant rat model of invasive infection. Infection and immunity **74:**6213-6225.

160. **Segal, N., N. Givon-Lavi, E. Leibovitz, P. Yagupsky, A. Leiberman, and R. Dagan.** 2005. Acute otitis media caused by Streptococcus pyogenes in children. Clin Infect Dis **41:**35-41.

161. **Sethi, S., J. M. Surface, and T. F. Murphy.** 1997. Antigenic heterogeneity and molecular analysis of CopB of Moraxella (Branhamella) catarrhalis. Infection and immunity **65:**3666-3671.

162. **Seydel, A., P. Gounon, and A. P. Pugsley.** 1999. Testing the '+2 rule' for lipoprotein sorting in the Escherichia coli cell envelope with a new genetic selection. Molecular microbiology **34:**810-821.

163. **Shaaban, K. M., and I. Hamadnalla.** 1993. The effect of duration of breast feeding on the occurrence of acute otitis media in children under three years. East African medical journal **70:**632-634.

164. **Shi, L., T. C. Squier, J. M. Zachara, and J. K. Fredrickson.** 2007. Respiration of metal (hydr)oxides by Shewanella and Geobacter: a key role for multihaem c-type cytochromes. Molecular microbiology **65:**12-20.

165. **Simon, A., and E. Biot.** 2010. ANAIS: analysis of NimbleGen arrays interface. Bioinformatics (Oxford, England) **26:**2468-2469.

166. **Skoner, D. P., P. K. Stillwagon, M. L. Casselbrandt, E. P. Tanner, W. J. Doyle, and P. Fireman.** 1988. Inflammatory mediators in chronic otitis media with effusion. Archives of otolaryngology--head & neck surgery **114:**1131-1133.

167. **Slevogt, H., J. Seybold, K. N. Tiwari, A. C. Hocke, C. Jonatat, S. Dietel, S. Hippenstiel, B. B. Singer, S. Bachmann, N. Suttorp, and B. Opitz.** 2007. Moraxella catarrhalis is internalized in respiratory epithelial cells by a trigger-like mechanism and initiates a TLR2- and partly NOD1-dependent inflammatory immune response. Cellular microbiology **9:**694-707.

168. **Slevogt, H., S. Zabel, B. Opitz, A. Hocke, J. Eitel, D. N'Guessan P, L. Lucka, K. Riesbeck, W. Zimmermann, J. Zweigner, B. Temmesfeld-Wollbrueck, N. Suttorp, and B. B. Singer.** 2008. CEACAM1 inhibits Toll-like receptor 2-triggered antibacterial responses of human pulmonary epithelial cells. Nature immunology **9:**1270-1278.

169. **Sritharan, M.** 2006. Iron and bacterial virulence. Indian journal of medical microbiology **24:**163-164.

170. **St Geme, J. W., 3rd.** 2000. The pathogenesis of nontypable Haemophilus influenzae otitis media. Vaccine **19 Suppl 1:**S41-50.

171. **St Geme, J. W., 3rd, S. Falkow, and S. J. Barenkamp.** 1993. High-molecular-weight proteins of nontypable Haemophilus influenzae mediate attachment to human epithelial cells. Proceedings of the National Academy of Sciences of the United States of America **90:**2875-2879.

172. **Tan, T. T., M. Morgelin, A. Forsgren, and K. Riesbeck.** 2007. Haemophilus influenzae survival during complement-mediated attacks is promoted by Moraxella catarrhalis outer membrane vesicles. The Journal of infectious diseases **195:**1661-1670.

173. **Theodorsson-Norheim, E.** 1986. Kruskal-Wallis test: BASIC computer program to perform nonparametric one-way analysis of variance and multiple comparisons on ranks of several independent samples. Computer methods and programs in biomedicine **23:**57-62.

174. **Thomas, C. E., W. Zhu, C. N. Van Dam, N. L. Davis, R. E. Johnston, and P. F. Sparling.** 2006. Vaccination of mice with gonococcal TbpB expressed in vivo from Venezuelan equine encephalitis viral replicon particles. Infection and immunity **74:**1612-1620.

175. **Thorne, M. C., L. Chewaproug, and L. M. Elden.** 2009. Suppurative complications of acute otitis media: changes in frequency over time. Archives of otolaryngology--head & neck surgery **135:**638-641.

176. **Thyrian, J. R., M. Hanke, W. Hannover, J. Grempler, K. Roske, C. Fusch, and U. John.** 2005. [Exposure to tobacco smoke (passive smoking) in the home and inpatient treatment of children under the age of 5 years in Germany]. Deutsche medizinische Wochenschrift (1946) **130:**1189-1194.

177. **Tonnaer, E. L., E. A. Sanders, and J. H. Curfs.** 2003. Bacterial otitis media: a new non-invasive rat model. Vaccine **21:**4539-4544.

178. **Toropainen, M., A. Raitolehto, I. Henckaerts, D. Wauters, J. Poolman, P. Lestrate, and H. Kayhty.** 2008. Pneumococcal Haemophilus influenzae protein D conjugate

vaccine induces antibodies that inhibit glycerophosphodiester phosphodiesterase activity of protein D. Infection and immunity **76:**4546-4553.

179. **Tristram, S., M. R. Jacobs, and P. C. Appelbaum.** 2007. Antimicrobial resistance in Haemophilus influenzae. Clinical microbiology reviews **20:**368-389.

180. **Trune, D. R., and Q. Y. Zheng.** 2009. Mouse models for human otitis media. Brain research **1277:**90-103.

181. **Upton, C., J. L. Macen, M. Schreiber, and G. McFadden.** 1991. Myxoma virus expresses a secreted protein with homology to the tumor necrosis factor receptor gene family that contributes to viral virulence. Virology **184:**370-382.

182. **Van Effelterre, T., M. R. Moore, F. Fierens, C. G. Whitney, L. White, S. I. Pelton, and W. P. Hausdorff.** 2010. A dynamic model of pneumococcal infection in the United States: implications for prevention through vaccination. Vaccine **28:**3650-3660.

183. **van Gils, E. J., R. H. Veenhoven, E. Hak, G. D. Rodenburg, W. C. Keijzers, D. Bogaert, K. Trzcinski, J. P. Bruin, L. van Alphen, A. van der Ende, and E. A. Sanders.** 2010. Pneumococcal conjugate vaccination and nasopharyngeal acquisition of pneumococcal serotype 19A strains. Jama **304:**1099-1106.

184. **Verduin, C. M., M. Jansze, C. Hol, T. E. Mollnes, J. Verhoef, and H. van Dijk.** 1994. Differences in complement activation between complement-resistant and complement-sensitive Moraxella (Branhamella) catarrhalis strains occur at the level of membrane attack complex formation. Infection and immunity **62:**589-595.

185. **Verhaegh, S. J., A. Streefland, J. K. Dewnarain, D. J. Farrell, A. van Belkum, and J. P. Hays.** 2008. Age-related genotypic and phenotypic differences in Moraxella catarrhalis isolates from children and adults presenting with respiratory disease in 2001-2002. Microbiology (Reading, England) **154:**1178-1184.

186. **Vidakovics, M. L., J. Jendholm, M. Morgelin, A. Mansson, C. Larsson, L. O. Cardell, and K. Riesbeck.** 2010. B cell activation by outer membrane vesicles--a novel virulence mechanism. PLoS pathogens **6:**e1000724.

187. **Vitovski, S., K. T. Dunkin, A. J. Howard, and J. R. Sayers.** 2002. Nontypeable Haemophilus influenzae in carriage and disease: a difference in IgA1 protease activity levels. Jama **287:**1699-1705.

188. **Wang, W., and E. J. Hansen.** 2006. Plasmid pWW115, a cloning vector for use with Moraxella catarrhalis. Plasmid **56:**133-137.

189. **Wang, W., L. Reitzer, D. A. Rasko, M. M. Pearson, R. J. Blick, C. Laurence, and E. J. Hansen.** 2007. Metabolic analysis of Moraxella catarrhalis and the effect of selected in

vitro growth conditions on global gene expression. Infection and immunity **75:**4959-4971.

190. **Webb, D. C., and A. W. Cripps.** 1999. Immunization with recombinant transferrin binding protein B enhances clearance of nontypeable Haemophilus influenzae from the rat lung. Infection and immunity **67:**2138-2144.

191. **Webb, D. C., and A. W. Cripps.** 2000. A P5 peptide that is homologous to peptide 10 of OprF from Pseudomonas aeruginosa enhances clearance of nontypeable Haemophilus influenzae from acutely infected rat lung in the absence of detectable peptide-specific antibody. Infection and immunity **68:**377-381.

192. **Whitby, P. W., T. W. Seale, T. M. VanWagoner, D. J. Morton, and T. L. Stull.** 2009. The iron/heme regulated genes of Haemophilus influenzae: comparative transcriptional profiling as a tool to define the species core modulon. BMC genomics **10:**6.

193. **Whitby, P. W., K. E. Sim, D. J. Morton, J. A. Patel, and T. L. Stull.** 1997. Transcription of genes encoding iron and heme acquisition proteins of Haemophilus influenzae during acute otitis media. Infection and immunity **65:**4696-4700.

194. **Williams, B. J., G. Morlin, N. Valentine, and A. L. Smith.** 2001. Serum resistance in an invasive, nontypeable Haemophilus influenzae strain. Infection and immunity **69:**695-705.

195. **Wilson, R.** 1998. The role of infection in COPD. Chest **113:**242S-248S.

196. **Winter, L. E., and S. J. Barenkamp.** 2009. Antibodies specific for the Hia adhesion proteins of nontypeable Haemophilus influenzae mediate opsonophagocytic activity. Clin Vaccine Immunol **16:**1040-1046.

197. **Yamanaka, N., M. Hotomi, and D. S. Billal.** 2008. Clinical bacteriology and immunology in acute otitis media in children. J Infect Chemother **14:**180-187.

198. **Yang, M., A. Johnson, and T. F. Murphy.** 2011. Characterization and evaluation of the Moraxella catarrhalis oligopeptide permease A as a mucosal vaccine antigen. Infection and immunity **79:**846-857.

199. **Yeh, S. H., A. Gurtman, D. C. Hurley, S. L. Block, R. H. Schwartz, S. Patterson, K. U. Jansen, J. Love, W. C. Gruber, E. A. Emini, and D. A. Scott.** 2010. Immunogenicity and safety of 13-valent pneumococcal conjugate vaccine in infants and toddlers. Pediatrics **126:**e493-505.

200. **Yellon, R. F., G. Leonard, P. T. Marucha, R. Craven, R. J. Carpenter, W. B. Lehmann, J. A. Burleson, and D. L. Kreutzer.** 1991. Characterization of cytokines present in middle ear effusions. The Laryngoscope **101:**165-169.

201. **Yu, R. H., R. A. Bonnah, S. Ainsworth, and A. B. Schryvers.** 1999. Analysis of the immunological responses to transferrin and lactoferrin receptor proteins from Moraxella catarrhalis. Infection and immunity **67:**3793-3799.

Books

202. **Crosa JH, Mey AR, Payne AM.** 2004. Iron transport in Bacteria. ASM Press.

203. **Enggist E, Thöny-Meyer L.** 2004. Advances in Photosynthesis and Respiration Volume 15. Respiration in Archaea and Bacteria. Diversity of Prokaryotic Electron Transport Carriers. Biogenesis of Cytochrome *c*, Chapter 11. Edited by Davide Zannoni. Kluwer Academic Publishers.

9 Equipment

9.1 Chemicals and materials

Chemicals

6x Loading Dye Solution	Fermentas
6x Orange Loading Dye Solution	Fermentas
ABTS	Sigma-Aldrich
AEBSF	Serva
Albumin, Bovine serum	Biomol
Amino acids	Sigma/Fluka/Merck
Aprotinin	Sigma-Aldrich
Aqua Bidestillata	Mayrhofer Pharmazeutika
Bestatin hydrochloride, min. 98%	Sigma-Aldrich
β-NAD	Sigma-Aldrich
Chemicals for media, buffers	Sigma-Adlrich/Fluka
Desferal®	Novartis
dNTP Mix	Invitrogen
DTT	Serva
E-64	Serva
Ethidium Bromide	Sigma-Aldrich
Ethanol	Merck
Fe-sulfate ($FeSO_4*7H_2O$)	Fluka
Gelatin from bovine skin	Sigma-Aldrich
GIBCO™ Kanamycin Sulfate	Invitrogen
HBSS	Gibco
Hemin	Fluka
Hemoglobin (human)	Sigma-Aldrich
Imidazole	Sigma-Aldrich
IPTG	Serva
Lane Marker Non-Reducing Sample Buffer	Pierce
Leupeptin	Serva

N-Lauroylsarcosine, Sodium Salt	AppliChem
Pepstatin A	Serva
Ponceau S Solution	Sigma-Aldrich
S.O.C. Medium	Invitrogen
SimplyBlue™ SafeStain	Invitrogen
Skim Milk Powder	Fluka
Sodium citrate tribasic dihydrate	Sigma-Aldrich
Sodium DL Lactate Solution	Sigma-Aldrich
Spectinomycin dihydrochloride pentahydrate	Sigma-Aldrich
SYTO® 60	Invitrogen
Triton® X-100	Fluka
Trizma® base	Sigma-Aldrich
Tween® 20 SigmaUltra	Sigma-Aldrich
UltraPure™ Agarose	Invitrogen
UltraPure™ Glycogen (20 μg/μl)	Invitrogen
UltraPure™ Phenol:Chloroform:Isoamyl Alcohol, (25:24:1, v/v)	Invitrogen

Antibodies

Penta-His Antibody, mouse anti-(H)5, BSA-free	Qiagen
Polyclonal Rabbit Anti-Mouse Immunoglobulins/HRP	Dako
Goat Anti-Mouse IgG (H + L), Peroxidase AffiniPure F(ab´)2 Fragment	Jackson ImmunoResearch

DNA and protein ladders

DNA Molecular Weight Marker II	Roche
O´GeneRuler™ 100 bp plus DNA ladder	Fermentas
PageRuler™ Plus Prestained Protein Ladder	Fermentas
SigmaMarker™ Wide Molecular Weight Range	Sigma-Aldrich
TrackIt™ 1Kb DNA ladder	Invitrogen

***E. coli* cells**

BL21-CodonPlus® Competent Cells	Stratagene
ElectroMAX™ DH10B™ Cells	Invitrogen
ElectroMAX™ DH5α-E™ Cells	Invitrogen

Enzymes

DN*ase* I	Roche
GoTaq® DNA Polymerase	Promega
Proteinase K Solution	Invitrogen
PWO DNA Polymerase	Roche
Restriction enzymes	New England Biolabs
RN*ase*-free DN*ase* set	Qiagen
RN*ase* A	Promega
SuperScript™ III Reverse Transcriptase (200 U/µl)	Invitrogen
T4 DNA Ligase (1 U/µl)	Invitrogen

Kits

BCA Protein Assay Kit	Pierce
DIG Easy Hyb	Roche
DIG Luminescent Detection Kit	Roche
DIG Wash and Block Buffer Set	Roche
ECL™ Western Blotting Detection Reagents (Amersham)	GE Healthcare
Expand High Fidelity PCR System	Roche
NimbleGen One-Color DNA Labeling Kit	Roche
PCR DIG Probe Synthesis Kit	Roche
PCR Purification Kit	Qiagen
Plasmid mini kit	Qiagen
PureLink™ HiPure Plasmid Filter Midiprep Kit	Invitrogen
PyroGene® recombinant factor C endotoxin detection system	Lonza
RNeasy mini kit	Qiagen
SuperScript® One-Cycle cDNA Kit	Invitrogen

SuperSignal West Femto Maximum Sensitivity Substrate Trial Kit	Pierce
Taxo™ Anaerobe Disc Set	BD diagnostic systems
TURBO DNA-free™ Kit	Ambion
Wizard® Genomic DNA Purification Kit	Promega

Supplementary material

ECL™ Western blotting Detection Reagents	Amersham Biosciences
Gene Pulser® Cuvette (0.1 cm)	Bio-Rad
Glass beads (1.7 – 2.0 mm)	Roth
Hybond-N Nylon membrane	Amersham Biosciences
Hypercassette™	Amersham Biosciences
Hyperfilm™ ECL (Amersham)	GE Healthcare
iBLOT® Gel Transfer Stacks Nitrocellulose	Invitrogen
Immobilon-P Transfer membrane PVDF filter	Millipore
MaxiSorp™ 96-well plates	Nunc
NimbleGen Gene Expression Microarrays	Roche
NimbleScan Software	Roche
Ni Sepharose™ 6 Fast Flow	GE Healthcare
PAGEr® Gold Precast Gels	Lonza
PLASTIBRAND® standard disposable cuvettes	Invitrogen
Random hexamers (3 µg/µl)	Sigma-Aldrich
RNAprotect™ Bacteria Reagent	Qiagen
Slide-A-Lyzer Dialysis Cassettes	Pierce
Spin-X® Centrifuge tube filter, 0.22 µm cellulose acetate in 2ml polypropylene tube	Costar
U96 DeepWell™ Plates	Nunc
Whatman® filter	Whatman International

9.2 Additional strains

M. catarrhalis and NTHI strains for gene distribution analysis. Strains were obtained from G.R. Micro Ltd. and are derived from AOM patients.

Species	Strain ID	Geographic origin
M. catarrhalis	1090122, 1090127, 1091216	Australia
M. catarrhalis	3681122	South Africa
M. catarrhalis	2084130, 2085119, 3079119	Japan
M. catarrhalis	1070122, 1071124, 2070120	South Korea
M. catarrhalis	3696117, 3696119, 3696126	Taiwan
M. catarrhalis	2660116, 2660119, 2660122	Turkey
M. catarrhalis	1510233	Belgium
M. catarrhalis	1502130, 3502122, 3502129	France
M. catarrhalis	3517132, 3518116, 3519121, 3522120	Germany
M. catarrhalis	3650122, 3650134	Hungary
M. catarrhalis	1530120, 2530126, 3530121	Italy
M. catarrhalis	2560117	Portugal
M. catarrhalis	2554135, 3552130, 3553117	Spain
M. catarrhalis	3590123, 3590127, 3590135	Sweden
M. catarrhalis	1041218, 3041116, 3041117	Brazil
M. catarrhalis	1022133, 1023257, 2022135	Canada
M. catarrhalis	1001118, 1001207, 1009124, 1009125	United States
NTHI	1090062, 1090068	Australia
NTHI	6681076, 6682077	South Africa
NTHI	4140081	China
NTHI	1120061	Indonesia
NTHI	1080086, 1081084	Japan
NTHI	1070090, 1071062	South Korea
NTHI	3696091	Taiwan
NTHI	2660082, 4662085	Turkey
NTHI	1130067, 3131080	Austria
NTHI	6400102	Bulgaria
NTHI	6620087	Czech Republic
NTHI	1501076, 6504071	France
NTHI	1521062, 1522072	Germany
NTHI	1530062, 1530079	Italy
NTHI	4641078, 4641092	Poland
NTHI	6671072, 6671084	Russia
NTHI	1551100, 6549074	Spain
NTHI	1610090	Switzerland
NTHI	1541075, 2541085	United Kingdom
NTHI	4051099, 4053085	Argentina
NTHI	1041099, 6040079	Brazil
NTHI	4690100	Colombia
NTHI	3691101	Ecuador
NTHI	3693080	Peru
NTHI	5692120	Venezuela
NTHI	1020080, 1020089	Canada
NTHI	1031068, 1031107	Mexico
NTHI	1001074, 1001081	United States

9.3 Buffers and media

Buffers and solutions

Blocking solution for Western blot	5% Milk powder in 1 x PBS
Laemmli Buffer (10x)	0.25 M Tris, 2 M Glycine, 1% SDS; pH8.5
PBS (10x)	80 g NaCl, 2.0 g KCl, 11.5 g Na_2HPO_4 * 7 H_2O, 2.0 g KH_2PO_4 (per litre); pH7.3
PBST (1x)	1x PBS, 0.05% Tween 20™
Protease inhibitor cocktail I (100x)	100 µl Pepstatin A (1 mg/ml in Ethanol), 10 µl Leupeptin (10 mg/ml in Aqua destillata), 20 µl Aprotinin (5 mg/ml in 10 mM Hepes pH8.0), 870 µl Aqua destillata
Protease inhibitor cocktail II (100x)	4 mM Bestatin 1 mM E-64 100 mM AEBSF (in Aqua destillata)
TAE Buffer (10x)	100 mM Tris, 50 mM Sodium acetate * 3 H_2O, 10 ml 0.5 M EDTA per litre buffer; pH7.8
TE Buffer (1x)	10 mM Tris, 1 mM EDTA; pH8.0
Trace metal stock for enriched LB-medium (2000x)	1.6 g $FeCl_3$ * $6H_2O$, 0.2 g $CoCl_2$, 0.1 g $CuCl_2$, 0.2 g $ZnCl_2$, 0.2 g Na_2MoO_4 * $2H_2O$, 0.05 g H_3BO_3, 10 ml HCl per Litre Aqua destillata

Solutions for Southern blot

SSC (20x)	3 M NaCl, 0.3 M Sodium citrate * $2H_2O$
Denaturation Solution	0.5 M NaOH, 1.5 M NaCl
Neutralization Solution	0.5 M Tris/HCl pH7.5, 1.5 M NaCl
Low Stringency Buffer	2x SSC, 0.1% SDS
High Stringency Buffer	0.5x SSC, 0.1% SDS

Media

BHI Medium (*M. catarrhalis*)	37 g BHI powder per litre Aqua destillata
BHI^+ Medium (NTHI)	BHI medium, 1 - 10 µg/ml hemin, 10 µg/ml NAD
Chemically defined medium for *M. catarrhalis* (1 L)	5.6 g Na_2HPO_4, 2 g KH_2PO_4, 1 g NH_4Cl, 20 ml of 60 % Sodium lactate, 780 ml Aqua destillata, 5 g Aspartic acid, 4 g Proline, 2 g Glycine, 1 g Arginine, 0.2 g L-Methionine, 1.7 mM $MgSO_4$, 0.07 mM $CaCl_2*2H_2O$
Columbia agar + 5% sheep blood	Biomérieux
Enriched LB-Medium	Stock solutions were prepared and added to LB-medium (final amounts per litre medium): 10 g Yeast extract[1], 15 g α-D-Glucose[1], 1.15 g KH_2PO_4[2], 6.27 g $K_2HPO_4*3H_2O$[2], 2 ml Glycerol[2], 250 mg/L $MgSO_4*7H_2O$[2], 1x Trace metal solution[1] [1], stock solution in Aqua destillata [2], stock solution in LB-Medium

LB-Medium	50 g Tryptone, 25 g Yeast extract, 50 g NaCl, 5 g Glucose, 5 g $MgCl_2$ * 6 H_2O, Aqua destillata ad 5 L
LB-Agar	LB medium, 15 g agar/L medium
Mueller Hinton Chocolate Agar	BD diagnostic systems

9.4 Laboratory devices

Block heater	Block heater QBT2, Grant Instruments, U.K.
Centrifuges	HERAEUS Multifuge 3S-R, Kendro Laboratory Products, U.K. Eppendorf Centrifuge 5415R, Eppendorf, Germany. Beckman Avanti™ J-25 Centrifuge, Beckman Coulter, U.S.A.
Concentrator 5301	Eppendorf, Germany.
GenePulser Xcell™	Bio-Rad, U.S.A.
Film processor	Optimax X-Ray Film Processor, Protec Medizintechnik GmbH & Co. KG, Germany.
Flow cytometer	Cell Lab Quanta™ SC Flow Cytometer, Beckman Coulter, U.S.A.
High pressure homogenizer	NS1001L, GEA Niro Soavi, Italy.

Incubators	HeraCell 150, Kendro Laboratory Products, U.K. HERAEUS Kelvitron® T, Kendro Laboratory Products, U.K.
Laminar flow	HeraSafe KS12, Kendro Laboratory Products, U.K.
Magenetic stirrer	MR 3001 K, Heidolph, Germany.
Microplate reader	Synergy 2 Multi-Mode Microplate Reader, BioTek, U.S.A.
Microscope	Axioskop 2 plus, Zeiss, Germany.
PCR Thermocycler	T3 Thermocycler, Biometra®, Germany.
pH Meter	SympHony SB70P, VWR, U.K.
Photometer	NanoDrop 1000 Spectrophotometer, Thermo Fisher Scientific, U.S.A. Eppendorf BioPhotometer, Germany.
Real-Time PCR System	7500 Fast Real-Time PCR System, Applied Biosystems, U.S.A.
Scales	TE1502S, Sartorius, Germany. CP224S, Sartorius, Germany.
Thermomixer	Eppendorf Thermomixer Comfort, Germany.

Ultrasonic homogenizer	Sonopuls Ultrasonic Homogenizer HD2200, Bandelin, Germany. Sonopuls Ultrasonic Homogenizer HD2070, Bandelin, Germany.
Ultracentrifuge	Beckman-Coulter System L8-70, U.S.A.
High Performance UV transilluminator	VWR, U.K.
Vortexer	Vortex Genie 2™, Bender & Hobein AG, Germany.
Western blotting device	iBLOT® Gel Transfer Device, Invitrogen, U.S.A.

10 Appendix I

Proteomics *M. catarrhalis*

***M. catarrhalis* overlaps of proteins identified by the antigenome technology and proteomic analyses.** 1, proteins identified by AIP®; 2, proteins identified from the whole membrane; 3, proteins identified from outer membrane vesicles; 4, proteins identified from outer membrane vesicles (iron-depleted conditions).

ORF	Annotation	1	2	3	4
MCR_0006	guaA; GMP synthase		x	x	
MCR_0008	glycerophosphoryl diester phosphodiesterase	x			
MCR_0015	thiC; thiamine biosynthesis protein ThiC			x	
MCR_0022	dnaK; chaperone protein DnaK		x	x	
MCR_0034	mpl; UDP-N-acetylmuramate:L-alanyl-gamma-D-glutamyl-meso-diaminopimelate ligase	x			
MCR_0036	gshA; glutamate-cysteine ligase	x			
MCR_0042	putative acyl-CoA dehydrogenase FadE		x		
MCR_0047	dapB; dihydrodipicolinate reductase	x			
MCR_0052	hypothetical protein	x	x	x	
MCR_0060	ompR; two-component system response regulator		x		
MCR_0061	RNA binding protein S1	x		x	
MCR_0063	hypothetical protein	x	x	x	
MCR_0064	gltA; citrate synthase			x	
MCR_0068	sdhA; succinate dehydrogenase subunit A	x	x	x	
MCR_0069	sdhB; succinate dehydrogenase subunit B		x		
MCR_0071	sucA; 2-oxoglutarate dehydrogenase E1 component	x	x	x	
MCR_0072	sucB; 2-oxoglutarate dehydrogenase E2 component		x	x	
MCR_0076	TonB-dependent receptor	x			
MCR_0078	hypothetical protein	x			x
MCR_0079	hypothetical protein				x
MCR_0081	prolyl endopeptidase	x			
MCR_0086	RdgB/HAM1 family non-canonical purine NTP pyrophosphatase		x		
MCR_0087	tig; trigger factor TF			x	
MCR_0088	clpP; ATP-dependent Clp protease proteolytic subunit ClpP		x		
MCR_0092	fadA; 3-ketoacyl-CoA thiolase FadA	x			
MCR_0096	cysD; sulfate adenylate transferase subunit 2		x		
MCR_0098	recG; ATP-dependent DNA helicase RecG	x			
MCR_0112	purL; phosphoribosylformylglycinamidine synthase	x	x		
MCR_0115	argA; amino-acid N-acetyltransferase		x		
MCR_0117	putative lipoprotein		x	x	
MCR_0121	dihydrouridine synthase	x			
MCR_0122	putative DNA helicase	x			
MCR_0124	ferredoxin-dependent glutamate synthase	x			
MCR_0130	rplT; 50S ribosomal protein L20		x		
MCR_0131	norB; nitric oxide reductase NorB	x	x		
MCR_0135	aniA; nitrite reductase AniA/Msp78		x	x	x
MCR_0136	hypothetical protein	x			
MCR_0138	SCO1/SenC family protein		x	x	
MCR_0140	pheS; phenylalanyl-tRNA synthetase alpha subunit		x		
MCR_0141	pheT; phenylalanyl-tRNA synthetase beta subunit	x	x		
MCR_0145	mutM; formamidopyrimidine-DNA glycosylase	x			
MCR_0149	putative ATP-dependent DEAD/DEAH box RNA-helicase	x			
MCR_0156	two-component system sensor histidine kinase	x			
MCR_0161	bioF; 8-amino-7-oxononanoate synthase	x	x		
MCR_0168	nadD; nicotinate nucleotide adenylyltransferase	x			
MCR_0169	uvrA; excinuclease ABC subunit A	x			
MCR_0176	metQ; D-methionine ABC transporter substrate binding protein MetQ		x	x	

ORF	Annotation	1	2	3	4
MCR_0180	two-component system response regulator		x	x	
MCR_0184	prsA; ribose-phosphate pyrophosphokinase	x			
MCR_0186	lolB; outer membrane lipoprotein LolB	x	x		
MCR_0187	lolB; outer membrane lipoprotein LolB		x		
MCR_0191	fixC; FAD-dependent oxidoreductase FixC		x		
MCR_0196	mltB; lytic murein transglycosylase	x	x		
MCR_0202	hypothetical protein	x			
MCR_0204	putative lipoprotein			x	
MCR_0207	dienelactone hydrolase		x		
MCR_0217	lbpB; lactoferrin binding protein B LbpB	x	x	x	x
MCR_0219	lbpA; lactoferrin binding protein A LbpA	x	x	x	x
MCR_0220	hypothetical protein		x		
MCR_0223	anthranilate synthase component I	x			
MCR_0225	hypothetical protein		x	x	
MCR_0226	rpsL; 30S ribosomal protein S12		x		
MCR_0227	rpsG; 30S ribosomal protein S7		x		
MCR_0228	fusA; translation elongation factor G		x	x	x
MCR_0229/0250	tuf; translation elongation factor Tu		x	x	
MCR_0233	aroE; shikimate 5-dehydrogenase		x		
MCR_0236	aminodeoxychorismate lyase family protein		x		
MCR_0238	dapA; dihydrodipicolinate synthase		x		
MCR_0240	purC; phosphoribosylaminoimidazole-succinocarboxamide synthase		x		
MCR_0246	hypothetical protein	x			
MCR_0253	rplK; 50S ribosomal protein L11		x		
MCR_0254	rplA; 50S ribosomal protein L1		x		
MCR_0255	rplJ; 50S ribosomal protein L10		x	x	
MCR_0256	rplL; 50S ribosomal protein L7/L12			x	
MCR_0257	rpoB; DNA-directed RNA polymerase subunit beta	x			
MCR_0258	rpoC; DNA-directed RNA polymerase subunit beta'	x	x	x	
MCR_0259	serA; D-3-phosphoglycerate dehydrogenase			x	
MCR_0264	C-terminal processing peptidase-1	x	x	x	x
MCR_0275	smc; condensin subunit Smc	x	x		
MCR_0276	rpsB; 30S ribosomal protein S2	x	x	x	
MCR_0277	tsf; translation elongation factor Ts		x		
MCR_0280	murG; undecaprenyldiphospho-muramoylpentapeptide beta-N-acetylglucosaminyltransferase MurG		x		
MCR_0283	murC; UDP-N-acetylmuramate-alanine ligase MurC	x	x		
MCR_0284	ddlB; D-alanine-D-alanine ligase B DdlB		x		
MCR_0286	LysR family transcriptional regulator		x		
MCR_0287	ahpC; alkyl hydroperoxide reductase subunit C			x	
MCR_0295	fbpA; iron (III) ABC transporter iron binding protein FbpA		x	x	x
MCR_0300	hypothetical protein	x			
MCR_0308	ftsZ; cell division protein FtsZ		x	x	
MCR_0318	TatD-related deoxyribonuclease		x		
MCR_0320	dapD; 2,3,4,5-tetrahydropyridine-2,6-dicarboxylate N-succinyltransferase		x		
MCR_0321	lysophospholipase-like protein	x	x		
MCR_0327	icd; isocitrate dehydrogenase NADP-dependent	x			
MCR_0329	uspA2H; ubiquitous surface protein A2H UspA2H	x	x	x	
MCR_0332	SmpA/OmlA family protein		x		
MCR_0337	nadE; NAD+ synthetase		x		
MCR_0347	dyp-type peroxidase family protein	x			
MCR_0363	uvrC; excinuclease ABC subunit C	x			
MCR_0366	ompJ; outer membrane protein J		x		
MCR_0373	znuA; zinc ABC transporter substrate binding protein ZnuA		x	x	
MCR_0378	atpF; ATP synthase F0 subunit B		x		
MCR_0380	atpA; ATP synthase F1 alpha subunit		x	x	
MCR_0383	atpD; ATP synthase F1 beta subunit		x	x	
MCR_0385	two-component system response regulator		x		
MCR_0391	rplS; 50S ribosomal protein L19		x		
MCR_0394	acnB; aconitase	x	x		
MCR_0400	electron transfer flavoprotein alpha/beta-subunit-like protein		x		
MCR_0401	electron transfer flavoprotein alpha subunit-like protein		x		
MCR_0405	tetratricopeptide repeat family protein	x	x	x	

ORF	Annotation	1	2	3	4
MCR_0406	dihydroorotase-like protein (aspartate carbamoyltransferase non-catalytic chain)	x	x		
MCR_0412	hypothetical protein	x			
MCR_0414	purE; phosphoribosylaminoimidazole carboxylase catalytic subunit	x	x		
MCR_0419	mcaP; Moraxella catarrhalis adherence protein McaP		x	x	x
MCR_0422	serB; phosphoserine phosphatase SerB		x		
MCR_0439	pbp1A; penicillin-binding protein 1A	x			
MCR_0440	htpG; chaperone protein HtpG		x	x	
MCR_0442	gdhA; NAD(P)-specific glutamate dehydrogenase			x	
MCR_0444	adhC; S-(hydroxymethyl)glutathione dehydrogenase/class III alcohol dehydrogenase		x		
MCR_0448	hypothetical protein	x			
MCR_0455	maeB; malate dehydrogenase (oxaloacetate-decarboxylating)		x	x	
MCR_0456	delta-aminolevulinic acid dehydratase		x		
MCR_0465	putative lipoprotein		x		
MCR_0466	ilvD; dihydroxy-acid dehydratase		x		
MCR_0471	histidine triad (HIT) protein		x		
MCR_0474	acrA; RND system membrane fusion protein AcrA	x	x		
MCR_0476	oprM; RND system membrane channel OprM	x	x	x	x
MCR_0477	hypothetical protein		x		
MCR_0488	homoserine dehydrogenase		x		
MCR_0489	protein-disulfide isomerase-like protein	x			
MCR_0491	guaB; inosine-5'-monophosphate dehydrogenase		x		
MCR_0492	copB; outer membrane protein CopB	x	x	x	x
MCR_0500	ileS; isoleucyl-tRNA synthetase	x	x		
MCR_0511	hypothetical protein		x	x	
MCR_0514	hypothetical protein	x			
MCR_0517	valS; valyl-tRNA synthetase	x	x		
MCR_0537	tkt; transketolase	x	x		
MCR_0539	pyrH; uridylate kinase	x	x		
MCR_0546	yaeT; outer membrane protein assembly complex protein YaeT	x	x	x	x
MCR_0555	thioredoxin family protein		x	x	
MCR_0560	hypothetical protein	x			
MCR_0569	NADPH dehydrogenase	x			
MCR_0574	hypothetical protein		x	x	
MCR_0577	purM; phosphoribosylformylglycinamidine cyclo-ligase		x		
MCR_0581	rpmB; 50S ribosomal protein L28		x		
MCR_0584	lysC; aspartate kinase		x		
MCR_0591	alaS; alanyl-tRNA synthetase	x	x		
MCR_0604	hscA; Fe-S protein assembly chaperone HscA	x			
MCR_0608	iscS; cysteine desulfurase IscS		x		
MCR_0614	purH; bifunctional phosphoribosylaminoimidazolecarboxamide formyltransferase/IMP cyclohydrolase		x		
MCR_0617	mid, hag; moraxella IgD binding protein/hemagglutinin MID/Hag	x	x	x	
MCR_0623	mapA; acid phosphatase autotransporter	x			
MCR_0625	pbp1B; penicillin-binding protein 1B	x	x	x	
MCR_0635	ubiE; demethylmenaquinone methyltransferase		x	x	
MCR_0657	YceI family protein		x	x	
MCR_0659	peptidyl-prolyl cis-trans isomerase B		x	x	
MCR_0661	glnS; glutaminyl-tRNA synthetase		x		
MCR_0666	hypothetical protein		x		
MCR_0670	ach1; acetyl-CoA hydrolase		x		
MCR_0677	rpoD; RNA polymerase sigma factor 70		x		
MCR_0681	putative lytic transglycosylase	x			
MCR_0686	msrAB; peptide methionine sulfoxide reductase MsrA/MsrB	x	x	x	x
MCR_0690	tbpA; transferrin binding protein A TbpA	x	x	x	x
MCR_0691	hypothetical protein	x	x	x	
MCR_0692	hypothetical protein	x	x	x	
MCR_0694	tbpB; transferrin binding protein B TbpB	x	x	x	x
MCR_0703	lolA; outer membrane lipocarrier protein LolA		x	x	
MCR_0713	nuoF; NADH-quinone oxidoreductase subunit F	x			
MCR_0714	nuoG; NADH-quinone oxidoreductase subunit G	x	x		
MCR_0728	phosphotyrosine protein phosphatase	x			

ORF	Annotation	1	2	3	4
MCR_0733	hypothetical protein	x			
MCR_0739	mhuA; hemoglobin utilization protein MhuA	x	x	x	x
MCR_0746	narG; nitrate reductase alpha subunit NarG	x			
MCR_0747	narH; nitrate reductase beta subunit NarH	x			
MCR_0754	modA; molybdate ABC transporter substrate binding protein ModA	x			
MCR_0782	DJ-1/PfpI family protein		x		
MCR_0787	msp75; succinic semialdehyde dehydrogenase Msp75	x			
MCR_0791	nadC; nicotinate-nucleotide diphosphorylase	x			
MCR_0795	nadB; L-aspartate oxidase	x			
MCR_0797	TonB-like protein		x		x
MCR_0798	tolQ; MotA/TolQ/ExbB proton channel		x	x	
MCR_0799	tolR; biopolymer transport protein ExbD/TolR			x	
MCR_0801	lon; ATP-dependent protease La		x		
MCR_0807	purA; adenylosuccinate synthetase	x	x		
MCR_0813	ion-like peptidase S16	x			
MCR_0815	parA; chromosome partitioning protein ParA		x		
MCR_0817	ParB-like chromosome partitioning protein	x			
MCR_0822	lldD; L-lactate dehydrogenase		x		
MCR_0828	putative lipoprotein		x		
MCR_0831	ndk; nucleoside diphosphate kinase		x	x	
MCR_0832	hypothetical protein		x	x	
MCR_0840	accC; acetyl-CoA carboxylase biotin carboxylase AccC		x	x	
MCR_0841	accB; acetyl-CoA carboxylase biotin carboxyl carrier protein AccB			x	
MCR_0846	nrdA; ribonucleoside-diphosphate reductase alpha subunit	x			
MCR_0850	trpS; tryptophanyl-tRNA synthetase		x		
MCR_0856	abcZ; ABC transporter ATP-binding protein	x	x		
MCR_0858	ompE; outer membrane protein E		x	x	
MCR_0860	ErfK/YbiS/YcfS/YnhG family protein		x	x	x
MCR_0863	fabH; 3-oxoacyl-ACP synthase III FabH		x	x	
MCR_0865	ung; uracil-DNA glycosylase		x		
MCR_0868	rpsA; 30S ribosomal protein S1	x	x	x	
MCR_0871	pyrF; orotidine 5'-phosphate decarboxylase		x		
MCR_0887	pheA; bifuctional prephenate dehydratase/chorismate mutase		x		
MCR_0888	aroA; 3-phosphoshikimate 1-carboxyvinyltransferase		x		
MCR_0892	aceE; pyruvate dehydrogenase E1 component pyruvate dehydrogenase complex		x	x	
MCR_0893	aceF; pyruvate dehydrogenase E2 component	x		x	
MCR_0894	glutathione S-transferase-like protein		x		
MCR_0896	cysP; sulfate ABC transporter substrate binding protein CysP		x		
MCR_0898	nrdF; ribonucleoside-diphosphate reductase 1 subunit beta		x		
MCR_0900	hypothetical protein		x	x	
MCR_0904	saccharopine dehydrogenase		x		
MCR_0909	arabinose 5-phosphate isomerase	x	x	x	
MCR_0915	delta-1-pyrroline-5-carboxylate dehydrogenase		x	x	
MCR_0917	M16-like peptidase	x	x	x	x
MCR_0918	M16-like peptidase	x	x	x	x
MCR_0920	hypothetical protein		x	x	
MCR_0926	putative lytic murein transglycosylase	x	x	x	
MCR_0934	polyphosphate kinase 2	x			
MCR_0938	peptidase S24-like protein	x			
MCR_0943	hypothetical protein	x			
MCR_0956	hypothetical protein		x	x	
MCR_0960	TP901 family phage tail tape measure protein	x			
MCR_0965	hypothetical protein		x	x	
MCR_0996	hypothetical protein	x		x	
MCR_0999	cysA; sulfate ABC transporter ATP-binding protein CysA		x		
MCR_1000	radA; DNA repair protein RadA	x			
MCR_1003	LysM domain protein	x	x		
MCR_1005	hypothetical protein		x	x	
MCR_1010	dacC; D-alanyl-D-alanine carboxypeptidase	x			
MCR_1011	nhaC; Na+/H+ antiporter NhaC	x			
MCR_1015	LysR family transcriptional regulator		x		
MCR_1018	lysS; lysyl-tRNA synthetase		x	x	

ORF	Annotation	1	2	3	4
MCR_1022	leuB; 3-isopropylmalate dehydrogenase		x		
MCR_1028	fbaB; fructose-bisphosphate aldolase class II		x	x	
MCR_1029	entericidin EcnAB		x	x	
MCR_1030	pgk; phosphoglycerate kinase		x	x	
MCR_1036	alr; alanine racemase Alr	x			
MCR_1038	bfrB; bacterioferritin B		x		
MCR_1039	bfrA; bacterioferritin A		x		
MCR_1041	sdaA; L-serine ammonia-lyase	x	x		
MCR_1042	hypothetical protein		x		
MCR_1053	yfiO; DNA uptake lipoprotein-like protein		x	x	x
MCR_1059	nucleoside-diphosphate-sugar epimerase-like protein	x			
MCR_1061	rpsT; 30S ribosomal protein S20		x		
MCR_1063	C-terminal processing peptidase		x	x	x
MCR_1067	permease family protein	x			
MCR_1070	putative cysteine ABC transporter CydDC	x			
MCR_1072	fumC; fumarate hydratase class II		x	x	
MCR_1078	fabI; NADH-dependent enoyl-ACP reductase FabI		x		
MCR_1082	phospholipase D/transphosphatidylase	x			
MCR_1095	lgt1; glucosyltransferase Lgt1		x		
MCR_1104	ppsA; phosphoenolpyruvate synthase/water dikinase		x		
MCR_1111	aminoglycoside phosphotransferase	x			
MCR_1113	LPS-assembly protein precursor	x	x		
MCR_1115	PpiC-type peptidyl-prolyl cis-trans isomerase	x	x	x	
MCR_1116	putative peptidase M23B	x	x		
MCR_1119	carB; carbamoyl-phosphate synthase large chain	x			
MCR_1128	aminotransferase class I and II	x			
MCR_1139	glnE; glutamate-ammonia-ligase adenylyltransferase	x			
MCR_1140	DsrE/DsrF-like protein	x			
MCR_1161	solanesyl diphosphate synthase		x		
MCR_1166	engA; GTP-binding protein EngA		x		
MCR_1168	yfgL; outer membrane assembly lipoprotein YfgL		x	x	x
MCR_1180	cysE; serine O-acetyltransferase		x		
MCR_1184	S49 family peptidase		x		
MCR_1193	permease family protein			x	
MCR_1198	uspA1; ubiquitous surface protein A1 UspA1	x		x	
MCR_1200	leuA; 2-isopropylmalate synthase	x			
MCR_1208	ABC transporter substrate binding protein		x		
MCR_1217	probable serine protease		x		
MCR_1222	gapA; glyceraldehyde-3-phosphate dehydrogenase		x	x	
MCR_1228	D15 surface antigen family protein	x	x		
MCR_1230	hypothetical protein		x	x	
MCR_1232	putative lipoprotein	x	x		
MCR_1233	adk; adenylate kinase		x		
MCR_1235	cytochrome c biogenesis family protein	x			
MCR_1236	dsbE; periplasmic thiol:disulfide oxidoreductase DsbE		x	x	
MCR_1241	asd; aspartate-semialdehyde dehydrogenase	x			
MCR_1247	outer membrane porin M35		x		x
MCR_1253	dcd; deoxycytidine triphosphate deaminase		x		
MCR_1267	secB; protein translocase chaperone SecB		x		
MCR_1273	hypothetical protein	x	x	x	
MCR_1276	rpsF; 30S ribosomal protein S6		x	x	
MCR_1279	gcvT; glycine cleavage system T protein		x		
MCR_1283	gcvP; glycine dehydrogenase	x		x	
MCR_1287	Na+ solute symporter	x			
MCR_1289	cobyrinic acid a,c-diamide synthase		x		
MCR_1292	phosphatidylethanolamine Kdo2-lipid A phosphoethanolamine transferase	x			
MCR_1295	leuS; leucyl-tRNA synthetase	x	x		
MCR_1301	hypothetical protein	x	x	x	
MCR_1302	hypothetical protein		x	x	
MCR_1303	oppA; oligopeptide ABC transport system substrate binding protein OppA	x	x	x	x
MCR_1311	humA; heme utilization protein HumA		x		
MCR_1317	eno; enolase		x		

ORF	Annotation	1	2	3	4
MCR_1318	kdsA; 3-deoxy-8-phosphooctulonate synthase KdsA		x		
MCR_1319	pyrG; CTP synthase		x		
MCR_1320	ccoP; cbb3-type cytochrome c oxidase subunit CcoP	x			
MCR_1326	ccoG; cbb3-type cytochrome c oxidase accessory protein CcoG	x			
MCR_1328	LysR family transcriptional regulator	x			
MCR_1331	pyrC; dihydroorotase homodimeric type		x		
MCR_1342	ffh; signal recognition particle subunit FFH/SRP54		x		
MCR_1347	hemerythrin HHE cation binding protein		x		
MCR_1350	gidA; tRNA uridine 5-carboxymethylaminomethyl modification enzyme GidA	x			
MCR_1353	rplM; 50S ribosomal protein L13			x	
MCR_1357	cyt1; cytochrome c1 family protein	x			
MCR_1362	clpB; ATP-dependent chaperone ClpB		x	x	
MCR_1366	ABC transporter substrate binding protein	x	x	x	x
MCR_1367	ABC transporter substrate binding protein		x	x	x
MCR_1370	putative lipoprotein		x	x	
MCR_1372	GDSL-like lipase/ccylhydrolase family protein	x			
MCR_1373	periplasmic protein	x			
MCR_1376	pepN; aminopeptidase N	x	x		
MCR_1377	pal; peptidoglycan-associated lipoprotein		x	x	
MCR_1380	ompG1b; outer membrane protein G1b	x	x	x	
MCR_1387	rph; ribonuclease PH	x	x		
MCR_1388	putative acyl-CoA synthetase (long-chain-fatty-acid-CoA ligase) FadD/FadK		x		
MCR_1393	putative lipoprotein		x	x	x
MCR_1397	cytochrome c4		x	x	
MCR_1398	cytochrome c5	x			
MCR_1400	cysS; cysteinyl-tRNA synthetase	x			
MCR_1403	thiG; thiazole biosynthesis protein ThiG		x		
MCR_1409	suhB; inositol-1-monophosphatase		x		
MCR_1411	dxs; 1-deoxy-D-xylulose-5-phosphate synthase	x			
MCR_1415	hemF; coproporphyrinogen 3 oxidase		x		
MCR_1416	msp22; cytochrome c class II Msp22	x			
MCR_1419	LysM domain protein	x	x	x	
MCR_1423	hypothetical protein		x	x	
MCR_1424	accD; acetyl-CoA carboxylase carboxyl transferase AccD	x			
MCR_1425	trpA; tryptophan synthase alpha subunit		x		
MCR_1433	cytochrome c class I		x	x	
MCR_1437	aroB; 3-dehydroquinate synthase		x		
MCR_1445	lytic transglycosylase	x	x		
MCR_1446	mdh; malate dehydrogenase		x	x	x
MCR_1451	thrS; threonyl-tRNA synthetase	x			
MCR_1458	nqrA; NADH:ubiquinone oxidoreductase Na(+)-translocating subunit A		x		
MCR_1463	nqrF; NADH:ubiquinone oxidoreductase Na(+)-translocating subunit F		x		
MCR_1467	metE; 5-methyltetrahydropteroyltriglutamate-homocysteine S methyltransferase		x		
MCR_1470	FKBP-type peptidyl-prolyl cis-trans isomerase		x		
MCR_1474	OmpA family protein		x	x	
MCR_1480	pta; phosphate acetyltransferase		x		
MCR_1481	ackA; acetate kinase		x	x	
MCR_1487	ubiquinone biosynthesis hydroxylase	x			
MCR_1493	groEL; chaperonin protein Cpn60			x	
MCR_1494	groES; chaperonin protein Cpn10	x			
MCR_1502	hypothetical protein	x			
MCR_1514	hypothetical protein	x			
MCR_1519	phage integrase		x		
MCR_1521	KWG Leptospira family protein		x	x	
MCR_1524	map; methionine aminopeptidase type I		x		
MCR_1527	comM; competence protein ComM	x			
MCR_1531	ispA; geranyltranstransferase		x		
MCR_1533	DNA/RNA non-specific endonuclease	x	x		
MCR_1535	hypothetical protein		x	x	
MCR_1537	murD; UDP-N-acetylmuramoylalanine-D-glutamate ligase MurD	x			

ORF	Annotation	1	2	3	4
MCR_1547	ilvN; acetolactate synthase small subunit		x		
MCR_1551	LysM domain protein		x	x	
MCR_1553	fabG; 3-oxoacyl-ACP reductase FabG		x		
MCR_1554	fabD; malonyl CoA-ACP transacylase FabD		x		
MCR_1560	rplQ; 50S ribosomal protein L17		x	x	
MCR_1563	rpsK; 30S ribosomal protein S11	x	x		
MCR_1564	rpsM; 30S ribosomal protein S13		x		
MCR_1565	secY; protein translocase subunit SecY		x		
MCR_1566	rplO; 50S ribosomal protein L15		x		
MCR_1568	rpsE; 30S ribosomal protein S5		x	x	
MCR_1569	rplR; 50S ribosomal protein L18		x		
MCR_1570	rplF; 50S ribosomal protein L6		x		
MCR_1572	rpsN; SSU ribosomal protein S14P		x	x	
MCR_1573	rplE; 50S ribosomal protein L5		x	x	
MCR_1575	rplN; 50S ribosomal protein L14		x		
MCR_1579	rpsC; 30S ribosomal protein S3		x	x	
MCR_1581	rpsS; 30S ribosomal protein S19		x		
MCR_1582	rplB; 50S ribosomal protein L2		x	x	
MCR_1584	rplD; 50S ribosomal protein L4		x	x	
MCR_1585	rplC; 50S ribosomal protein L3		x		
MCR_1586	rpsJ; 30S ribosomal protein S10		x		
MCR_1591	beta-lactamase family protein BRO-2		x	x	
MCR_1592	gatB; aspartyl/glutamyl(asn/Gln)-tRNA amidotransferase subunit B		x		
MCR_1594	cytochrome c class I		x	x	
MCR_1595	OmpA/MotB domain protein		x	x	
MCR_1596	phospholipid/glycerol acyltransferase	x			
MCR_1603	rplY; 50S ribosomal protein L25		x		
MCR_1619	ribonuclease E	x			
MCR_1641	glyS; glycyl-tRNA synthetase beta subunit		x		
MCR_1642	glyQ; glycyl-tRNA synthetase alpha subunit		x		
MCR_1651	pyridine nucleotide-disulfide oxidoreductase family protein	x			
MCR_1652	mcmA; peptidase M16 inactive domain protein McmA	x	x		
MCR_1653	universal stress family protein		x		
MCR_1660	acetoin reductase			x	
MCR_1661	hypothetical protein		x	x	
MCR_1664	hypothetical protein		x		
MCR_1666	FKBP-type peptidyl-prolyl cis-trans isomerase		x	x	
MCR_1667	ABC transporter ATPase subunit		x		
MCR_1668	putative lipoprotein		x	x	
MCR_1672	pepSY-associated membrane protein	x			
MCR_1678	parC; DNA topoisomerase IV subunit A		x		
MCR_1681	prfC; peptide chain release factor 3	x			
MCR_1682	putative lipoprotein		x	x	
MCR_1683	polA; DNA polymerase I	x			
MCR_1685	topA; DNA topoisomerase I	x			
MCR_1689	aotP; arginine/ornithine transport ATP-binding protein AotP	x			
MCR_1690	extracellular solute-binding protein family 3	x		x	
MCR_1691	extracellular solute-binding protein family 3		x	x	
MCR_1692	extracellular solute-binding protein family 3	x			
MCR_1697	typA; GTP-binding protein TypA		x		
MCR_1698	ompCD; outer membrane protein CD	x	x	x	x
MCR_1720	luciferase-like monooxygenase		x		
MCR_1728	Ppx/GppA phosphatase	x			
MCR_1730	phoB; two-component system phosphate regulon response regulator PhoB		x		
MCR_1731	pstB; phosphate ABC transporter ATPase subunit PstB	x			
MCR_1734	pstS; phosphate ABC transporter substrate binding protein PstS	x		x	
MCR_1735	M48 family zinc metallopeptidase	x	x	x	
MCR_1737	sulfate transporter	x			
MCR_1742	outer membrane protein	x			
MCR_1750	putative phospholipid binding protein		x	x	
MCR_1760	rpsO; 30S ribosomal protein S15		x		
MCR_1761	olpA; OPA-like protein A	x	x		
MCR_1763	rbfA; ribosome-binding factor A	x			

ORF	Annotation	1	2	3	4
MCR_1764	hypothetical protein		x		
MCR_1766	hypothetical protein		x	x	
MCR_1768	infB; translation initiation factor IF-2	x	x		
MCR_1774	murF; UDP-N-acetylmuramoyl-tripeptide--D-alanyl-D-alanine ligase MurF		x		
MCR_1776	ftsI; peptidoglycan synthetase FtsI	x	x		
MCR_1777	ftsL; cell division protein FtsL	x			
MCR_1778	mraW; S-adenosyl-methyltransferase MraW	x			
MCR_1797	HSP33 protein		x		
MCR_1810	plsB; glycerol-3-phosphate acyltransferase		x		
MCR_1818	aromatic-amino-acid aminotransferase		x	x	
MCR_1821	putative hemolysin-related protein	x			
MCR_1825	ubiG; 3-demethylubiquinone-9 3-O-methyltransferase		x		
MCR_1827	DsbA oxidoreductase		x	x	
MCR_1836	pcnB; poly(A) polymerase	x			
MCR_1837	comEA; competence protein ComEA	x			
MCR_1839	cysK; cysteine synthase A		x	x	
MCR_1842	phosphomannomutase		x		
MCR_1845	major facilitator superfamily protein	x			
MCR_1846	fabF; 3-oxoacyl-ACP synthase II FabF		x	x	
MCR_1852	recN; DNA repair protein RecN	x			
MCR_1853	def; peptide deformylase		x		
MCR_1863	hypothetical protein	x	x	x	x
MCR_1867	afeA; chelated iron ABC transporter substrate binding protein AfeA		x		
MCR_1894	thrC; threonine synthase	x			
MCRH_0211*	not found	x			
MCRH_0267*	not found	x			
MCRH_0372*	not found	x			
MCRH_0432*	-	x			
MCRH_0655*	Acriflavin resistance protein - Psychrobacter s(strain PRwf-1)	x			
MCRH_0682*	not found	x			
MCRH_1397*	not found	x			
MCRH_1671*	not found	x			
MCRH_1878*	not found	x			
MCRH_2399*	not found	x			
MCRH_2916*	not found	x			
MCRH_3146*	not found	x			
MCRH_3320*	not found		x		
MCRH_3578*	not found	x			
MCRH_4402*	Putative uncharacterized protein - Anaerostipes caccae DSM 14662		x	x	
MCRH_4597*	not found		x		
MCRH_4750*	not found	x			
MCRH_5260*	not found	x			
MCRH_5451*	not found	x			
MCRH_5640*	not found	x			
MCRH_5644*	not found	x			
MCRH_5753*	not found	x			
MCRH_5787*	not found	x			
MCRH_5882*	not found	x			
Total number		**214**	**309**	**148**	**31**

MCRH_*, Internal Intercell annotation, ORFs not present in published genome (40).

Proteomics NTHI

NTHI overlaps of proteins identified by the antigenome technology and proteomic analyses. 1, proteins identified by AIP®; 2, proteins identified from the outer membrane; 3, proteins identified from whole membrane.

ORF	Annotation	1	2	3
NTHI0007	fdxG; formate dehydrogenase major subunit	x	x	
NTHI0010	fdxH; formate dehydrogenase, iron-sulfur subunit		x	
NTHI0039	mrdA; penicillin-binding protein 2; K05515 penicillin-binding protein 2	x		
NTHI0079	amiB; N-acetylmuramoyl-L-alanine amidase AmiB precursor	x		
NTHI0083	recN; DNA repair protein RecN	x		
NTHI0088	nrdD; anaerobic ribonucleoside triphosphate reductase	x		
NTHI0126	hypothetical protein	x		
NTHI0127	hypothetical protein	x		
NTHI0128	hypothetical protein	x		
NTHI0130	hypothetical protein	x		
NTHI0131	hypothetical protein	x		
NTHI0132	hypothetical protein	x		
NTHI0134	hypothetical protein	x		
NTHI0145	hypothetical protein	x		
NTHI0166	thrB; homoserine kinase	x		
NTHI0193	hsdR1; putative type I site-specific restriction-modification system, R subunit	x		
NTHI0202	hemR; hemin receptor	x		
NTHI0203	rlmL; 23S rRNA m(2)G2445 methyltransferase	x		
NTHI0206	hypothetical protein	x		
NTHI0208	znuA, yebL; high-affinity zinc transporter periplasmic component	x	x	
NTHI0210	mpl; UDP-N-acetylmuramate:L-alanyl-gamma-D-glutamyl-meso-diaminopimelate ligase	x		
NTHI0225	ompP2; outer membrane protein P2 precursor	x	x	x
NTHI0228	nanA; N-acetylneuraminate lyase	x		
NTHI0239	hflK; HflK; K04088 membrane protease subunit HflK	x		
NTHI0254	nqrA; Na(+)-translocating NADH-quinone reductase subunit A		x	x
NTHI0266	hypothetical protein		x	x
NTHI0269	pflB; formate acetyltransferase	x		
NTHI0291	potassium efflux protein KefA	x	x	
NTHI0303	nadN; NAD nucleotidase		x	x
NTHI0306	aroB; 3-dehydroquinate synthase	x		
NTHI0321	arcB; aerobic respiration control sensor protein ArcB	x		
NTHI0324	guaB; inosine 5'-monophosphate dehydrogenase		x	
NTHI0334	pnp; polynucleotide phosphorylase/polyadenylase	x	x	x
NTHI0338	putative transglycosylase	x		
NTHI0346	secD; preprotein translocase subunit SecD			x
NTHI0351	queA; S-adenosylmethionine:tRNA ribosyltransferase-isomerase	x		
NTHI0353	hypothetical protein		x	
NTHI0354	hap; adhesion and penetration protein Hap	x		x
NTHI0358	tonB; TonB	x		
NTHI0363	lipoprotein	x		
NTHI0369	hxuC; heme-hemopexin utilization protein C	x	x	x
NTHI0370	hxuB; heme-hemopexin-binding protein B	x		
NTHI0371	hxuA; heme-hemopexin-binding protein A	x		
NTHI0374	narQ; nitrate/nitrite sensor protein NarQ	x		
NTHI0375	murB; UDP-N-acetylenolpyruvoylglucosamine reductase	x		
NTHI0382	gltX; glutamyl-tRNA synthetase	x		
NTHI0389	udp; uridine phosphorylase		x	
NTHI0407	pilC; putative type IV pilin secretion protein	x		
NTHI0408	pilB; putative type IV pilin secretion protein	x		
NTHI0448	oapA; opacity associated protein	x		
NTHI0458	priA; primosome assembly protein PriA	x		
NTHI0463	napA; nitrate reductase catalytic subunit	x		
NTHI0472	lic3A; CMP-Neu5Ac--lipooligosaccharide alpha 2-3 sialyltransferase	x		

ORF	Annotation	1	2	3
NTHI0482	hypothetical protein		x	
NTHI0493	hscA; chaperone protein HscA			x
NTHI0501	pal; outer membrane protein P6 precursor		x	x
NTHI0503	tolA; cell envelope integrity inner membrane protein TolA	x		
NTHI0510	lcfA; long-chain-fatty-acid--CoA ligase	x		
NTHI0522	ompP1; long-chain fatty acid ABC transporter	x		x
NTHI0525	mesJ; putative cell cycle protein MesJ	x		
NTHI0529	znuB; high-affinity zinc uptake system membrane protein ZnuB	x		
NTHI0532	metalloprotease	x		
NTHI0538	rne; ribonuclease E		x	
NTHI0567	mrcA; penicillin-binding protein 1A	x		
NTHI0573	fruA; PTS system, fructose-specific IIBC component	x		
NTHI0574	fruK; 1-phosphofructokinase	x		
NTHI0585	lav; autotransported protein Lav	x		
NTHI0588	surA; survival protein SurA-like protein	x		
NTHI0611	atpA; F0F1 ATP synthase subunit alpha			x
NTHI0625	hslU; ATP-dependent protease ATP-binding subunit HslU	x		
NTHI0630	rbsA; D-ribose transporter ATP binding protein	x		
NTHI0642	rplA; 50S ribosomal protein L1			x
NTHI0645	nucleoside permease	x		
NTHI0652	ribonuclease I	x		
NTHI0657	rpsU; 30S ribosomal protein S21		x	
NTHI0668	groES; co-chaperonin GroES	x		
NTHI0669	groEL; chaperonin GroEL		x	x
NTHI0670	rplI; 50S ribosomal protein L9	x		
NTHI0716	rseB; periplasmic negative regulator of sigmaE	x		
NTHI0739	C4-dicarboxylate transporter	x		
NTHI0741	cpdB; bifunctional 2',3'-cyclic nucleotide 2'-phosphodiesterase/3'-nucleotidase periplasmic precursor protein	x		
NTHI0745	rpsL; 30S ribosomal protein S12	x	x	
NTHI0748	tuf; elongation factor Tu		x	x
NTHI0762	glmU; bifunctional N-acetylglucosamine-1-phosphate uridyltransferase/glucosamine-1-phosphate acetyltransferase	x		
NTHI0779	ABC transporter ATP-binding protein	x		
NTHI0782	hgpB; hemoglobin-haptoglobin binding protein B	x	x	x
NTHI0813	glpK; glycerol kinase		x	x
NTHI0816	hel; outer membrane protein P4, NADP phosphatase	x	x	x
NTHI0830	lppB; lipoprotein	x		
NTHI0831	tnaA; tryptophanase		x	
NTHI0834	mutS; DNA mismatch repair protein MutS	x		
NTHI0870	fucK; L-fuculokinase	x		
NTHI0877	metQ; putative D-methionine-binding lipoprotein MetQ		x	x
NTHI0899	pgmB; phosphoglucomutase			x
NTHI0921	mltC; murein transglycosylase C	x		
NTHI0941	rplB; 50S ribosomal protein L2		x	
NTHI0945	rpsC; 30S ribosomal protein S3	x	x	
NTHI0954	rpsN; 30S ribosomal protein S14		x	
NTHI0956	rplF; 50S ribosomal protein L6		x	
NTHI0960	rplO; 50S ribosomal protein L15	x		
NTHI0963	rpsK; 30S ribosomal protein S11			x
NTHI0978	alaS; alanyl-tRNA synthetase		x	
NTHI1012	dsbA; thiol:disulfide interchange protein DsbA	x		
NTHI1021	hbpA; heme-binding protein A		x	x
NTHI1024	polA; DNA polymerase I	x		
NTHI1028	clpB; ClpB	x		
NTHI1030	vacB; ribonuclease R	x		
NTHI1034	lic3A2; CMP-neu5Ac--lipooligosaccharide alpha 2-3 sialyltransferase	x		
NTHI1036	glnA; glutamine synthetase		x	
NTHI1038	pepB; aminopeptidase B		x	
NTHI1048	dipZ; thiol:disulfide interchange protein precursor	x		
NTHI1059	putative membrane-fusion protein	x		
NTHI1063	emrA; multidrug resistance protein A	x		
NTHI1080	rpsB; 30S ribosomal protein S2		x	

ORF	Annotation	1	2	3
NTHI1083	omp26; outer membrane protein 26	x		
NTHI1084	protective surface antigen D15	x		x
NTHI1085	zinc metalloprotease	x		
NTHI1093	glyS; glycyl-tRNA synthetase subunit beta	x		
NTHI1094	hypothetical protein	x		
NTHI1114	nrdR; transcriptional regulator NrdR	x		
NTHI1116	degS; protease DegS		x	
NTHI1127	dut; deoxyuridine 5'-triphosphate nucleotidohydrolase	x		
NTHI1139	rpsT; 30S ribosomal protein S20		x	
NTHI1145	accC; acetyl-CoA carboxylase biotin carboxylase subunit	x		
NTHI1160	leuA; 2-isopropylmalate synthase	x		
NTHI1164	iga1; IgA-specific serine endopeptidase	x		
NTHI1168	tbp1; transferrin-binding protein 1	x		
NTHI1169	tbp2; transferrin-binding protein 2 precursor	x		
NTHI1175	yidC; putative inner membrane protein translocase component YidC	x	x	
NTHI1188	bioB; biotin synthase	x		
NTHI1199	ATPase	x		
NTHI1207	dmsA; anaerobic dimethyl sulfoxide reductase chain A precursor	x		
NTHI1231	hrpA; ATP-dependent RNA helicase HrpA	x		
NTHI1236	cyoA; cytochrome oxidase subunit I		x	
NTHI1238	pyrG; CTP synthetase	x		
NTHI1240	pnuC; nicotinamide riboside transporter		x	
NTHI1244	murA; UDP-N-acetylglucosamine 1-carboxyvinyltransferase	x		
NTHI1253	ccmA; cytochrome c biogenesis protein CcmA	x		
NTHI1265	ligA; NAD-dependent DNA ligase LigA	x		
NTHI1266	zipA; cell division protein ZipA	x		
NTHI1286	oppF; oligopeptide transport ATP-binding protein	x		
NTHI1292	oppA; periplasmic oligopeptide-binding protein	x		
NTHI1299	ftsI; peptidoglycan synthetase FtsI	x		
NTHI1300	murE; UDP-N-acetylmuramoylalanyl-D-glutamate--2,6-diaminopimelate ligase	x		
NTHI1308	ddl; D-alanine--D-alanine ligase	x		
NTHI1323	Na+/dicarboxylate symporter	x		
NTHI1326	cydD; cysteine/glutathione ABC transporter membrane/ATP-binding component	x		
NTHI1332	ompP5; outer membrane protein P5	x	x	x
NTHI1342	opa; opacity protein	x		
NTHI1374	pta; phosphate acetyltransferase		x	x
NTHI1375	ackA; acetate kinase		x	
NTHI1390	hup; heme utilization protein	x	x	x
NTHI1403	ppc; phosphoenolpyruvate carboxylase	x		
NTHI1423	aspC; aromatic amino acid aminotransferase	x		
NTHI1448	hmw2C; HMW2C, putative glycosyltransferase involved in glycosylation of HMW1A and HMW2A	x	x	
NTHI1449	hmw2B; HMW2B, OMP-85-like protein required for HMW1A and HMW2A secretion	x		x
NTHI1450	hmw2A; HMW2A, high molecular weight adhesin 2	x		
NTHI1458	recombination factor protein RarA	x		
NTHI1473	pcp; outer membrane lipoprotein PCP precursor		x	
NTHI1474	lgtD; UDP-GlcNAc--lipooligosaccharide N-acetylglucosamine glycosyltransferase	x		
NTHI1512	hypothetical protein	x		
NTHI1517	hypothetical protein		x	
NTHI1542	phage-related minor tail protein	x		
NTHI1552	tail fiber protein	x		
NTHI1569	hypothetical protein	x		
NTHI1593	sppA; protease IV	x		
NTHI1600	fabB; 3-oxoacyl-(acyl carrier protein) synthase I		x	
NTHI1638	serine/threonine protein phosphatase family protein	x		
NTHI1642	rpmI; 50S ribosomal protein L35		x	
NTHI1643	rplT; 50S ribosomal protein L20		x	
NTHI1667	hypothetical protein	x	x	
NTHI1668	hypothetical protein			x
NTHI1683	folE; GTP cyclohydrolase I		x	
NTHI1702	trpB; tryptophan synthase subunit beta	x		
NTHI1707	ABC transporter periplasmic protein	x		

ORF	Annotation	1	2	3
NTHI1746	trpH; TrpH	x		
NTHI1760	valS; valyl-tRNA synthetase	x		
NTHI1772	ftnB; ferritin		x	
NTHI1773	ftnA; ferritin like protein 1		x	
NTHI1774	pstS; phosphate-binding periplasmic protein precursor PstS	x		x
NTHI1784	mukB; cell division protein MukB	x		
NTHI1809	glgB; glycogen branching enzyme	x		
NTHI1812	glnS; glutaminyl-tRNA synthetase	x		
NTHI1816	cdd; cytidine deaminase	x		
NTHI1823	potD1; spermidine/putrescine-binding periplasmic protein 1 precursor		x	x
NTHI1825	deoxyguanosinetriphosphate triphosphohydrolase-like protein	x		
NTHI1838	hsdM3; putative type I restriction enzyme HindVIIP M protein	x		
NTHI1849	hypothetical protein	x		
NTHI1857	tail fiber protein	x		
NTHI1885	major capsid protein	x		
NTHI1905	htoA; periplasmic serine protease do/HhoA-like precursor	x		
NTHI1915	ABC transporter permease	x		
NTHI1920	mao2; malic enzyme		x	
NTHI1925	hypothetical protein	x		
NTHI1929	dnaK; molecular chaperone DnaK	x		x
NTHI1933	aceE; pyruvate dehydrogenase subunit E1		x	x
NTHI1935	lpdA; dihydrolipoamide dehydrogenase			x
NTHI1945	tetratricopeptide repeat protein	x		
NTHI1948	rpsA; 30S ribosomal protein S1		x	
NTHI1950	pyridoxal biosynthesis lyase PdxS			x
NTHI1955	tldD; hypothetical protein	x		
NTHI1957	putative lipoprotein	x		x
NTHI1963	sucB; dihydrolipoamide succinyltransferase component of 2-oxoglutarate dehydrogenase complex		x	
NTHI1964	sucA; 2-oxoglutarate dehydrogenase E1 component	x		
NTHI1983	hmw1A; HMW1A, high molecular weight adhesin 1	x		x
NTHI1994	rnfG; electron transport complex protein RnfG	x		
NTHI2013	pepA; leucyl aminopeptidase		x	
NTHI2041	rnb; exoribonuclease II	x		
NTHI2048	metR; HTH-type transcriptional regulator MetR	x		
NTHI2049	lldD; L-lactate dehydrogenase			x
NTHI2052	spoT; guanosine-3',5'-bis 3'-pyrophosphohydrolase		x	
Total number		**156**	**60**	**37**

Microarray analysis

Differential gene expression analyzed by Microarray analysis under iron-rich and iron-depleted culture conditions. Log_2 ratios (gene expression in the presence of 1.25 μM Desferal versus 0 μM Desferal) are shown. nd, not detected.

ORF	Protein name	Log_2 ratio wt 1.25 μM vs. 0 μM	Log_2 ratio *msp22*Δ 1.25 μM vs. 0 μM
Upregulated genes during iron depletion			
MCR_0119	Imelysin family protein	1.5	0.9
MCR_0120	Putative iron-dependent peroxidase	1.4	0.9
MCR_0157	Putative membrane protein	1.3	0.9
MCR_0159	Membrane protein	2.0	1.5
MCR_0160	Adenosylmethionine-8-amino-7-oxononanoate transaminase	1.4	0.8
MCR_0161	8-amino-7-oxononanoate synthase	1.0	0.7
MCR_0216	Hypothetical protein	1.7	1.7
MCR_0217	Lactoferrin binding protein B LbpB	2.0	1.7
MCR_0218	Hypothetical protein	2.9	2.3
MCR_0219	Lactoferrin binding protein A LbpA	2.1	1.6
MCR_0220	Conserved hypothetical protein	2.3	2.0
MCR_0294	Iron (III) ABC transporter membrane permease FbpB	1.0	0.5
MCR_0487	Putative membrane protein	1.3	0.7
MCR_0490	Putative membrane protein	1.1	0.7
MCR_0493	Hypothetical protein	1.2	0.5
MCR_0611	Hypothetical protein	1.1	0.5
MCR_0693	Hypothetical protein	1.7	1.3
MCR_0694	Transferrin binding protein B TbpB	1.2	1.0
MCR_0796	Hypothetical protein	1.3	nd
MCR_0797	TonB-like protein	1.4	1.0
MCR_0798	Mota/tolq/exbb proton channel	1.3	1.3
MCR_0799	Biopolymer transport protein ExbD/TolR	1.3	1.3
MCR_0810	Heme oxygenase	1.2	0.8
MCR_0811	Hypothetical protein	1.3	0.7
MCR_1040	Putative bacterioferritin-associated ferredoxin	1.1	0.7
MCR_1072	Fumarate hydratase class II	1.3	0.7
MCR_1121	Hypothetical protein	1.0	-0.5
MCR_1224	Hypothetical protein	1.5	1.4
MCR_1621	Malate synthase G	1.2	nd
MCR_1867	Chelated iron ABC transporter substrate binding protein AfeA	1.3	0.8
MCR_1868	Chelated iron ABC transporter atpase subunit AfeB	1.6	0.8
MCR_1869	Chelated iron ABC transporter permease protein AfeC	1.4	1.0
MCR_1870	Chelated iron ABC transporter permease protein AfeD	1.3	0.9
MCR_1871	Putative membrane protein	1.9	nd
MCR_1872	Hypothetical protein	1.3	0.6
Downregulated genes during iron depletion			
MCR_0056	Trar/DksA family transcriptional regulator	-1.1	-0.3
MCR_0074	Conserved hypothetical protein	-0.9	nd
MCR_0075	Hypothetical protein	-0.9	nd
MCR_0137	Hypothetical protein	-1.0	-0.6
MCR_0349	Hypothetical protein	-1.1	nd
MCR_0460	Hypothetical protein	-1.1	nd
MCR_0568	Putative nitroreductase	-1.0	-0.4
MCR_0593	Putative membrane protein	-1.8	-0.5
MCR_0638	Hypothetical protein	-1.0	nd
MCR_0745	Carbonic anhydrase	-1.8	nd
MCR_0750	Ppic-type peptidyl-prolyl cis-trans isomerase	-2.1	-1.2

ORF	Protein name	Log_2 ratio wt 1.25 µM vs. 0 µM	Log_2 ratio *msp22*Δ 1.25 µM vs. 0 µM
MCR_0751	Molybdopterin molybdochelatase	-1.5	nd
MCR_0760	Molybdenum cofactor biosynthesis protein B	-1.2	-0.9
MCR_0761	MOSC domain protein	-1.3	-1.1
MCR_0762	Molybdenum cofactor biosynthesis protein A	-1.3	nd
MCR_0766	Nitrate transporter nark1	-0.9	nd
MCR_0767	IS1016 transposase	-1.0	nd
MCR_0858	Outer membrane protein E	-1.5	nd
MCR_0934	Polyphosphate kinase 2	-1.4	nd
MCR_0956	Hypothetical protein	-0.9	-0.5
MCR_0963	Hypothetical protein	-1.1	nd
MCR_1038	Bacterioferritin B	-2.7	-1.8
MCR_1039	Bacterioferritin A	-2.2	-1.3
MCR_1223	NUDIX hydrolase	-0.9	nd
MCR_1535	Hypothetical protein	-1.1	nd
MCR_1594	Cytochrome c class I	-0.9	-0.4
MCR_1627	Hypothetical protein	-0.9	-0.6
MCR_1684	Hypothetical protein	-0.9	nd
MCR_1743	Osmc family protein	-1.3	-0.7
MCR_1744	Fumarate hydratase class I	-1.2	nd
MCR_1886	Conserved hypothetical protein	-0.9	nd

11 Appendix II

11.1 Plasmid maps and sequences

Multiple cloning site of pET28b+. blue, T7 promoter and T7 terminator regions.

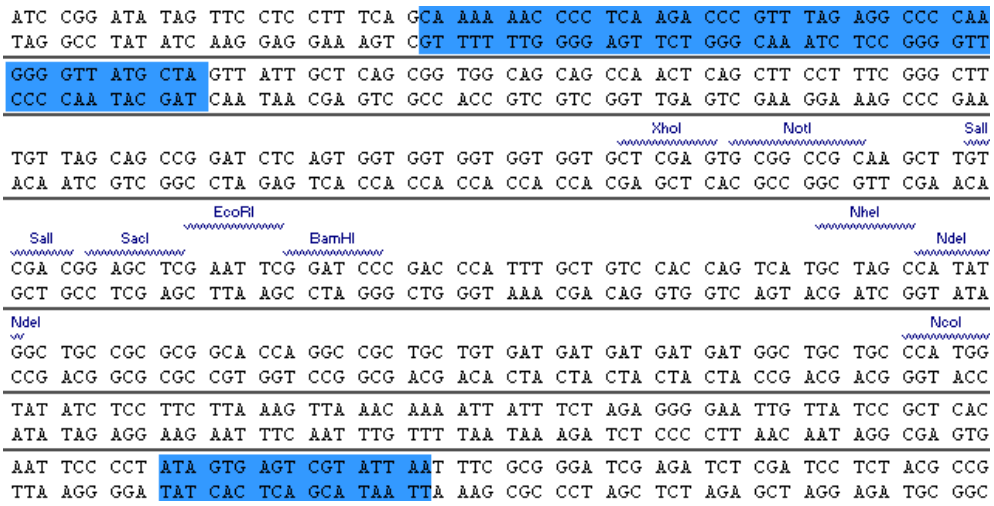

Promoter prediction for *msp22*. 1-8, potential prokaryotic promoters predicted by www.fruitfly.org (promoter predictions, score cutoff 0.80).

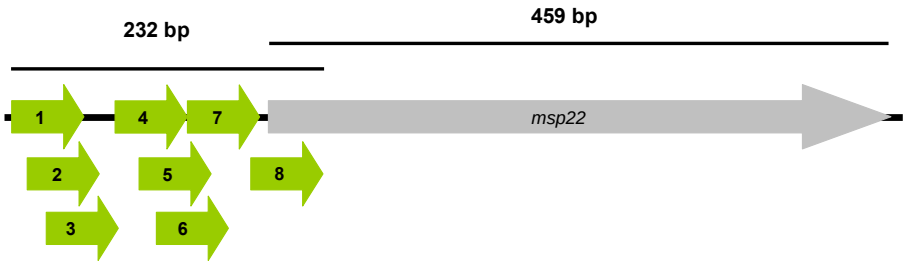

Score	Promoter Sequence
0.93	CATAACATAAATTGCCGTTGTCTTGGCTGGTCAATCAAATTTGGTCAATT
0.99	ATTGCCGTTGTCTTGGCTGGTCAATCAAATTTGGTCAATTTTTAGGTAT
0.83	GGTCAATCAAATTTGGTCAATTTTTTAGGTATTGTTTCATCAAAAAACAC
0.88	GTTATCCTGATTGCATGTCATCATTGTTTGTAATCAGAATAGACATTTCA
0.83	CATCATTGTTTGTAATCAGAATAGACATTTCATCAATCATTTTGGTAAAT
0.88	AATCAGAATAGACATTTCATCAATCATTTTGGTAAATAATATTAGGTTAC
0.98	CAATCATTTTGGTAAATAATATTAGGTTACCAAATAACCTATTTTACCAA
0.99	TAAGGTATTTTAACAAAACGGAGCCGCCGCCATGTTTCATAAAATTACCT

pEMCJH04-KAN-Msp22-HIS (5418 bp).

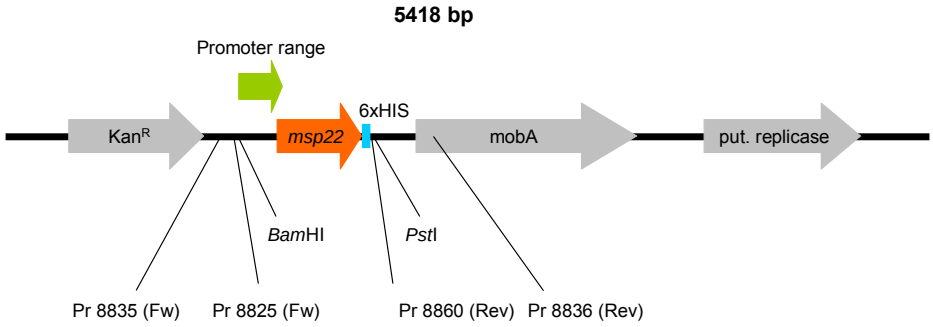

Heterologous expression of Msp22 in *M. catarrhalis*. Msp22 in pEMCJH04-KAN. Green: promoter range; red, *msp22* gene start and stop.

```
                                                                                                BamHI
GTTCAAAATC ACCAACTGGT CCACCTACAA CAAAGCTCTC ATCAACCGTG GCGGGGATCC CATAACATAA ATTGCCGTTG TCTTGGCTGG TCAATCAAAT
CAAGTTTTAG TGGTTGACCA GGTGGATGTT GTTTCGAGAG TAGTTGGCAC CGCCCCTAGG GTATTGTATT TAACGGCAAC AGAACCGACC AGTTAGTTTA

TTGGTCAATT TTTTAGGTAT TGTTTCATCA AAAAACACTG TTATCCTGAT TGCATGTCAT CATTGTTTGT AATCAGAATA GACATTTCAT CAATCATTTT
AACCAGTTAA AAAATCCATA ACAAAGTAGT TTTTTGTGAC AATAGGACTA ACGTACAGTA GTAACAAACA TTAGTCTTAT CTGTAAAGTA GTTAGTAAAA

                                                                                    Met  Phe  His  Lys  Ile  Thr  Leu  Ala  Ala
GGTAAATAAT ATTAGGTTAC CAAATAACCT ATTTTACCAA AATAAGGTAT TTTAACAAAA CGGAGCCGCC GCCATGTTTC ATAAAATTAC CTTAGCTGCT
CCATTTATTA TAATCCAATG GTTTATTGGA TAAAATGGTT TTATTCCATA AAATTGTTTT GCCTCGGCGG CGGTACAAAG TATTTTAATG GAATCGACGA

 Ala  Cys  Phe  Met  Thr  Val  Ile  Leu  Ala  Gly  Cys  Asn  Ser  Ser  Gly  Thr  Ala  Thr  Ala  Asn  Asn  Pro  Gln  Val  Glu  Asp  Arg  Ala  Lys  Leu  Met  Lys  Asp  Trp
GCATGTTTTA TGACTGTTAT TTTAGCAGGT TGCAACAGCT CAGGGACTGC CACCGCCAAT AATCCACAGG TTGAAGACCG TGCCAAACTC ATGAAAGATT
CGTACAAAAT ACTGACAATA AAATCGTCCA ACGTTGTCGA GTCCCTGACG GTGGCGGTTA TTAGGTGTCC AACTTCTGGC ACGGTTTGAG TACTTTCTAA

 Trp  Arg  His  Ala  Asn  Glu  Gly  Met  Lys  Ala  Met  Ile  Glu  Asp  Pro  Ser  Arg  Phe  Asp  Ala  Ile  Thr  Phe  Lys  Glu  Arg  Ala  Asp  Phe  Ile  Ala  Asp  Thr  Asn
GGCGTCATGC CAATGAAGGT ATGAAGGCAA TGATTGAAGA CCCAAGTCGC TTTGATGCCA TCACCTTTAA AGAGCGAGCT GATTTTATTG CTGATACCAA
CCGCAGTACG GTTACTTCCA TACTTCCGTT ACTAACTTCT GGGTTCAGCG AAACTACGGT AGTGGAAATT TCTCGCTCGA CTAAAATAAC GACTATGGTT

 Asn  Ala  Thr  Met  Trp  Val  His  Phe  Glu  Gly  Glu  Met  Ala  Gln  Gly  Gly  His  Ala  Lys  Asp  Glu  Ile  Trp  Thr  Asp  Pro  Glu  Gly  Phe  Gln  Thr  Lys  Ile  Glu
TGCCACCATG TGGGTACACT TTGAAGGAGA AATGGCTCAA GGTGGTCATG CTAAAGATGA GATATGGACA GACCCTGAAG GCTTTCAAAC CAAAATCGAA
ACGGTGGTAC ACCCATGTGA AACTTCCTCT TTACCGAGTT CCACCAGTAC GATTTCTACT CTATACCTGT CTGGGACTTC CGAAAGTTTG GTTTTAGCTT

 Ala  Phe  Thr  Ser  Ser  Ile  Asn  Ala  Leu  Ala  Leu  Ala  Ala  Ser  Glu  Ala  Ala  Ser  Ala  Ala  Asp  Val  Glu  Ala  Ser  Tyr  Gly  Glu  Met  Ala  Ser  Gln  Cys  Gly
GCGTTTACCA GCTCAATTAA TGCACTTGCC TTGGCAGCAT CAGAAGCTGC CTCGGCGGCT GATGTTGAAG CAAGCTATGG TGAAATGGCC AGCCAGTGTG
CGCAAATGGT CGAGTTAATT ACGTGAACGG AACCGTCGTA GTCTTCGACG GAGCCGCCGA CTACAACTTC GTTCGATACC ACTTTACCGG TCGGTCACAC

                                                                                                PstI
 Gly  Ser  Cys  His  Lys  Ala  Tyr  Lys  Lys  Lys  His  His  His  His  His  His  ***
GTTCTTGCCA TAAGGCTTAT AAGAAAAAAC ACCACCACCA CCACCACTAG CTGCAGGCAT GCAAGCTTCA GGGTTGAGAT GTGTATAAGA GACAGCCTAT
CAAGAACGGT ATTCCGAATA TTCTTTTTTG TGGTGGTGGT GGTGGTGATC GACGTCCGTA CGTTCGAAGT CCCAACTCTA CACATATTCT CTGTCGGATA
```

pR412T7 (4640 bp).

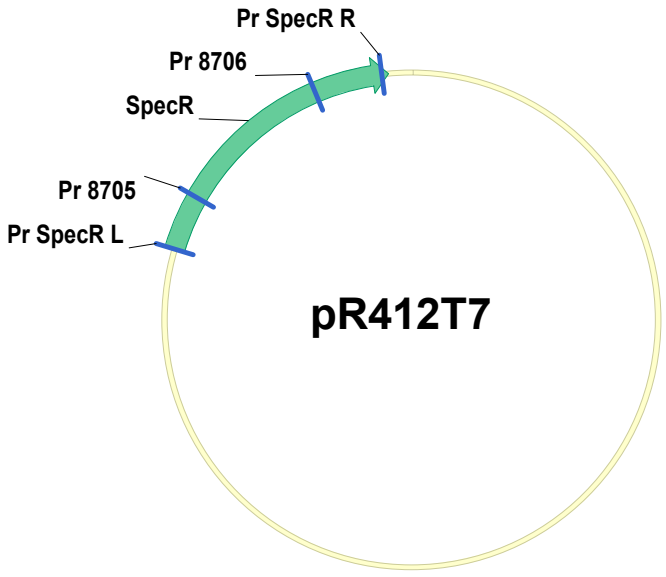

Sequence of the Spectinomycin resistance cassette (within pR412T7). Red, Primers SpecR L and SpecR R; green, Spectinomycin gene start and stop.

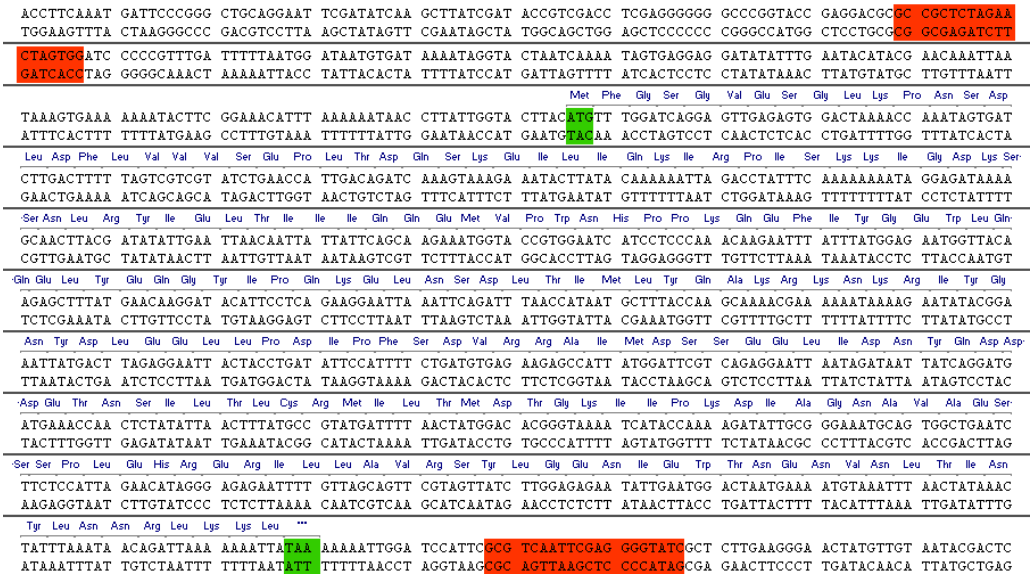

11.2 Primer sequences

Cloning of *M. catarrhalis* and NTHI antigens for recombinant expression (Materials and methods 4.7)

Primers for amplification of genes from genomic DNA (*M. catarrhalis* RH4, NTHI86-028NP). Restriction digests performed with *Nco*I/*Xho*I, *Bsp*HI/*Xho*I, *Afl*III/*Xho*I or *Nco*I/*Not*I. Restriction sites are underlined,

Specificity	Primer sequence (5′ - 3′)	Product size (bp)	kDa
MCR_0076-1	Fw: ATATATCCATGGATAATACCAAGCTGGGTGAAGAGC Rev: ATATATCTCGAGATCAACAACATTAATCACACCAGCTG	420	15.7
MCR_0136	Fw: ATATATTCATGATTAAAACTGACACCAATGCCATGG Rev: ATATATCTCGAGATCTTTTGCACAGCGAAATCC	717	28.1
MCR_0196	Fw: ATATATCCATGGCTAATGATTCTCCCAATCTTAGCAACAG Rev: ATATATCTCGAGTTTAACTAATATCCAAGATGAGCTGCC	1350	50.8
MCR_0560-1	Fw: ATATATCCATGGCTTCTGAGTCTGTATCTGAAGATGATTTGAC Rev: ATATATCTCGAGATCCACAGAATCATCAGTCTGAGC	657	29.4
MCR_0686	Fw: ATATATCCATGGGTAAACCCAGCAAAATTCATACAC Rev: ATATATCTCGAGAGGTTGGGCAGGCTTAATGAG	1593	60.3
MCR_0739-1	Fw: ATATATCCATGGAGGATACCCTTAAGGATGTGCC Rev: ATATATCTCGAGCGAACCTGTTAAGGTGTTGATACC	438	16.3
MCR_0996	Fw: ATATATCCATGGCTAAAACTGCTGCCCCCAAAG Rev: ATATATCTCGAGGTTTTTGGGAGTTTTAAGCACTTG	366	14.7
MCR_1003	Fw: ATATATCCATGGCTAGTAGCACAGGCACACCTGCTAAAC Rev: ATATATCTCGAGTCCATAGCCTTTTAAAGAAGCCAGC	1038	39.3
MCR_1010	Fw: ATATATACATGTCTTTTTCGGTTGATAACAGTCAGCAG Rev: ATATATCTCGAGCTGGCGATAAGCCAATTCAG	1080	41.0
MCR_1303nHIS	Fw: ATATATCCATGGCTAGCAATAATAGCACGACAGCATCAC Rev: ATATATCTCGAGATTCGCTGTTGTCGTATCCGTG	1968	73.8
MCR_1416	Fw: ATATATCCATGGCTAACAGCTCAGGGACTGCCAC Rev: ATATATCTCGAGTTTTTTCTTATAAGCCTTATGGCAAG	396	15.7
MCR_1698	Fw: ATATATCCATGGGTGTGACAGTCAGCCCACTAC Rev: ATATATCTCGAGTTGAACAATCATATCTTTGGTTTG	1281	47.0
NTHI0811	Fw: ATATATCCATGGCAATACCCAAATGAAATCAGACAAAATCAT Rev: ATATATCTCGAGTTTTATTCCTTTTAAGAATTCCACGC	1011	40.4
NTHI0358	Fw: ATATATCCATGGCTTTATGGAATTGGAATGAGCC Rev: ATATATGCGGCCGCTTGAAGAGTAAAACTAATTTGCACAC	717	27.5
NTHI0370	Fw: ATATATCCATGGCTTTAGGTCAGCCAGATACTGGATCATTG Rev: ATATATCTCGAGGAAAGTTTTAATCATAGAAAGCCAAAATTGGTG	1617	61.2
NTHI0371-1	Fw: ATATATCCATGGCTACACAGGGTTTGCCACAAGAG Rev: ATATATCTCGAGAGCCACAAAACTAACCATATCCCCTTTAATATTAC	831	31.0
NTHI1169-2	Fw: ATATATCCATGGCTAGAAAAACTGATATTCAACAATATGAAAAG Rev: ATATATCTCGAGCTTGTTGGTTTTTTCTACTTGTCTTTTAG	1137	43.1

Primers for the confirmation of positive clones.

Primer ID (in vector pET28b+)	Primer sequence (5′ - 3′)
ICC102	TAATACGACTCACTATAGGG
ICC103	GCTAGTTATTGCTCAGCGG

M. catarrhalis gene deletion mutants (Materials and methods 4.12.1)

Location of primers for the generation and confirmation of gene deletion mutants.

ORF	Primer sequence (5´ - 3´)	Primer location
MCR_0076	ACGGTCAAGATAAACAGCAT	L1
MCR_0076	**CCACTAGTTCTAGAGCGGC**GACTTTAGGTTTGACGGCTA	L2
MCR_0076	**GCGTCAATTCGAGGGGTATC**TCACCCAGCTTGGTATTATC	R2
MCR_0076	GTTGCTACGACGCTTAAAAT	R1
MCR_0076	TAAAAGCACCTGATCATCCT	C
MCR_0076	CGCTCTAAAGTGGCATTATT	P1
MCR_0076	TGCTCAACTTCTTTCTTGGT	P2
MCR_0136	TGGGCAGACTTCTTTACAAT	L1
MCR_0136	**CCACTAGTTCTAGAGCGGC**CCTAAAAAGCTTGGGATTTC	L2
MCR_0136	**GCGTCAATTCGAGGGGTATC**CACGCAGTTAAGTGAGTCAA	R2
MCR_0136	GCTTGCCAACTCTGACTATC	R1
MCR_0136	AAACCTGTGGTGAATGTCTC	C
MCR_0136	AAAGTCCAATGTTCATCAGC	P1
MCR_0136	ACAAGCAATTGATACCCAAG	P2
MCR_0560	GACTTGATTGGACAGCTCAT	L1
MCR_0560	**CCACTAGTTCTAGAGCGGC**GAGGTTCTTGGTAATGCAGA	L2
MCR_0560	**GCGTCAATTCGAGGGGTATC**GAGTATGAGCGTGCATTTTT	R2
MCR_0560	CCAATTTGGTACAGGTTGTT	R1
MCR_0560	CTTTGGTGATTGTTCCAAGT	C
MCR_0560	TGTTATGTCTGTTGGTGCAT	P1
MCR_0560	CCTTGACATTAAGTTTGTCG	P2
MCR_0686	ATGTCAAAGTCCTGCCTAAA	L1
MCR_0686	**CCACTAGTTCTAGAGCGGC**GCAAGCAGAGAGCATAGTTAG	L2
MCR_0686	**GCGTCAATTCGAGGGGTATC**GACATGGAAAAACAAGGCTA	R2
MCR_0686	ATGTGTCAGCGTTACTGTGT	R1
MCR_0686	GAGTGTCCAAATCCACCTTA	C
MCR_0686	TCTGATGATGAGCGTGATTA	P1
MCR_0686	GGCATAATCCATACGATCAC	P2
MCR_0739	GCGTTTTACTCGTACACAAA	L1
MCR_0739	**CCACTAGTTCTAGAGCGGC**CCAAAGGGCGTTCTTTATTA	L2
MCR_0739	**GCGTCAATTCGAGGGGTATC**CCTGTTATCATCATCGCTTT	R2
MCR_0739	GTGCGATGGATTTGGTTA	R1
MCR_0739	CTTTGGGGCTAAAAGTAGTG	C
MCR_0739	CAAAACGACCCTTAACAATC	P1
MCR_0739	AAGCCTACAAAGCTGACAAG	P2
MCR_0996	GCTTAATTGCTGCAAACACT	L1
MCR_0996	**CCACTAGTTCTAGAGCGGC**CAAACCACGCATCCATTTAT	L2
MCR_0996	**GCGTCAATTCGAGGGGTATC**GATCAAGTGCTTAAAACTCC	R2
MCR_0996	ATATCCAGCATACGATCAGC	R1
MCR_0996	GATGAGATCCTTCAGCTCAG	C
MCR_0996	AGGTGTGTAAACCATTGACC	P1
MCR_0996	TACTTTCAGGTGCAATCTCA	P2
MCR_1303	GTCTGTGGTGCGTTTTATTT	L1
MCR_1303	**CCACTAGTTCTAGAGCGGC**ACTGTGGCAAATAACTTCGT	L2
MCR_1303	**GCGTCAATTCGAGGGGTATC**ATACGACAACAGCGAATTG	R2
MCR_1303	CAATCAAATGCCCTATCACT	R1
MCR_1303	TAGCATTCACAGGGAATAGG	C
MCR_1303	TATTGCCTGAACATCTGACA	P1
MCR_1303	GGTGATTTTGCTCATAAAGG	P2
MCR_1416	TGATATTCGCTGAGATGTGA	L1
MCR_1416	**CCACTAGTTCTAGAGCGGC**AGTGTGGTTCTTGCCATAAG	L2
MCR_1416	**GCGTCAATTCGAGGGGTATC**TAAAACATGCAGCAGCTAAG	R2
MCR_1416	GATGGCATCATACCAATCTT	R1
MCR_1416	ATGTGGGTACACTTTGAAGG	C
MCR_1416	ATTGCTGTTGTACAGGGTGT	P1
MCR_1416	CATCAGGTGGCTTATGAGTT	P2
SpecR	GCCGCTCTAGAACTAGTGG	SpecR L
SpecR	GATACCCCTCGAATTGACGC	SpecR R
SpecR	TTTTACCCGTGTCCATAGTT	A

Southern blot analysis (Materials and methods 4.2.4)

Specificity (ORF)	Primer #	Primer sequence (5′ - 3′)	Probe size (unlabeled)	Probe start – stop (within respective gene)
MCR_0076	8840	Fw: GCAAATAACTCTACCGTTGG	832 bp	709 - 1540
	8839	Rev: GCTGGTCATATTCAATTGGT		
MCR_1416	8842	Fw: CTGTTATTTTAGCAGGTTGC	368 bp	41 - 408
	8841	Rev: ACCATAGCTTGCTTCAACAT		
MCR_1303	8837	Fw: GTATACCTCAGATGGCGAAG	749 bp	324 - 1072
	8838	Rev: CGACAGTTTGTGCTTGATAA		
SpecR	8705	Fw: GTTTGGATCAGGAGTTGAGA	503 bp	3 - 505
	8706	Rev: TTTTACCCGTGTCCATAGTT		

qRT-PCR analysis (Materials and methods 4.16.5)

Specificity (ORF)	Primer sequence (5′ - 3′)	Gene start - stop
MCR_0056	Fw: TGCTGCCAGTCGTGATGAA	135 – 153
	Rev: GTCCTTGCTCGGCCTCAAT	190 - 172
MCR_0096	Fw: GCCGTAATCCTGCTCTGCTATT	86 - 107
	Rev: TGCCAGTGCAAGTAGCACAAC	147 - 127
MCR_0159	Fw: GCCATGATAACACCGCTCAA	16 - 35
	Rev: CCGCTCGCATCAAAGCA	91 - 75
MCR_0218	Fw: GCCCAAGGCACTGTTTCAAA	21 - 40
	Rev: CGCTTGACCGACAGTTGATG	89 - 70
MCR_0219	Fw: TGTTCTTTGCGATGATTATCAAGAG	1266 - 1290
	Rev: GCATAAGCCAGTTTTGGAATGG	1370 - 1349
MCR_0294	Fw: CGCTTGTGGCTTGGTCTGT	31 - 49
	Rev: GCAAAGACAATGACGGATAATGG	92 - 70
MCR_0361	Fw: CGAAATTACGCATCATCAAGATG	72 - 94
	Rev: TCATTGGCAATCACACGCATA	140 - 120
MCR_0492	Fw: GGTGAGTGCCGCTTTTACAAC	36 - 56
	Rev: GGCGATCACTGACCACTGTATC	124 - 103
MCR_0593	Fw: TTATTGGCGTGTTGATGATTGTT	50 - 72
	Rev: ACAGCACCAATGATATGCATACCT	119 - 96
MCR_0677	Fw: GCAGCAGTACTAGCCTCTGTTGAA	271 - 294
	Rev: CCGTACCCATCTCACGCATA	352 - 333
MCR_0694	Fw: CGAACGCACCGCTACCA	1662 - 1678
	Rev: CCTACCCAGTTCCCCAAATATTT	1736 - 1714
MCR_0760	Fw: CTGATACTCGCATACTGGACGAA	95 - 117
	Rev: TGCCTCCACTAGGCTATCTACCA	159 - 137
MCR_0798	Fw: GGGCATCATGCGTGTGATT	93 - 111
	Rev: GGCAGTTAGCTCATCAACAATATTTG	156 - 131
MCR_0810	Fw: GCCGAGCGTCTCAAAGAAGA	19 - 38
	Rev: CTGACATGACCGTCTCATCGA	82 - 62
MCR_0858	Fw: AATTTGGATACAAAGCGCTGAGT	11 - 33
	Rev: TGCTGCGGTTGCGGTTA	69 - 53
MCR_0920	Fw: GCCATGTTTGGCTCATTGC	127 - 145
	Rev: TTGGTGCCGTGGTGGAA	181 - 165
MCR_1039	Fw: AGCTTGGTGCTCGTGATCAA	53 - 72
	Rev: ACCAAAACTCCACTCCGCATA	114 - 94
MCR_1040	Fw: GGTACTTGTTGTGGTTGCTGTGTAC	103 - 127
	Rev: CGATCACATTGGCTTGATGCT	172 - 152
MCR_1057	Fw: CATACGCCGAAGATCCAAATATT	578 - 600
	Rev: GATACCGCTTCTGCCATGGATA	678 - 657
MCR_1731	Fw: CCAACCATGAACACAGCGTTT	28 - 48
	Rev: GGCGGCAGTTTGGCTTAG	93 - 76
MCR_1868	Fw: CGACCAAAACCAAAGGATTACC	337 - 358
	Rev: GCTAATTTGTCGATTGGCAAGA	420 - 399

Heterologous expression of MCR_1416 (Msp22) (Materials and methods 4.12.3 and 4.13.1)

PCR primers for amplification of *msp22* from *M. catarrhalis* genomic DNA (8825, 8826 and 8860) and for colony PCR (8835 and 8836). Restriction sites are underlined, gene specific nucleotides are **bold**. The 6xHIS-tag coding sequence is represented in *italic*.

Specificity	Primer #	Primer sequence (5′ - 3′)	Gene start - stop
MCR_1416	8825	Fw: ATATATGGATCC**CATAACATAAATTGCCGTTGTCTTGG**	Upstream *msp22*
MCR_1416	8826	Rev: ATATATCTGCAG**CTATTTTTTCTTATAAGCCTTATGGC**	459 - 434
MCR_1416	8860	Rev*: AAAACTGCAGCTA*GTGGTGGTGGTGGTGGTG***TTTTTTCTTATAAGC**	456 - 442
pEMCJH04-KAN	8835	Fw: ACTTTTGCTGAGTTGAAGGA	
pEMCJH04-KAN	8836	Rev: ACAAAATGTTGTAGCGGTCT	

NTHI gene deletion mutant (*hxuA*Δ) (Materials and methods 4.14)

Primer sequences for the generation and confirmation of an *hxuA* gene deletion mutant. L1, L2, primers for generation of fragment A (flanking region of 1425 bp); R2, R1, for generation of fragment B (flanking region of 1444 bp).

Specificity or Primer #	Primer sequence (5′ - 3′)	Primer location
Upstream NTHI0371	Fw: GGCAAATGAGATCAGCGAAT	L1
Upstream NTHI0371	Rev: CGCACCAGTGTAAGTGGTCA	L2
Downstream NTHI0371	Fw: CAACAATTCGGCGATAAAGG	R2
Downstream NTHI0371	Rev: TCCACGCTTTCTGGTTGTTC	R1
8030	GGCGAGCTCTCTACCCGTTTTGGTGTAAC	Control primer 1
7956	CCCAAGCTTAACCACCACACATAAAAAGG	Control primer 2

12 Abbreviations

ABTS	2,2´-Azino-Bis-(3-Ethylbenzthiazoline-6-Sulfonic Acid)
AEBSF	4-(2-Aminoethyl)-Benzenesulfonyl Fluoride
AIP®	Antigen Identification Program (Intercell)
AOM	Acute otitis media
BHI medium	Brain Heart Infusion Medium
bp	Base pair
CFA	Complete Freund´s Adjuvant
CFU	Colony Forming Unit
COPD	Chronic Obstructive Pulmonary Disease
DIG	Digoxigenin-dUTP
DNA	Deoxyribonucleic Acid
dNTP	Deoxyribonucleotide triphosphate
DTT	Dithiothreitol
EDTA	Ethylenediaminetetraacetic Acid
ELISA	Enzyme-linked Immunosorbent Assay
Fc	Fragment crystallizable region
Fw primer	Forward primer
HBSS	Hank´s Buffered Salt Solution
HIS-tag	6x Histdine-tag
HRP	Horseradish Peroxidase
IFA	Incomplete Freund´s Adjuvant
IFN	Interferon
Ig	Immunoglobulin
IL	Interleukin
IPTG	Isopropyl β-D-1-Thiogalactopyranoside
kDa	Kilodalton
LB-medium	Luria-Bertani medium
Lbp	Lactoferrin-binding protein
LOS	Lipooligosaccharide
LPS	Lipopolysaccharide
Mbp	Mega base pair

MW	Molecular Weight
MWM	Molecular Weight Marker
NAD	Nicotinamide Adenine Dinucleotide
NTHI	Nontypeable *Haemophilus influenzae*
OD	Optical Density
OD_{600}	OD_{600nm}
OME	Otitis media with effusion
OMV	Outer membrane vesicle
ORF	Open Reading Frame
PBS	Phosphate-Buffered Saline
PBST	Phosphate-Buffered Saline + Tween®20
PCR	Polymerase Chain Reaction
qRT-PCR	Quantitative Real-Time PCR
Rev primer	Reverse primer
RNA	Ribonucleic Acid
SDS	Sodium Dodecylsulfate
SDS-PAGE	SDS-Polyacrylamide Gel Electrophoresis
TAE Buffer	Tris Acetate EDTA Buffer
Tbp	Transferrin-binding protein
TE Buffer	Tris EDTA Buffer
Tris	TRIZMA®Base
Tx-100	Triton X-100
Vol	Volume

13 Curriculum Vitae

Personal information	
Name	Margarita Smidt
Place of birth	Vienna, Austria
Date of birth	11th March 1983
Nationality	Austrian

Education	
04/2008 – 03/2011	PhD thesis *"Characterization of potential vaccine antigens from Moraxella catarrhalis and nontypeable Haemophilus influenzae with focus on iron metabolism"* Supervisor: Univ. Prof. Dr. Alexander von Gabain Institute: Intercell AG Molecular Microbiology Department Campus Vienna Biocenter 3, Vienna, Austria
02/2008	MSc Degree (Mag.rer.nat.) in Genetics and Microbiology
11/2006 – 10/2007	Diploma thesis *"Identification of antigens for the development of a vaccine to prevent otitis media disease"* Supervisor: Univ. Prof. Dr. Alexander von Gabain Institute: Intercell AG Antigen Discovery Department Campus Vienna Biocenter 3, Vienna, Austria
2004 – 2007	Studies of Genetics and Microbiology at the University of Vienna
2002 – 2004	Study of Biology at the University of Vienna
06/2001	"Matura" (school leaving exam) with distinction
1993 – 2001	Secondary school, BRG XIII Wenzgasse (Vienna, Austria)
1989 – 1993	Elementary school, Speisingerstraße 44 (Vienna, Austria)

Stays abroad

10/2010	Microarray analysis (PhD-related work) at the Radboud University Medical Center (Nijmegen, The Netherlands)
03/2006 – 07/2006	Erasmus program, Studies of Genetics and Microbiology at the University of Geneva (Geneva, Switzerland)
07/2004 – 08/2004	Work experience in Las Quebradas Biological Centre (San Isidro de El General, Costa Rica)
07/1999 – 06/2000	AFS Student exchange year (North Canterbury, New Zealand)

Presentations and Conferences

10/2010	Poster presentation at the 4th Vaccine and ISV Annual Global Congress (Vienna, Austria) *"Moraxella catarrhalis and nontypeable Haemophilus influenzae proteins for otitis media vaccine development"*
04/2009	Poster presentation at the 4th Semmering Vaccine Symposium (Baden, Austria) *"Moraxella catarrhalis and nontypeable Haemophilus influenzae iron-regulated proteins as potential vaccine candidates"*
11/2008	Oral presentation at the VBC Student Symposium II (Campus Vienna Biocenter, Vienna, Austria) *"Antigen identification of otitis media causing pathogens"*
2008	Member of the organizing committee of the VBC Student Symposium II (Campus Vienna Biocenter, Vienna, Austria)
10/2007	Poster presentation at the VBC Student Symposium I (Campus Vienna Biocenter, Vienna, Austria) *"Identification of novel antigens for the development of vaccines (AIP®)"*

Publications

Smidt M.[1], Bättig P.[1], Verhaegh S.J., Oleksiewicz M.O., Niebisch A., Hanner M., Schlick P., Noiges B., Schüler W., Lundberg U., Nagy E., Meinke A., Hays J., Selak S.[2], Henriques-Normark B. Identification of novel *Moraxella catarrhalis* vaccine candidates by the ANTIGENome technology. *Manuscript in preparation.*